Supporting information

Redox-active Ligand Based Mn(I)-Catalyst for Hydrosilylative Ester Reduction

*Soumi Chakraborty, Arpan Das and Swadhin K. Mandal**

Department of Chemical Sciences, Indian Institute of Science Education and Research-Kolkata, Mohanpur-741246, India.

*E-mail: swadhin.mandal@iiserkol.ac.in

Contents:

I. General considerations and instrumentations.

All catalytic and control reactions were performed under oxygen free atmosphere (Argon or nitrogen) using standard Schlenk techniques or inside a glovebox. All solvents used in the experiments were dried over sodium/benzophenone mixture or CaH_2 and distilled prior to use. All chemicals were purchased from Sigma-Aldrich or Merck or Alfa Aesar and used as received. Analytical thin layer chromatography (TLC) was performed on a Merck 60 F254 silica gel plate (0.25 mm thickness). Column chromatography was performed on Merck 60 silica gel (100-200 mesh). The ^{1}H and ^{13}C NMR spectra were recorded on JEOL ECS 400 MHz spectrometer and on a Bruker Avance III 500 MHz spectrometer in $CDCl_3$ or DMSO-d_6 or CD_3CN with residual undeuterated solvent (eg. $CDCl_3$, 7.26/77.0) as an internal standard. Chemical shifts (δ) are given in ppm, and J values are given in Hz. All chemical shifts were reported in ppm using tetramethylsilane as a reference. Chemical shifts (δ) downfield from the reference standard were assigned positive values. Evaporation of solvents was performed under reduced pressure using a rotary evaporator. All the glassware and NMR tubes used for experiments were kept in oven at 120 °C for overnight (12h). EPR spectroscopic measurements were performed in Bruker (X-band) spectrometer. X-ray crystallographic measurements were performed in Agilent X-ray diffractometer. GC-MS experiments were performed on a Perkin Elmer Clarus 590 gas chromatography using Clarus SQ 8 S mass spectrometer. Cyclic voltammetry was performed using CH instrument with glassy carbon and platinum wire electrodes, Ag/AgCl reference electrode, tetrabutylammonium perchlorate electrolyte, under N_2 atmosphere. Ester synthesis from corresponding carboxylic acid was performed following Fischer esterification process.[1] N,N,O-PLY (**1**) was synthesized following reported literature.[2]

II. Experimental Procedures.

*a) Synthetic Procedure **2**.*

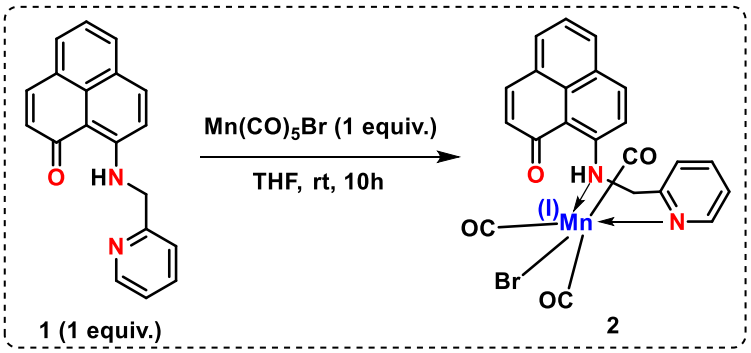

In a 50 mL Schlenk flask, N,N,O-PLY ligand (**1**) (0.3 g, 1.04 mmol) and $Mn(CO)_5Br$ (1 mmol) were taken in dry THF and stirred under nitrogen atmosphere in dark for 10 hours at room temperature. After completion, bright orange precipitate was observed in the reaction mixture. The solvent was decanted and the precipitate was washed with dry THF several times in aerobic atmosphere. Finally, the orange compound was dried over high vacuum and stored in dark. Crystals suitable for SC-XRD were grown from concentrated THF solution of the orange solid at room temperature in 3-4 days. The complex was characterized by X-ray diffraction, elemental analysis, NMR, IR and UV-vis spectroscopy. ^{1}H NMR (DMSO-d_6, rt, 400 MHz): 12.53 (s, 1H), 8.67 (d, 1H, J = 4Hz), 8.24 (d, 1H, J = 8Hz), 8.11-8.05 (m, 3H), 7.94-7.92 (m, 1H), 7.56-7.52 (m, 2H), 7.49-7.47 (m, 2H), 6.91 (d, 1H, J = 4Hz). ^{13}C{^{1}H} NMR (DMSO-d_6, rt, 500 MHz): 157.3, 157.2, 157.2, 155.7, 153.8, 149.2, 149.2, 146.1, 139.5, 139.0, 138.9, 132.4, 132.1, 128.9, 128.1, 125.0, 124.5, 123.3, 122.4, 120.9, 115.8, 67.5. IR (400-2000 cm^{-1}): 2909, 2818, 1989, 1898, 1607, 1573, 1464, 1344, 1253, 1230, 1190, 1179, 1093, 1053, 1008, 893, 836, 761, 676, 625, 533. Anal. calculated for $C_{26}H_{22}BrMnN_2O_5$: C, 54.09; H, 3.84; N 4.85. Found: C, 54.04; H, 3.84; N, 4.83. The molecular formula was calculated from crystallographically determined unit which contains lattice held THF molecule (used as crystallization solvent).

*b) Synthetic procedure of **3**.*

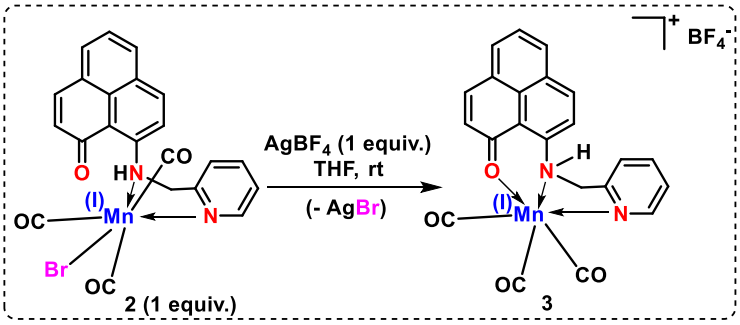

In a nitrogen filled glove box, compound **2** (120 mg, 0.24 mmol) and $AgBF_4$ (0.24 mmol) were taken in a 50 mL Schlenk flask in dry THF (6 mL). The flask was closed properly with glass stopper and stirred at room temperature for 4 hours. A sharp colour change from bright orange to dark red was clearly observed through the course of the reaction. After completion, the reaction mixture was allowed to settle down, when pale yellow precipitate was observed at the bottom of the flask. The reaction mixture was filtered through celite plug under nitrogen atmosphere and dried over high vacuum to get dark red solid compound. Red colored block shaped single crystals suitable to X-ray diffraction were grown from concentrated THF solution layered by ether (6:1 *v/v*) at room temperature under nitrogen atmosphere. The compound was finally characterized with X-ray diffraction, elemental analysis, HRMS and IR spectroscopy. IR (400-2000 cm^{-1}): 3212, 2933, 2013, 1898, 1607, 1556, 1515, 1482, 1424, 1350, 1242, 1008, 841, 796, 767, 681, 625, 568. HRMS calculated for $C_{22}H_{14}MnN_2O_4$ $[M]^+$: m/z 425.0329. Found: 425.0307. Anal. calculated for $C_{22}H_{14}BF_4MnN_2O_4$: C, 51.60; H, 2.76; N 5.47. Found: C, 51.55; H, 2.75; N, 5.43.

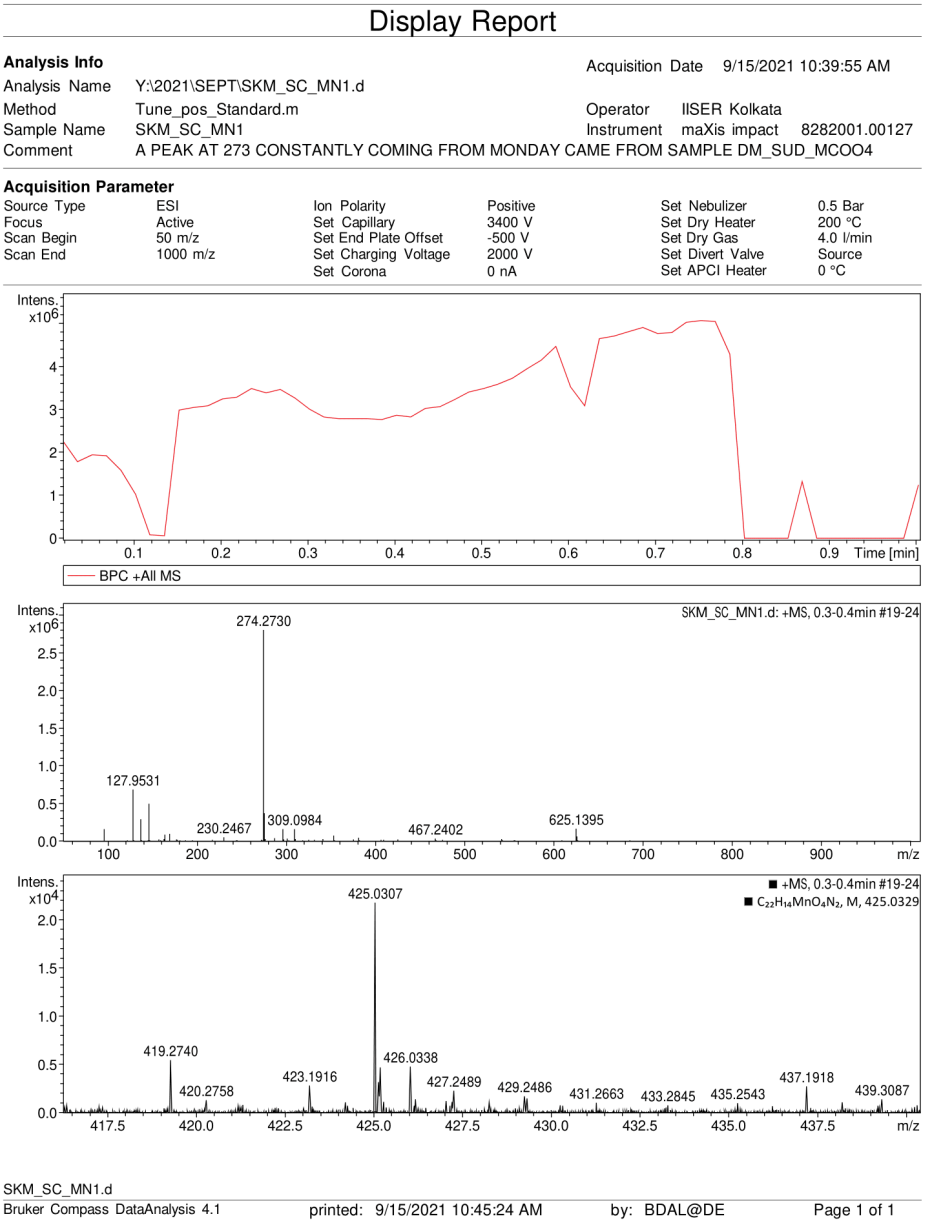

Fig. S1 HRMS spectrum of Mn(I) complex **3**.

*c) General Procedure for optimization of catalytic ester hydrosilylation using **3**.*

In a nitrogen filled glovebox, **3** (5 mol%) and potassium hydride (5 mol%) were taken in a pressure tube equipped with a stir bar. 800µL solvent was added to that and kept for stirring for 5 min. at room temperature. PMHS (2 equiv.) was added to it followed by addition of methyl-4-chlorobenzoate (1 equiv.). The tube was closed with a glass-stopper and kept for stirring at 50 ºC for 12 hours. After completion, the reaction mixture was exposed to air and

treated with MeOH (1 mL) and 1(M) NaOH solution (1 mL) and stirred at room temperature for an hour. 1,4-dimethoxybenzene was used as internal standard. The organic part was extracted in EtOAc and dried over rotary evaporator. Conversion of product was calculated from ^{1}H NMR spectroscopy with respect to the internal standard. Alcohol product was isolated through silica column with 15% EtOAc-hexane mixture and characterized by ^{1}H and ^{13}C NMR spectroscopy. By varying solvent, temperature and reductant, the reaction condition was optimized.

Table S1. Optimization of Reaction Condition for Ester Hydrosilylation Using **3** as a Catalyst.

Entry	**Cat. (mol%)**	**Reductant (mol%)**	**PMHS (equiv.)**	**Solvent**	**Temp. (^{o}C)**	**Conversion (yield) in %**
1	3 (5)	KH (5)	1	THF	50	48
2	**3 (5)**	**KH (5)**	**2**	**THF**	**50**	**99 (95)**
3	3 (5)	KH (5)	2	MeCN	50	92
4	-	KH (5)	2	THF	50	25
5	3 (5)	-	2	THF	50	-
6	3 (5)	KH (5)	2	THF	- (at RT)	-
7	3 (5)	KH (5)	2	THF	50	98 (performed in dark)
8	$AgBF_4$ (5)	KH (5)	2	THF	50	-
9	3 (5)	KH (5)	HMTS (2)	THF	50	94 (92)

*d) General Procedure for catalytic ester hydrosilylation using **3**.*

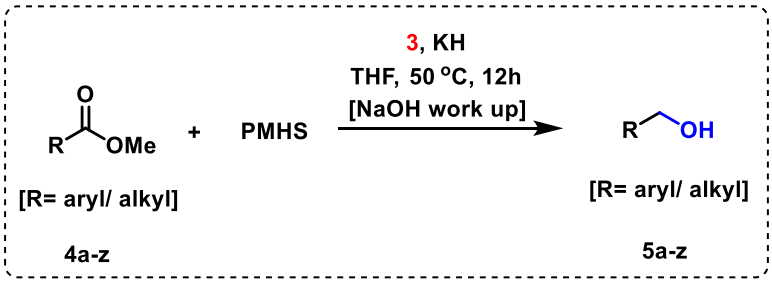

In a nitrogen filled glovebox, **3** (5 mol%) and potassium hydride (5 mol%) were taken in a pressure tube equipped with a stir bar. 800 µL THF was added to the reaction mixture and kept for stirring for 5 min. at room temperature. PMHS (2 equiv.) was added to it followed by addition of ester (1 equiv.). The tube was closed with a glass-stopper and kept for stirring at 50 °C for 8-12 hours. Following this, the reaction mixture was exposed to air and treated with MeOH (1 mL) and 1(M) NaOH solution (1 mL) and stirred at room temperature for an hour. The organic part was extracted in EtOAc and dried over a rotary evaporator. Alcohol products were isolated through silica column with 10-40% EtOAc-hexane mixture and characterized by ^{1}H and ^{13}C NMR spectroscopy.

e) Procedure for ester hydrosilylation in presence of radical scavengers.

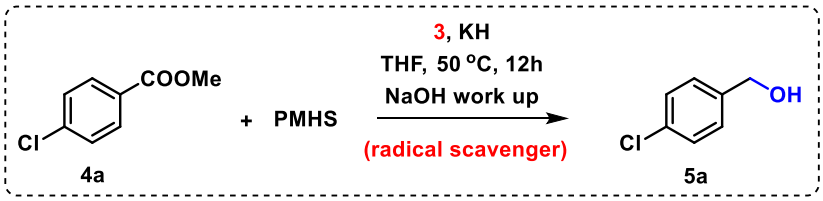

In a nitrogen filled glovebox, **3** (5 mol%) and potassium hydride (5 mol%) were taken in a pressure tube equipped with a stir bar. THF (800µL) was added to it and allowed to stir for 5 minutes at room temperature. PMHS (0.48 mmol) was added to it followed by addition of methyl-4-chlorobenzoate (0.24 mmol) and radical scavenger (0.48 mmol). The tube was closed properly with a glass-stopper and kept for stirring at 50 °C for 12 hours. After completion, the reaction mixture was treated with MeOH (1 mL) and 1(M) NaOH solution (1 mL) and stirred

at room temperature for an hour. 1,4-dimethoxybenzene was added to it as an internal standard. The organic part was extracted in EtOAc and dried over a rotary evaporator. Conversion of product was calculated from ^{1}H NMR spectroscopy with respect to the internal standard.

Table S2. Catalytic reaction in presence of radical scavenger.

Entry	**Radical Scavenger**	**Conversion**
1	TEMPO	No conversion
2	Galvinoxyl free radical	No conversion

*f) Synthesis procedure of **6**.*

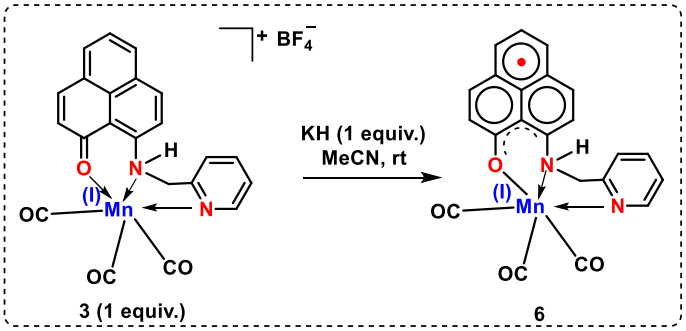

In a nitrogen filled glove box, **3** (120 mg, 0.24 mmol) was taken in a 50 mL Schlenk flask in acetonitrile (6 mL) and stirred at room temperature for 3-5 minutes to obtain a clear solution. Potassium hydride (0.24 mmol) was added to the solution and the reaction pot was closed properly with glass stopper and stirred at room temperature for 2 hours. A sharp colour change from deep red to dark green was observed within 30 minutes of the reaction. After completion, the reaction mixture was filtered through celite plug under nitrogen atmosphere and dried over high vacuum to get dark green solid compound, which was highly sensitive to air and moisture, and stored inside the glove box. The compound was characterized with HRMS and EPR spectroscopy (at 100K, in acetonitrile solution). HRMS calculated for $C_{22}H_{14}MnN_2O_4$ $[M]^+$: m/z 425.0329. Found: 425.0338.

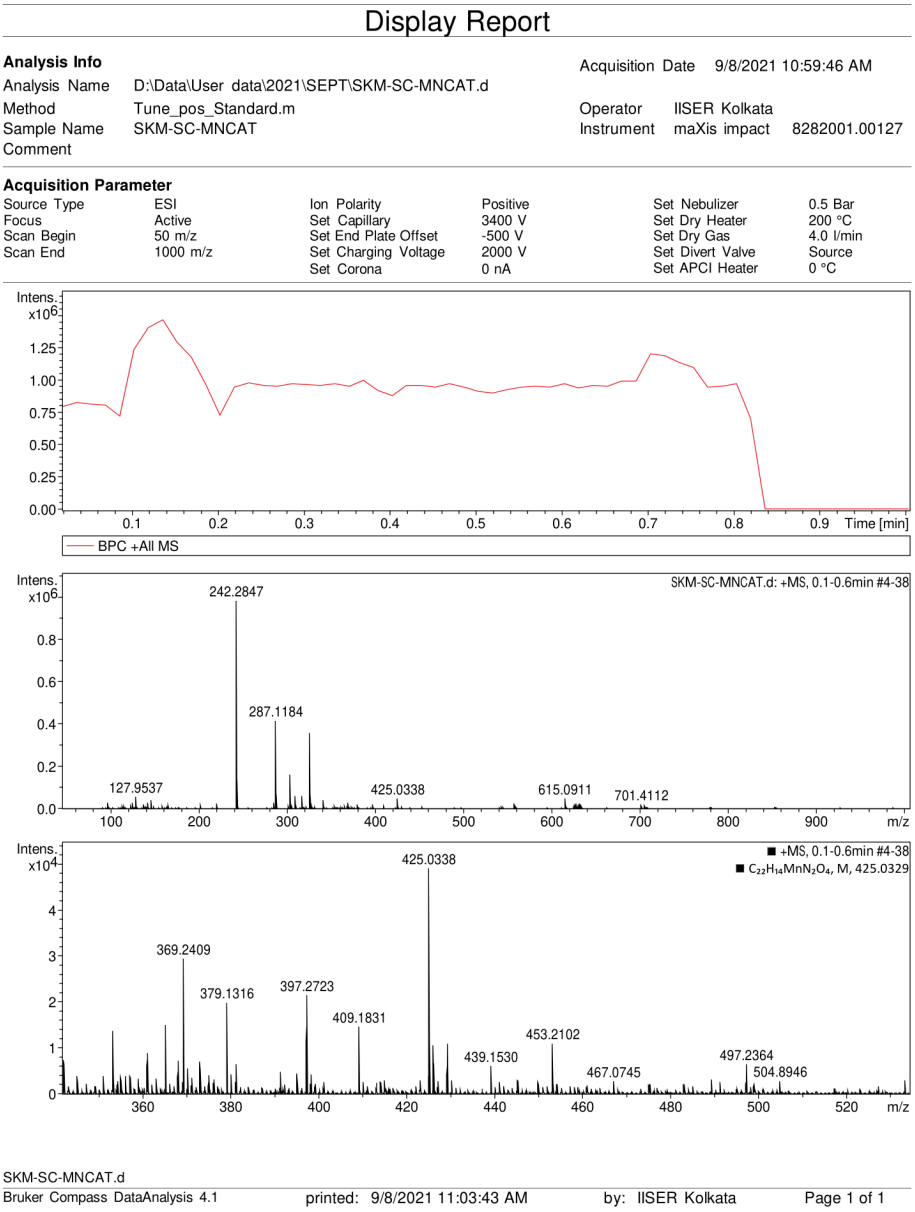

Fig. S2 HRMS spectrum of Mn(I) radical species **6**.

*g) Procedure for catalytic ester hydrosilylation with active catalyst **6**.*

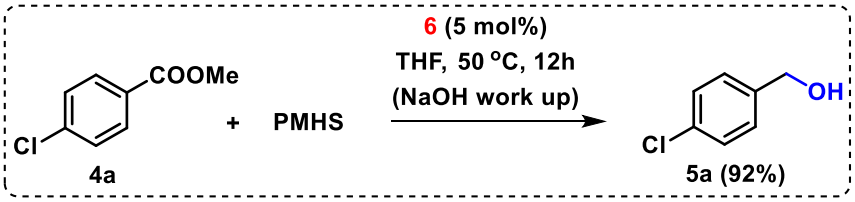

In a nitrogen filled glovebox, **6** (5 mol%) was taken in a pressure tube equipped with a stir bar followed by THF (800µL). PMHS (2 equiv.) was added to it followed by addition of methyl-

4-chlorobenzoate (1 equiv.). The tube was closed with a glass-stopper and kept for stirring at 50 °C for 12 hours. After completion, the reaction mixture was exposed to air and treated with MeOH (1 mL) and 1(M) NaOH solution (1 mL) and stirred at room temperature for an hour. The organic part was extracted in EtOAc and dried over a rotary evaporator. Product was isolated through silica column with 15% EtOAc-hexane mixture and characterized with NMR spectroscopy. Isolated yield of the product was reported by taking average yield of two results.

h) Procedure for characterization of TEMPO-trapped silyl radical intermediate (7).

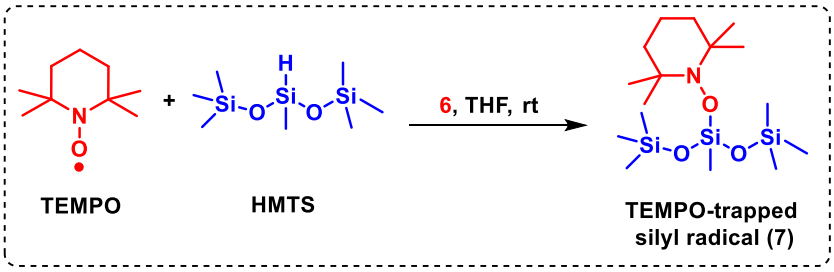

In a nitrogen filled glovebox, **6** (1 equiv.) was taken in a pressure tube equipped with a stir bar. 800 µL THF was added to that and kept for stirring for 5 minutes at room temperature. HMTS (1 equiv.) and TEMPO (1 equiv.) were added to it and continued to stir for 6 hours at room temperature. After completion, the reaction mixture was analyzed by HRMS to detect the TEMPO-trapped silyl radical species. HRMS calculated for $C_{16}H_{39}NO_3Si_3$ $[M+H]^+$: m/z 378.2311. Found: 378.2330.

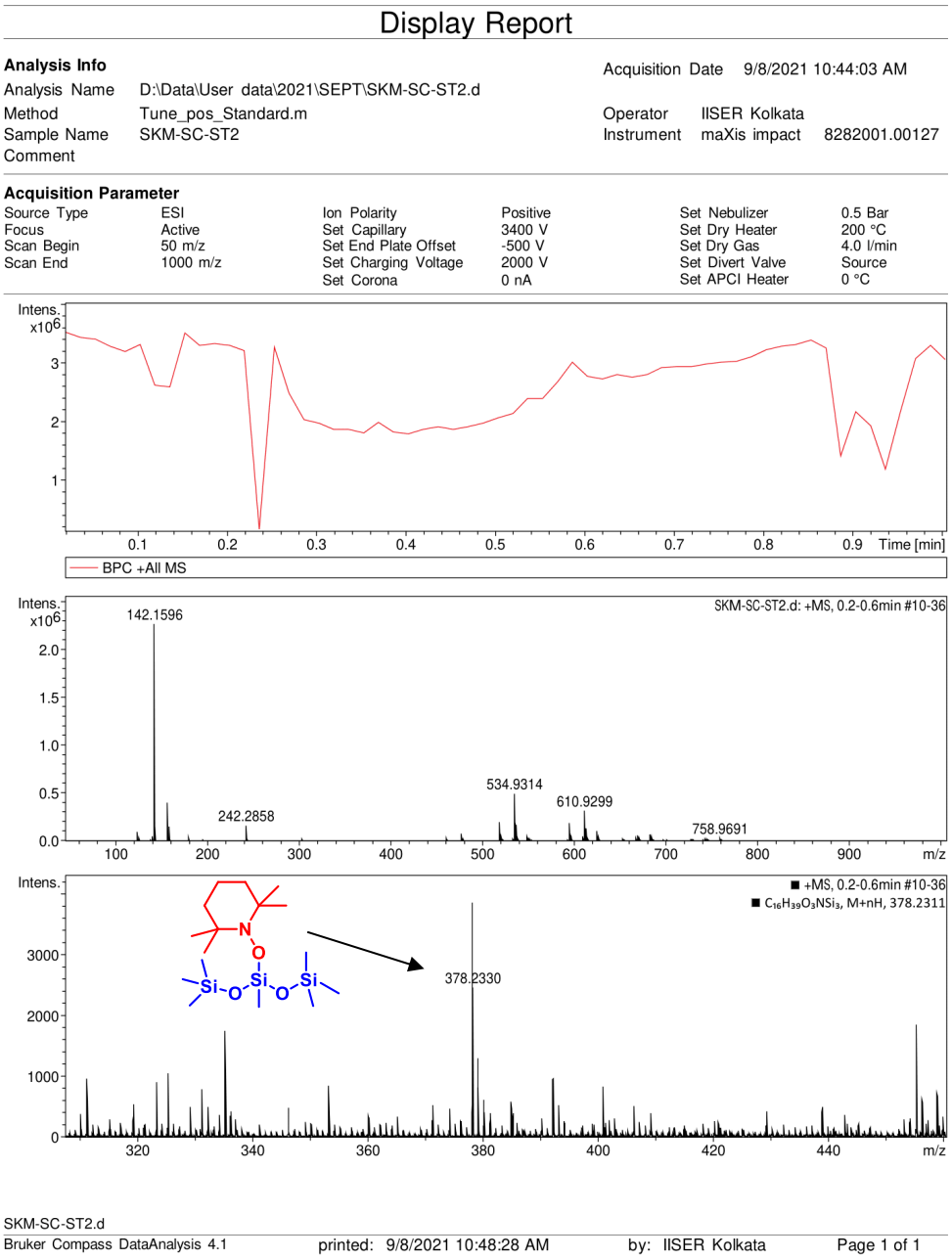

Fig. S3 HRMS spectrum of TEMPO-trapped silyl radical compound **7**.

*i) Procedure for characterization of [Mn(I)-H] species (**8**).*

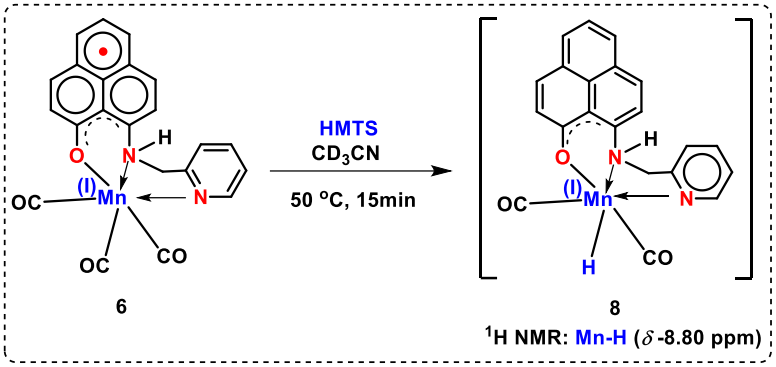

In a nitrogen filled glovebox, **6** (0.06 mmol) was taken in a screw cap NMR tube in 600 µL CD_3CN stirred by hand for a few minutes to get the green solution. HMTS (0.06 mmol) was added to the reaction mixture and the NMR tube was closed properly with a screw cap and tied with parafilm. The tube was heated at 50 °C for 15 minutes and analyzed with ^1H NMR spectroscopy. Singlet at δ -8.80 ppm confirms the presence of Mn(I)-H species in the reaction mixture.[3]

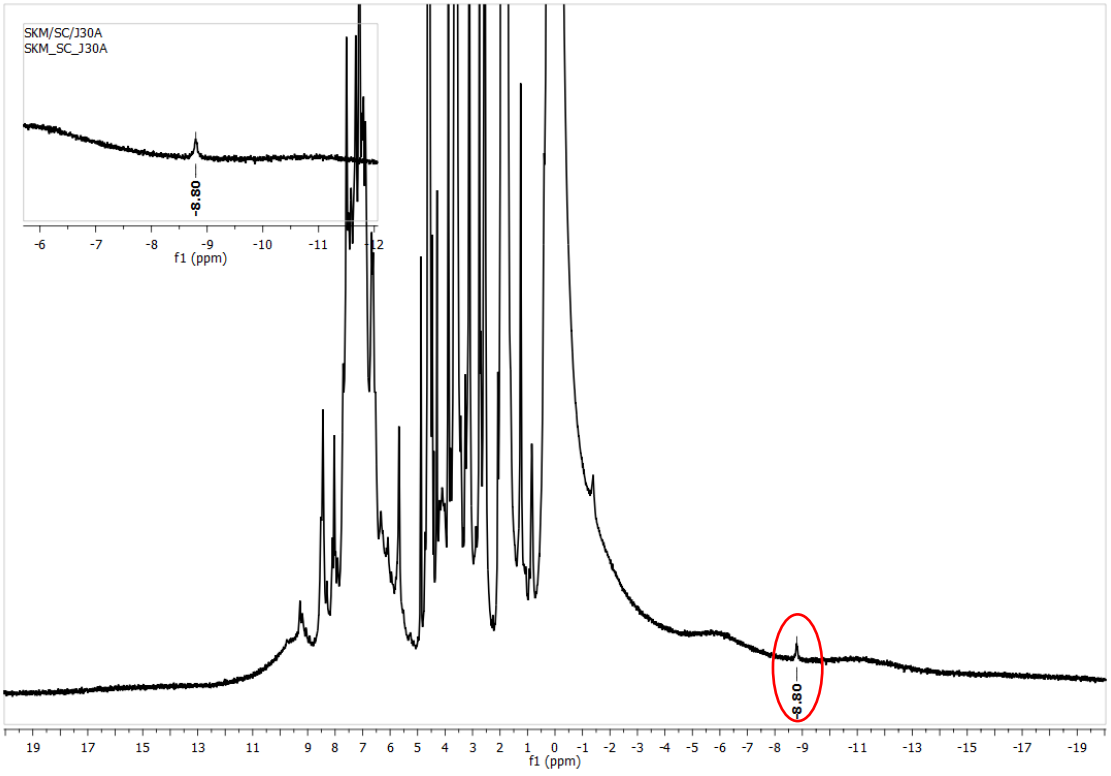

Fig. S4. ^1H NMR spectrum (CD_3CN, 400 MHz, rt) displaying the [Mn(I)-H] resonance at δ -8.80 ppm (**8**).

l) Procedure for characterization of silylated products.

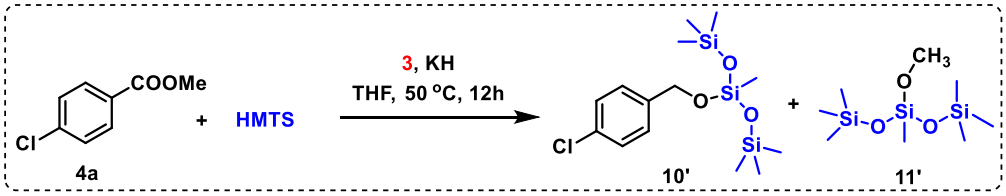

In a nitrogen filled glovebox, **3** (5 mol%) and a potassium hydride (5 mol%) were taken in a pressure tube equipped with a stir bar. 800µL THF was added to that and kept for stirring for 5 min. at room temperature. HMTS (2 equiv.) was added to it followed by addition of methyl-4-chlorobenzoate (1 equiv.). The tube was closed with a glass-stopper and kept for stirring at 50 °C for 12 hours. After completion, the reaction mixture was analyzed by GC-MS (in THF solution) technique. Formation of silylated product **10'** and side product **11'** were confirmed by the respective mass spectra. Further, to isolate the silylated product **10'**, the reaction mixture was passed through silica column with 30% EtOAc-hexane mixture. The eluent was dried over a rotary evaporator to get yellow oil type compound. The compound was characterized by ^{1}H ^{13}C and ^{29}Si NMR spectroscopy and HRMS to further confirm the formation of **10'**. HRMS calculated for $C_{14}H_{27}ClO_3Si_3$ $[M+H]^+$: m/z 362.1951. Found: 362.1938.

GC-MS Method applied for detection of silylated products.

GC Control

Instrument Name	: inst1	Injection	: AUTO	Inlet A	: PSSI
Experiment Time	: 28.00 min	Injection Volume	: 1.0 µL	Inlet B	: PKD
Delay Time	: 0.00 min	Sampling Rate	: 1.56250 pts/s	Detector A	: FID
Run Time	: 28.00 min	Channel	: NONE	Detector B	: TCD+R

Oven Temperature Program :
Initial Temperature : 50 deg for 2.00 min
Ramp 1 : 20.0 deg/min to 270 deg, hold for 15.00 min

Retention time plot.

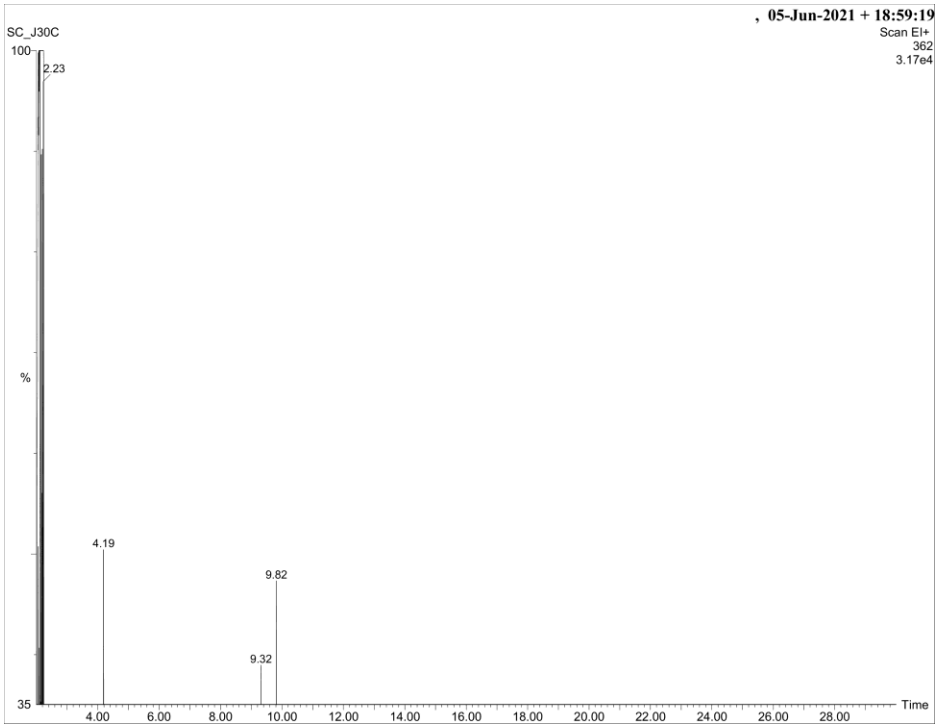

Fig. S5. Retention time plot for GC-MS.

Retention time- 4.19 minutes.

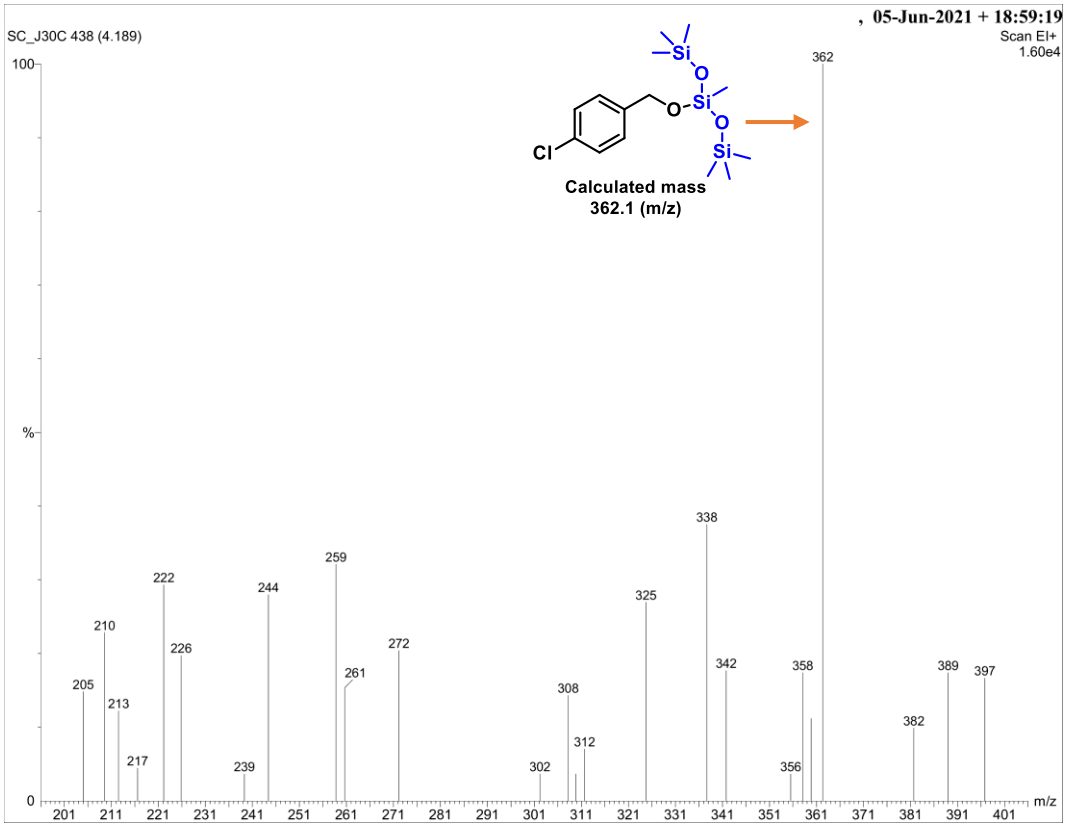

Retention time- 9.32 minutes

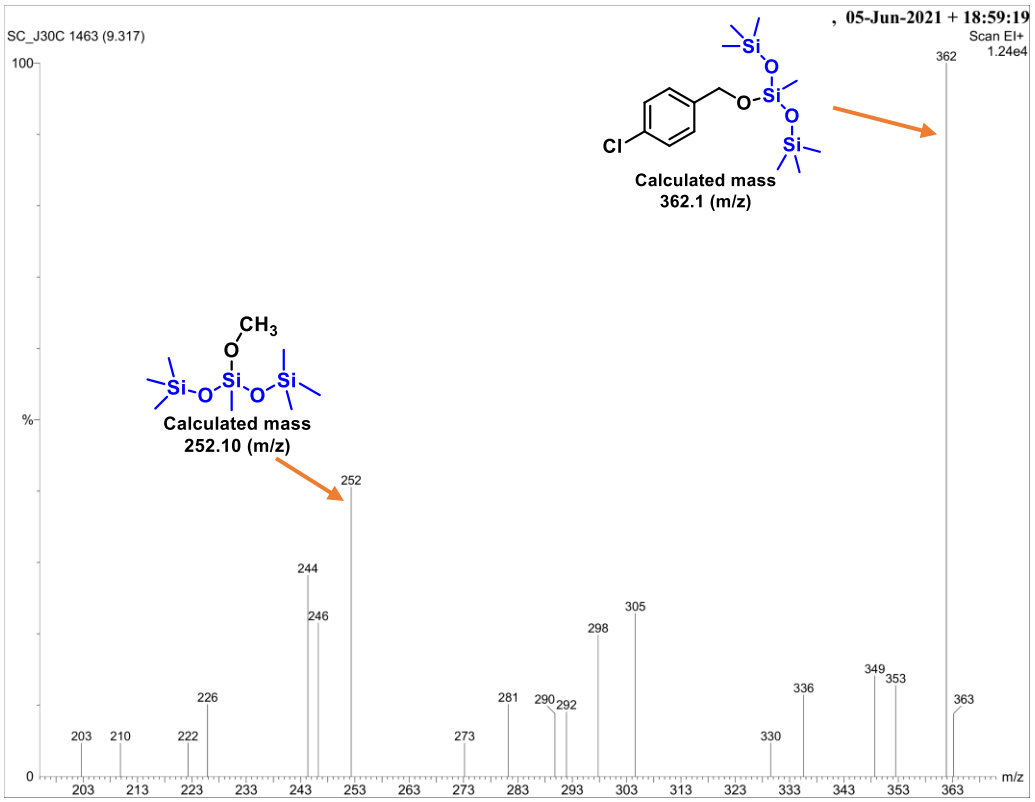

Retention time- 9.82 minutes

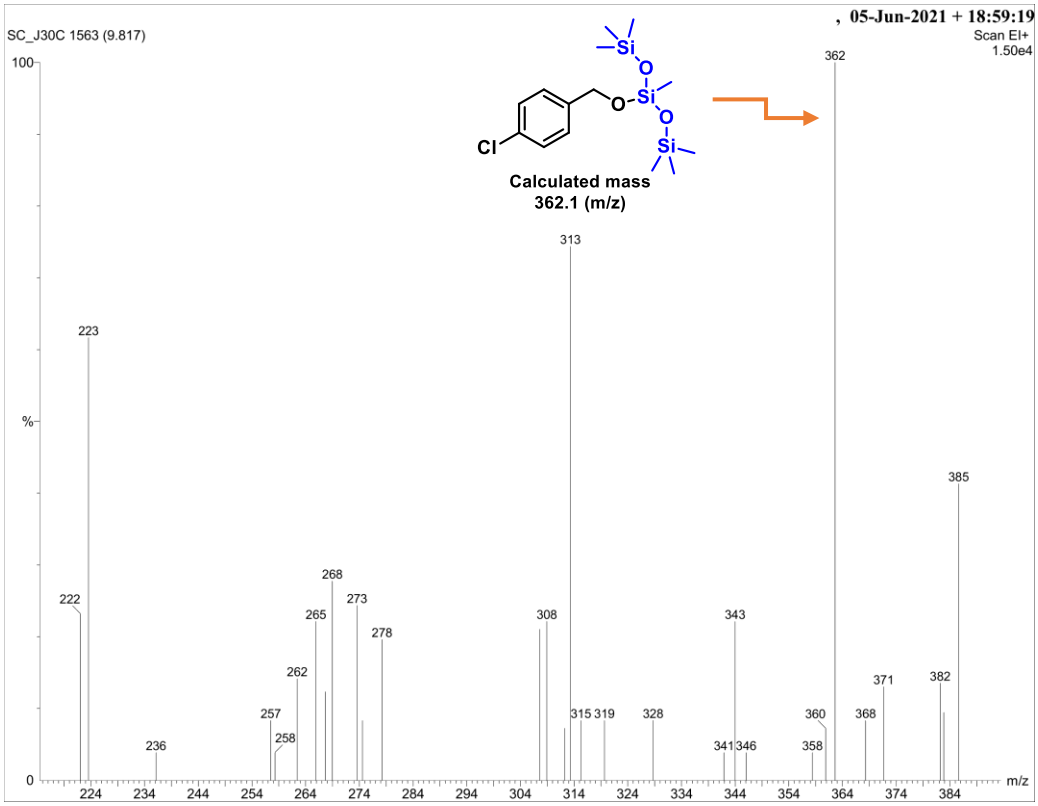

Fig. S6. Mass spectra for compound **10'** and **11'**.

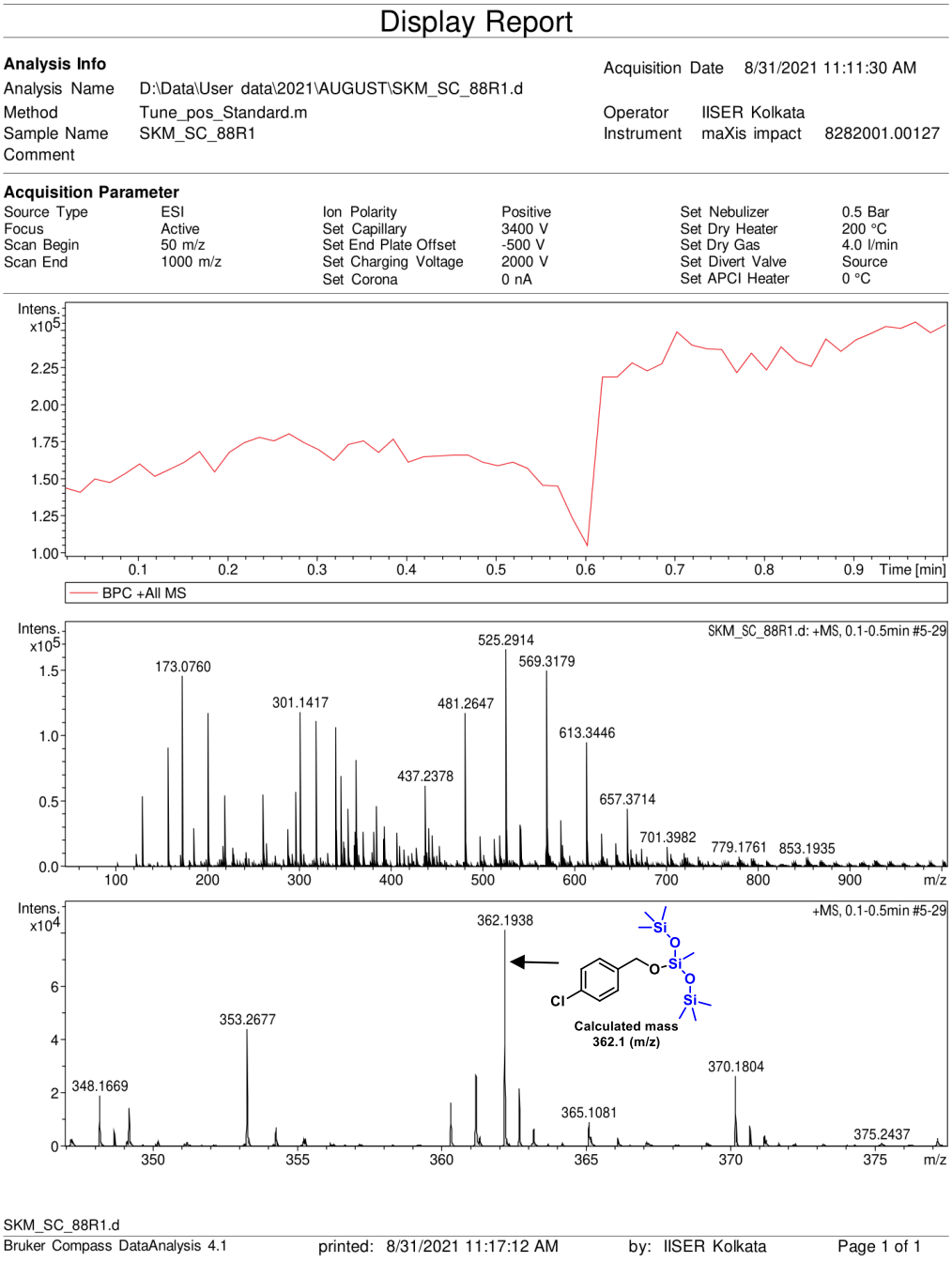

Fig. S7. HRMS spectrum for compound **10'**.

III. Electrochemical data.

Cyclic Voltammetry study.

Cyclic voltammetry was performed using a glassy carbon working electrode and a platinum wire counter electrode, Ag/AgCl reference electrode, tetrabutylammonium perchlorate electrolyte, under N_2 atmosphere in dry acetonitrile solvent.

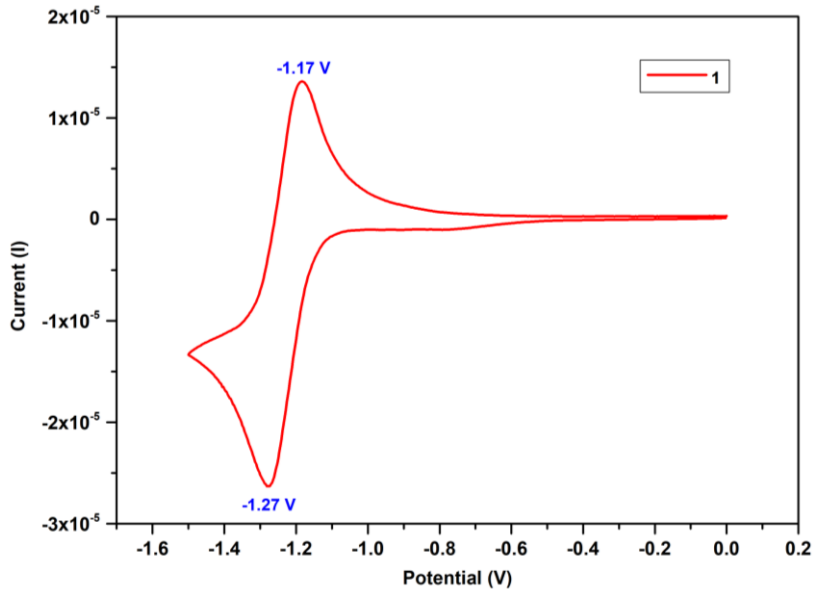

Fig. S8. Cyclic voltammogram of N,N,O-PLY (**1**) in acetonitrile.

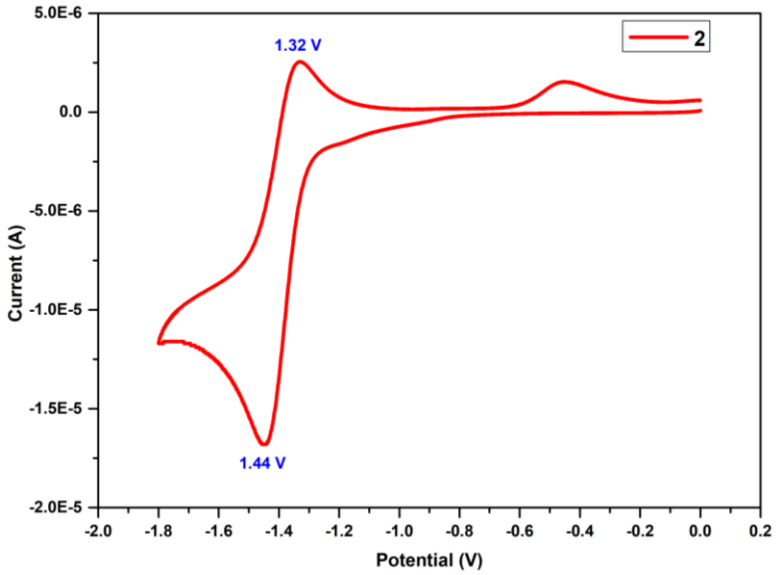

Fig. S9. Cyclic voltammogram of Mn(I)-complex (**2**) in acetonitrile.

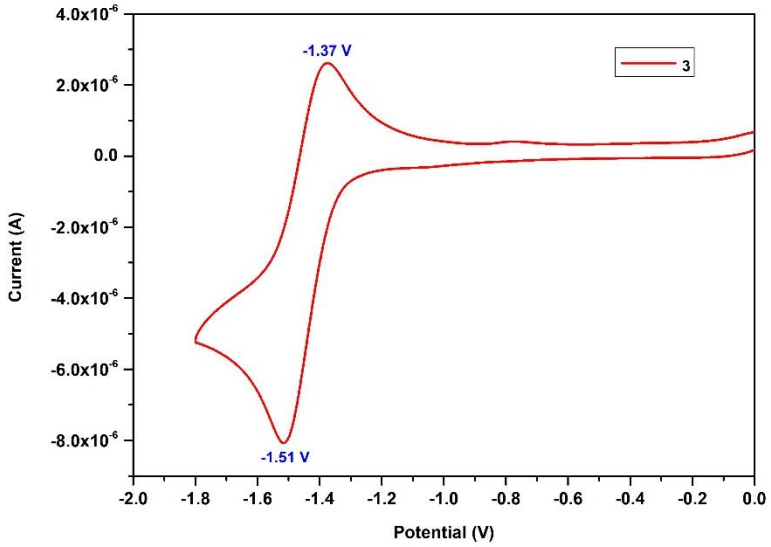

Fig. S10. Cyclic voltammogram of Mn(I)-complex (**3**) in acetonitrile.

IV. Spectroscopic characterization data of Mn-complex.

a) *NMR spectroscopy for characterization of **2**.*

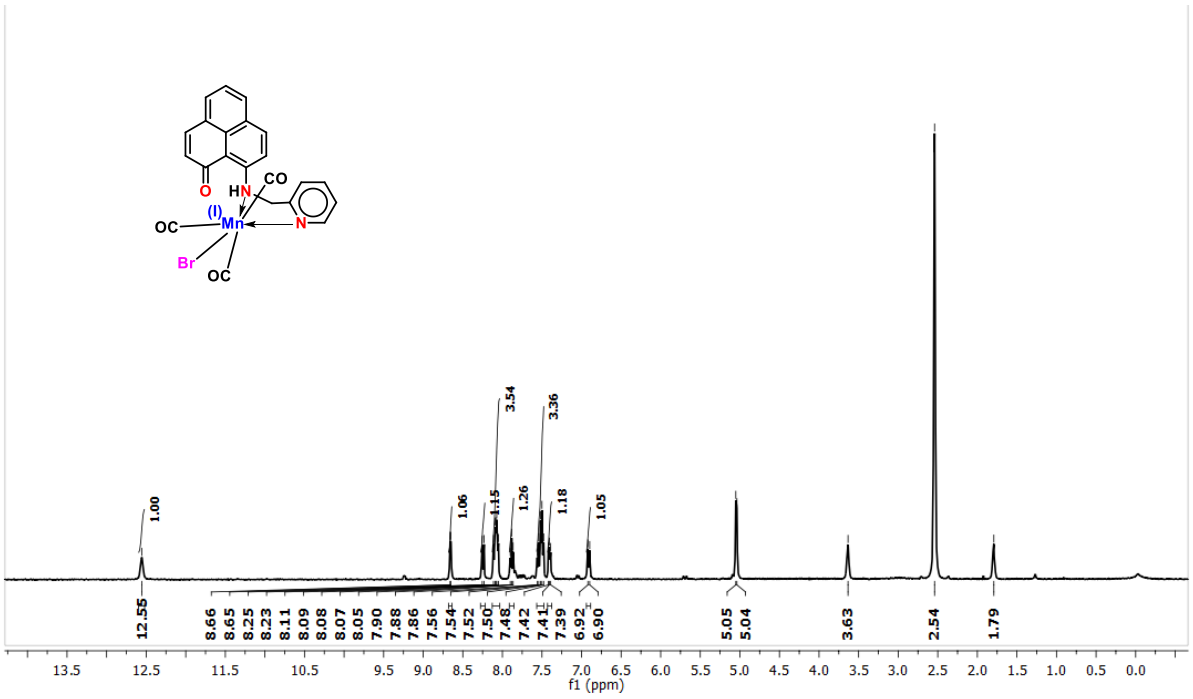

Fig. S11. ^{1}H NMR spectrum (DMSO-d_6, 400 MHz, rt) of **2**.

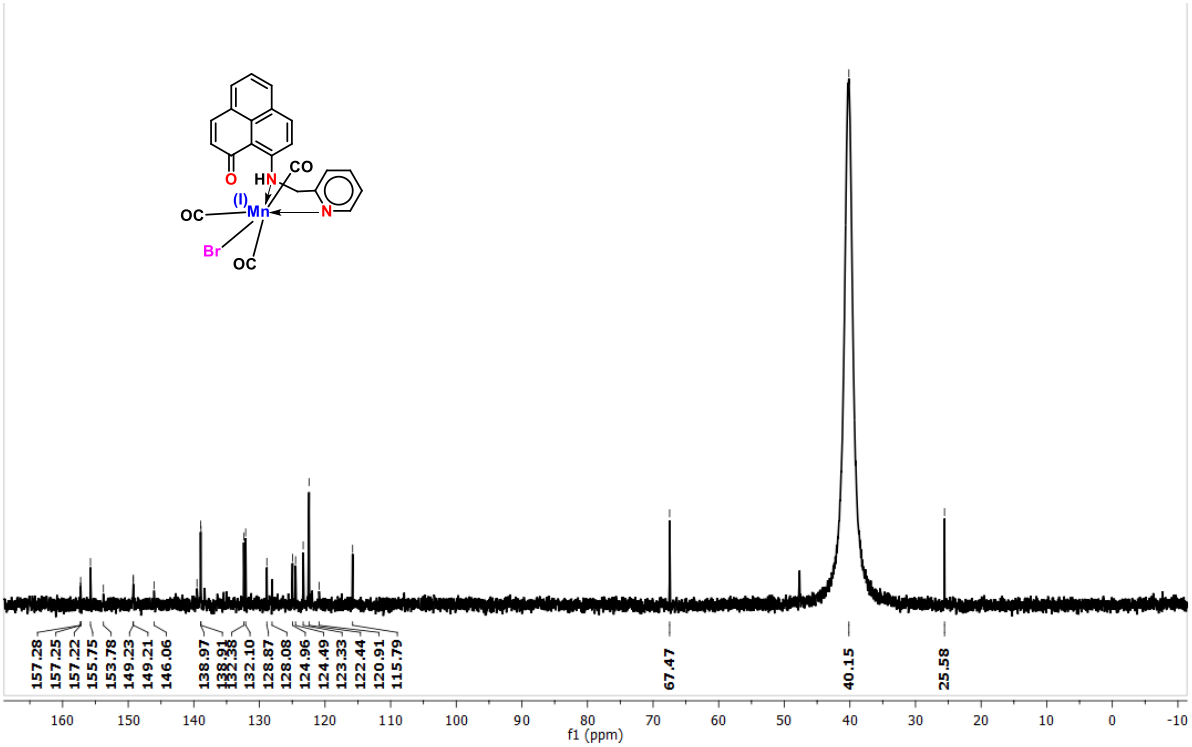

Fig. S12. $^{13}C\{^{1}H\}$ NMR spectrum (DMSO-d_6, 500 MHz, rt) of **2**.

b) EPR spectroscopy of ***6****.*

EPR spectrum of **6** was recorded in acetonitrile solution at 100K (in X-band), packed under N_2 atmosphere.

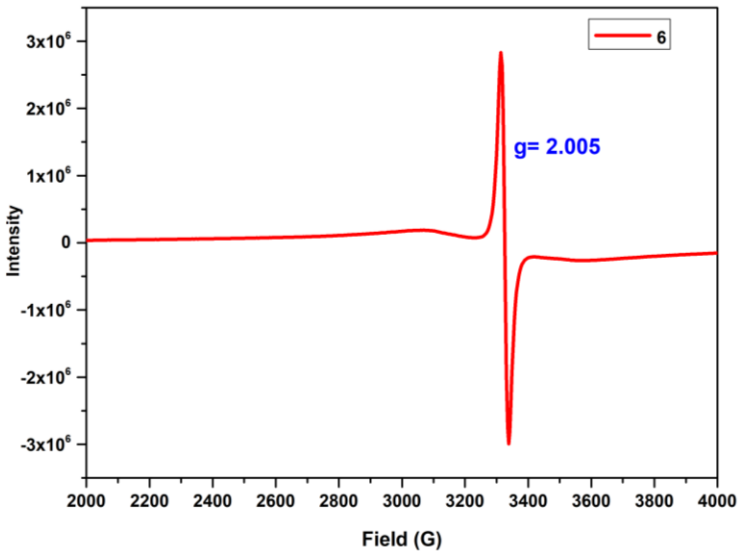

Fig. S13. EPR spectrum of Mn(I)-radical species **6** in acetonitrile solution at 100K.

b) *UV-Vis spectroscopy of **2**.*

UV-vis spectrum was recorded in dry acetonitrile solution at room temperature under nitrogen atmosphere.

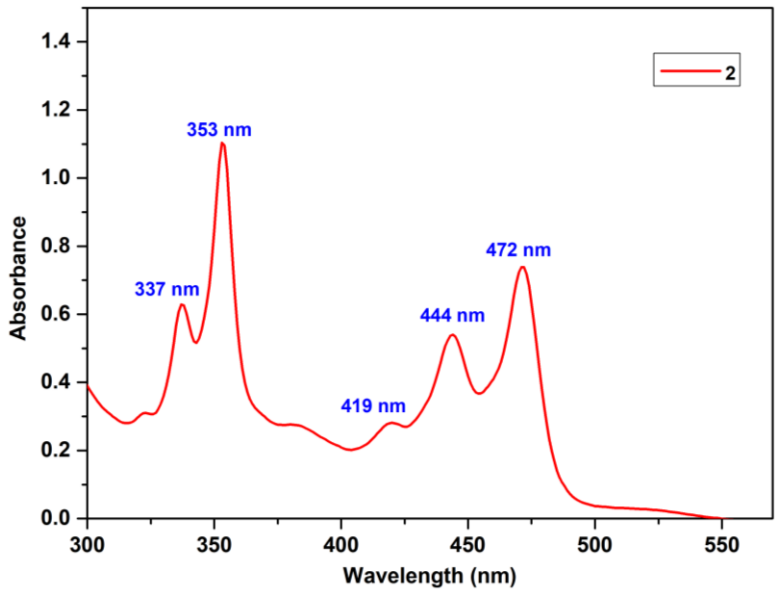

Fig. S14. UV-Vis spectrum of Mn(I)-N,N,O-PLY complex **2**.

V. Characterization data for alcohol products.

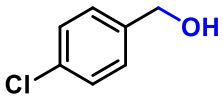

4-Chlorobenzyl alcohol (**5a**)[4]: Colorless liquid. Yield 95%. The crude product was purified by column chromatography using silica gel (100-200 mesh) with 15% of EtOAc in hexane.

^{1}H-NMR (400 MHz, $CDCl_3$, 298 K) δ (ppm) 7.32-7.26 (m, 4H), 4.64 (s, 2H), 2.02 (br. s, 1H).

$^{13}C\{^{1}H\}$ NMR (100 MHz, $CDCl_3$, 298 K) δ (ppm) 139.2, 133.3, 128.6, 128.2, 64.4.

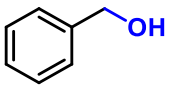

Benzyl alcohol (**5b**)[4]: Colorless liquid. Yield 92%. The crude product was purified by column chromatography using silica gel (100-200 mesh) with 15% of EtOAc in hexane.

^{1}H-NMR (400 MHz, $CDCl_3$, 298 K) δ (ppm) 7.33-7.27 (m, 5H), 4.65 (s, 2H), 2.19 (br. s, 1H).

$^{13}C\{^{1}H\}$ NMR (100 MHz, $CDCl_3$, 298 K) δ (ppm) 140.8, 128.4, 127.5, 126.9, 65.1.

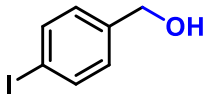

4-Iodobenzyl alcohol (**5c**)[5]: Pale white liquid. Yield 92%. The crude product was purified by column chromatography using silica gel (100-200 mesh) with 20% of EtOAc in hexane.

^{1}H-NMR (400 MHz, $CDCl_3$, 298 K) δ (ppm) 7.66 (d, 2H, J = 8Hz), 7.07 (d, 2H, J = 8Hz), 4.59 (s, 2H), 2.46 (br. s, 1H).

$^{13}C\{^{1}H\}$ NMR (100 MHz, $CDCl_3$, 298 K) δ (ppm) 140.4, 137.5, 128.8, 92.9, 64.4.

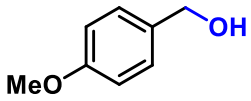

4-Methoxybenzyl alcohol (**5d**)[6]: Colorless liquid. Yield 90%. The crude product was purified by column chromatography using silica gel (100-200 mesh) with 20% of EtOAc in hexane.

^{1}H-NMR (400 MHz, $CDCl_3$, 298 K) δ (ppm) 7.27 (d, 2H, J = 8Hz), 6.87 (d, 2H, J = 8Hz), 4.59 (s, 2H), 3.79 (s, 3H), 2.06 (br. s, 1H).

$^{13}C\{^{1}H\}$ NMR (100 MHz, $CDCl_3$, 298 K) δ (ppm) 159.2, 133.1, 128.6, 113.9, 65.0, 55.3.

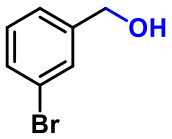

3-Bromobenzyl alcohol (**5e**)[7]: Colorless liquid. Yield 90%. The crude product was purified by column chromatography using silica gel (100-200 mesh) with 20% of EtOAc in hexane.

^{1}H-NMR (400 MHz, $CDCl_3$, 298 K) δ (ppm) 7.41 (s, 1H), 7.32 (d, 1H, J = 8Hz), 7.17-7.10 (m, 2H), 4,52 (s, 2H).

$^{13}C\{^{1}H\}$ NMR (100 MHz, $CDCl_3$, 298 K) δ (ppm) 143.0, 130.5, 130.0, 129.8, 125.3, 122.5, 64.1.

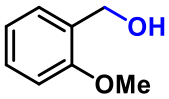

2-Methoxybenzyl alcohol (**5f**)[4]: Colorless liquid. Yield 85%. The crude product was purified by column chromatography using silica gel (100-200 mesh) with 20% of EtOAc in hexane.

^{1}H-NMR (400 MHz, $CDCl_3$, 298 K) δ (ppm) 7.30-7.26 (m, 2H), 6.97-6.93 (t, 1H, J_1 = 8Hz, J_2 = 8Hz), 6.89 (d, 1H, J = 4Hz), 4.68 (s, 2H), 3.87 (s, 3H).

$^{13}C\{^{1}H\}$ NMR (100 MHz, $CDCl_3$, 298 K) δ (ppm) 157.4, 129.0, 128.9, 128.7, 120.6, 110.2, 62.1, 55.2.

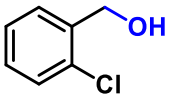

2-Chlorobenzyl alcohol (**5g**)[8]: Colorless liquid. Yield 88%. The crude product was purified by column chromatography using silica gel (100-200 mesh) with 20% of EtOAc in hexane.

^{1}H-NMR (400 MHz, $CDCl_3$, 298 K) δ (ppm) 7.46-7.34 (m, 2H), 7.26-7.22 (m, 2H), 4.74 (s, 2H), 2.94 (br. s, 1H)

$^{13}C\{^{1}H\}$ NMR (100 MHz, $CDCl_3$, 298 K) δ (ppm) 138.1, 132.5, 129.2, 128.6, 128.5, 126.9, 62.4.

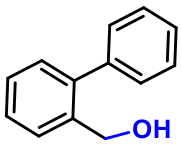

2-Phenylbenzyl alcohol (**5h**)[9]: Colorless liquid. Yield 80%. The crude product was purified by column chromatography using silica gel (100-200 mesh) with 20% of EtOAc in hexane.

^{1}H-NMR (400 MHz, $CDCl_3$, 298 K) δ (ppm) 7.55-7.57 (dd, 1H), 7.44-7.37 (m, 7H), 7.31-7.28 (m, 1H), 4.62 (s, 2H).

$^{13}C\{^{1}H\}$ NMR (100 MHz, $CDCl_3$, 298 K) δ (ppm) 141.3, 140.6, 138.0, 130.0, 129.1, 128.4, 128.2, 127.7, 127.6, 127.2, 63.1.

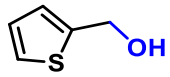

2-Thiophenemethanol (**5i**)[10]: Colorless liquid. Yield 81%. The crude product was purified by column chromatography using silica gel (100-200 mesh) with 20% of EtOAc in hexane.

^{1}H-NMR (400 MHz, $CDCl_3$, 298 K) δ (ppm) 7.29-7.26 (m, 1H), 7.01-7.00 (m, 1H), 6.99-6.97 (m, 1H), 4.81 (s, 2H).

$^{13}C\{^{1}H\}$ NMR (100 MHz, $CDCl_3$, 298 K) δ (ppm) 143.9, 126.8, 125.5, 125.4, 59.9.

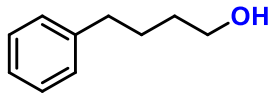

4-Phenyl-1-butanol (**5j**)[11]: Colorless liquid. Yield 70%. The crude product was purified by column chromatography using silica gel (100-200 mesh) with 20% of EtOAc in hexane.

^{1}H-NMR (400 MHz, $CDCl_3$, 298 K) δ (ppm) 7.30-7.28 (m, 2H), 7.19-7.18 (m, 3H), 3.65 (m, 2H), 2.64-2.63 (m, 2H), 1.69-1.61 (m, 4H).

$^{13}C\{^{1}H\}$ NMR (100 MHz, $CDCl_3$, 298 K) δ (ppm) 142.3, 128.4, 128.2, 125.7, 62.7, 35.6, 32.2, 27.5.

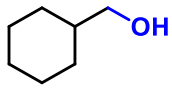

Cyclohexane-1-methanol (**5k**)[4]: Colorless liquid. Yield 95%. The crude product was purified by column chromatography using silica gel (100-200 mesh) with 20% of EtOAc in hexane.

^{1}H-NMR (400 MHz, $CDCl_3$, 298 K) δ (ppm) 3.40 (s, 2H), 1.71-1.64 (m, 5H), 1.45 (br. s, 1H), 1.23-1.12 (m, 4H), 0.94-0.86 (m, 2H).

^{13}C{^{1}H} NMR (100 MHz, $CDCl_3$, 298 K) δ (ppm) 68.6, 40.4, 29.5, 26.5, 25.8.

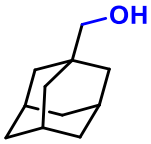

Adamentane-1-methanol (**5l**): Pale white solid. Yield 85%. The crude product was purified by column chromatography using silica gel (100-200 mesh) with 20% of EtOAc in hexane.

^{1}H-NMR (400 MHz, $CDCl_3$, 298 K) δ (ppm) 3.18 (s, 2H), 1.97 (br. s, 1H), 1.70-1.62 (m, 7H), 1.50-1.49 (m, 5H).

^{13}C{^{1}H} NMR (100 MHz, $CDCl_3$, 298 K) δ (ppm) 73.8, 39.0, 37.1, 34.4, 28.1.

HRMS calculated for $C_{11}H_{18}ONa$ [M + Na]+ 189.1301, found 189.1300.

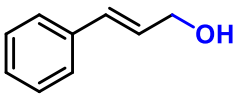

Cinnamyl alcohol (**5m**)[12]: Colorless oil. Yield 85%. The crude product was purified by column chromatography using silica gel (100-200 mesh) with 20% of EtOAc in hexane.

^{1}H-NMR (400 MHz, $CDCl_3$, 298 K) δ (ppm) 7.39-7.37 (m, 2H), 7.33-7.29 (m, 2H), 7.26-7.24 (m, 1H), 6.62-6.58 (d, 1H, J = 16 Hz), 6.38-6.32 (m, 1H), 4.30 (d, 2H, J = 8 Hz).

^{13}C{^{1}H} NMR (100 MHz, $CDCl_3$, 298 K) δ (ppm) 136.6, 131.0, 128.5, 128.4, 127.6, 126.4, 63.5.

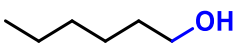

1-Hexanol (**5n**)[4]: Colorless liquid. Yield 75%. The crude product was purified by column chromatography using silica gel (100-200 mesh) with 30% of EtOAc in hexane.

^{1}H-NMR (400 MHz, $CDCl_3$, 298 K) δ (ppm) 3.70-3.57 (t, 2H), 1.56 (br. m, 2H), 1.41-1.25 (m, 6H), 0.97-0.89 (m, 3H).

$^{13}C\{^{1}H\}$ NMR (100 MHz, $CDCl_3$, 298 K) δ (ppm) 63.1, 32.7, 31.6, 25.4, 22.6, 14.0.

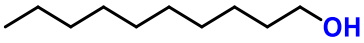

Capric alcohol or 1-decanol (**5o**)[6]: Pale yellow oil. Yield 84%. The crude product was purified by column chromatography using silica gel (100-200 mesh) with 30% of EtOAc in hexane.

^{1}H-NMR (400 MHz, $CDCl_3$, 298 K) δ (ppm) 3.62-3.59 (t, 2H, J_1= 4Hz, J_2= 8Hz), 1.56-1.52 (t, 2H, J_1= 8Hz, J_2= 8Hz), 1.25 (m, 14H), 0.88-0.84 (t, 3H, J_1= 8Hz, J_2= 8Hz).

$^{13}C\{^{1}H\}$ NMR (100 MHz, $CDCl_3$, 298 K) δ (ppm) 62.9, 32.7, 31.8, 29.6, 29.5, 29.4, 29.3, 25.7, 22.6, 14.0.

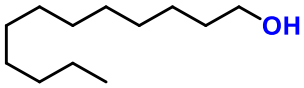

Lauryl alcohol or 1-dodecanol (**5p**)[6]: Pale yellow oil. Yield 88%. The crude product was purified by column chromatography using silica gel (100-200 mesh) with 30% of EtOAc in hexane.

^{1}H-NMR (400 MHz, $CDCl_3$, 298 K) δ (ppm) 3.61-3.58 (t, 2H, J_1= 4Hz, J_2= 8Hz), 1.53-1.52 (m, 2H) 1.39-1.24 (m, 18H), 0.87-0.84 (t, 3H, J_1= 8Hz, J_2= 4Hz).

$^{13}C\{^{1}H\}$ NMR (100 MHz, $CDCl_3$, 298 K) δ (ppm) 62.9, 32.7, 31.9, 29.6, 29.6, 29.6, 29.6, 29.4, 29.3, 25.7, 22.6, 14.0.

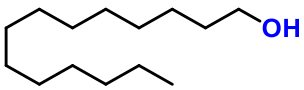

Myristyl alcohol or 1-tetradecanol (**5q**)[6]: Pale white solid. Yield 85%. The crude product was purified by column chromatography using silica gel (100-200 mesh) with 30% of EtOAc in hexane.

^{1}H-NMR (400 MHz, $CDCl_3$, 298 K) δ (ppm) 3.64-3.61 (t, 2H, J_1= 4Hz, J_2= 8Hz), 1.55-1.52 (m, 2H) 1.33-1.25 (m, 22H), 0.89-0.85 (t, 3H, J_1= 8Hz, J_2= 8Hz).

^{13}C{^{1}H} NMR (100 MHz, $CDCl_3$, 298 K) δ (ppm) 63.0, 32.8, 31.9, 29.6, 29.6, 29.6, 29.6, 29.5, 29.4, 29.3, 29.3, 25.7, 22.7, 14.1.

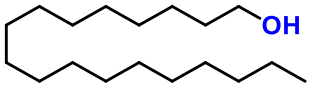

Steryl alcohol or 1-octaecanol (**5r**): Pale yellow solid. Yield 85%. The crude product was purified by column chromatography using silica gel (100-200 mesh) with 30% of EtOAc in hexane.

^{1}H-NMR (400 MHz, $CDCl_3$, 298 K) δ (ppm) 3.63-3.60 (t, 2H, J_1= 12Hz, J_2= 4Hz), 1.70 (br. s, 1H), 1.58-1.51 (m, 2H) 1.32-1.20 (m, 30H), 0.88-0.85 (t, 3H, J_1= 4Hz, J_2= 8Hz).

^{13}C{^{1}H} NMR (100 MHz, $CDCl_3$, 298 K) δ (ppm) 63.0, 32.8, 31.9, 29.7, 29.6, 29.6, 29.6, 29.4, 29.3, 25.7, 22.7, 14.1.

HRMS calculated for $C_{18}H_{38}ONa$ [M + Na]+ 293.2886, found 293.1884.

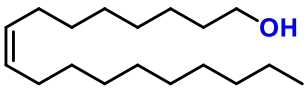

Oleyl alcohol (**5t**)[6]: Pale yellow oil. Yield 88%. The crude product was purified by column chromatography using silica gel (100-200 mesh) with 30% of EtOAc in hexane.

^{1}H-NMR (400 MHz, $CDCl_3$, 298 K) δ (ppm) 5.35-5.32 (m, 2H), 3.63-3.60 (t, 2H J_1= 4Hz, J_2= 8Hz), 2.01-1.99 (m, 4H), 1.57-1.53 (m, 2H), 1.29-1.24 (m, 21H), 0.89-0.85 (m, 3H).

^{13}C{^{1}H} NMR (100 MHz, $CDCl_3$, 298 K) δ (ppm) 129.9, 129.8, 127.9, 62.9, 32.7, 31.9, 29.7, 29.7, 29.6, 29.5, 29.4, 29.3, 29.2, 27.2, 25.7, 25.6, 22.6, 14.1.

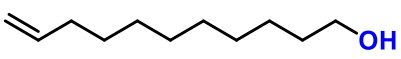

1-Undecylenic alcohol (**5u**)[6]: Colorless oil. Yield 86%. The crude product was purified by column chromatography using silica gel (100-200 mesh) with 30% of EtOAc in hexane.

^{1}H-NMR (400 MHz, $CDCl_3$, 298 K) δ (ppm) 5.79-5.75 (m, 1H), 4.99-4.89 (m, 2H), 3.61-3.58 (t, 2H, J_1= 4Hz, J_2= 8Hz), 2.02-2.01 (m, 2H), 1.53-1.52 (m, 2H), 1.26-1.15 (m, 13H).

^{13}C{^{1}H} NMR (100 MHz, $CDCl_3$, 298 K) δ (ppm) 139.1, 114.0, 62.8, 33.7, 32.7, 29.5, 29.4, 29.3, 29.0, 28.8, 25.7.

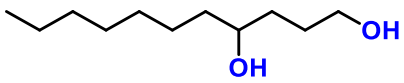

1,4-Undecandiol (**5v**): Pale white oil. Yield 88%. The crude product was purified by column chromatography using silica gel (100-200 mesh) with 30% of EtOAc in hexane.

^{1}H-NMR (400 MHz, $CDCl_3$, 298 K) δ (ppm) 3.64-3.58 (m, 3H), 3.31 (br. s., 1H), 2.50 (br. s, 1H), 1.67-1.64 (m, 2H), 1.43-1.41 (m, 4H), 1.26 (m, 10H), 0.88-0.84 (m, 3H).

^{13}C{^{1}H} NMR (100 MHz, $CDCl_3$, 298 K) δ (ppm) 71.8, 62.8, 37.5, 34.3, 31.8, 29.6, 29.3, 29.0, 25.7, 22.6, 14.0.

HRMS calculated for $C_{11}H_{24}O_2Na$ [M + Na]+ 211.1718, found 211.1721.

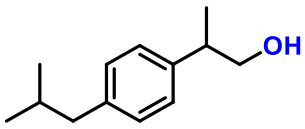

2-(4-isobutylphenyl)propan-1-ol (**5w**)[13]: Pale yellow oil. Yield 84%. The crude product was purified by column chromatography using silica gel (100-200 mesh) with 30% of EtOAc in hexane.

^{1}H-NMR (400 MHz, $CDCl_3$, 298 K) δ (ppm) 7.15-7.10 (m, 4H), 3.69 (d, 2H, J= 8Hz), 2.97-2.88 (sextette, 1H), 2.45 (d, 2H, J= 8Hz), 1.88-1.82 (m, 1H), 1.36 (br. s, 1H), 1.27 (d, 3H, J= 8Hz), 0.90 (d, 6H, J= 4Hz).

^{13}C{^{1}H} NMR (100 MHz, $CDCl_3$, 298 K) δ (ppm) 140.7, 140.1, 129.4, 127.1, 68.8, 45.0, 42.0, 30.2, 22.4, 17.6.

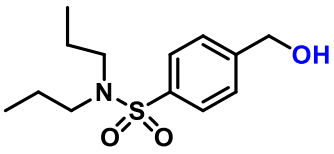

4-(hydroxymethyl)-N,N-dipropylbenzenesulfonamide (**5x**)[14]: Pale yellow oil. Yield 90%. The crude product was purified by column chromatography using silica gel (100-200 mesh) with 30% of EtOAc in hexane.

^{1}H-NMR (400 MHz, $CDCl_3$, 298 K) δ (ppm) 7.66 (d, 2H, J= 8Hz), 7.41 (d, 2H, J= 8Hz), 4.70 (s, 2H), 3.03-2.99 (dt, 4H, J_d = 2Hz, J_t = 4Hz), 1.53-1.47 (m, 4H), 0.85-0.81 (dt, 6H, J_d = 2Hz, J_t = 4Hz).

^{13}C{^{1}H} NMR (100 MHz, $CDCl_3$, 298 K) δ (ppm) 145.8, 138.5, 127.0, 126.8, 63.9, 49.9, 21.9, 11.1.

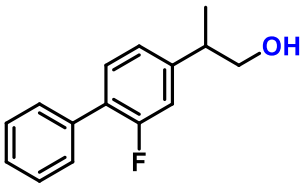

2-(2-fluoro-[1,1'-biphenyl]-4-yl)propan-1-ol (**5y**)[15]: Pale yellow oil. Yield 82%. The crude product was purified by column chromatography using silica gel (100-200 mesh) with 30% of EtOAc in hexane.

^{1}H-NMR (400 MHz, $CDCl_3$, 298 K) δ (ppm) 7.56-7.54 (m, 2H), 7.47-7.35 (m, 4H), 7.12-7.04 (m, 2H), 3.75 (d, 2H, J= 8Hz), 3.03-2.98 (m, 1H), 1.31 (d, 3H, J= 4Hz).

^{13}C{^{1}H} NMR (100 MHz, $CDCl_3$, 298 K) δ (ppm) 160.8, 158.8, 145.5, 145.4, 130.7, 130.7, 128.9, 128.8, 128.4, 127.5, 123.5, 123.4, 115.0, 114.8, 68.3, 41.9, 17.4.

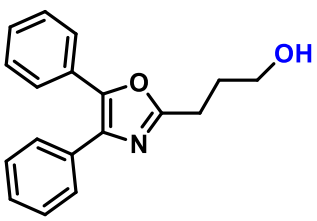

3-(4,5-diphenyloxazol-2-yl)propan-1-ol (**5z**)[14]: Pale yellow oil. Yield 85%. The crude product was purified by column chromatography using silica gel (100-200 mesh) with 30% of EtOAc in hexane.

^{1}H-NMR (400 MHz, $CDCl_3$, 298 K) δ (ppm) 7.62-7.60 (m, 2H), 7.57-7.55 (m, 2H), 7.35-7.30 (m, 5H), 3.79-3.76 (t, 2H, J_1= 8Hz, J_2= 4Hz), 3.00-2.96 (t, 2H, J_1= 8Hz, J_2= 8Hz), 2.12-2.06 (m, 2H).

^{13}C{^{1}H} NMR (100 MHz, $CDCl_3$, 298 K) δ (ppm) 163.5, 145.3, 134.7, 132.2, 128.8, 128.6, 128.5, 128.4, 128.1, 127.8, 126.4, 61.8, 29.4, 25.2.

VI. X-ray crystallographic details.

Suitable single crystals of **2** and **3** were selected and mounted under nitrogen atmosphere using the X-TEMP2 and intensity data were collected on a Super Nova, Dual, Cu at zero, Eos diffractometer. All the crystals were kept at 100 K during data collection. Using Olex2,[16] the structure was solved with the ShelXT[17] structure solution program using Intrinsic Phasing and refined with the ShelXL[18] refinement package using Least Squares minimisation. All nonhydrogen atoms were refined with anisotropic displacement parameters. Crystallographic data (including structure factors) for the structures have been deposited with the Cambridge Crystallographic Data Centre. Copies of the data can be obtained free of charge from the Cambridge Crystallographic Data Centre *via* 2101729 and 2101730 contain the supplementary crystallographic data of compounds **2** and **3**, respectively for this paper.

Crystallographic and data collection parameters for 2 and 3.

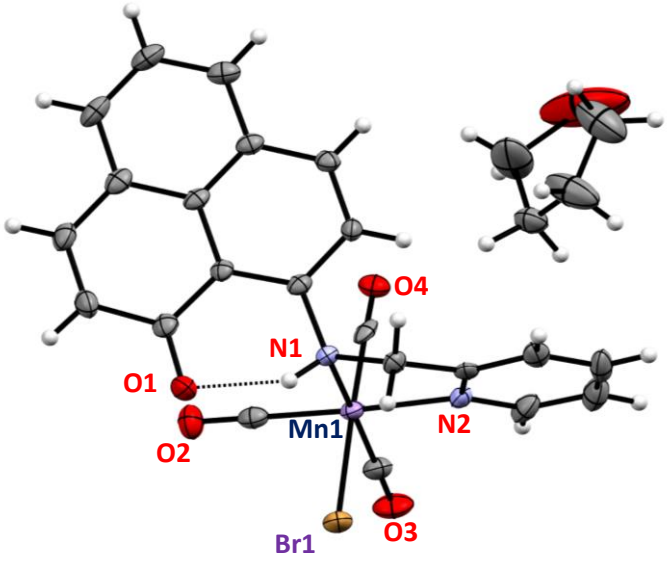

Fig. S15. Molecular structure of **2**. Thermal ellipsoids represent 50% probability. Selected bond distances (Å) and angles (degree) in **2**: Mn-N1 2.130, Mn-N2 2.060, Mn-Br 2.520, N1-Mn-N2 80.62.

Table S3. Crystal data and structure refinement for 2.

CCDC	2101729
Identification code	MnBr1
Empirical formula	$C_{22}H_{14}BrMnN_2O_4$
Formula weight	505.20
Temperature/K	100.00(10)
Crystal system	monoclinic
Space group	$P2_1/n$
a/Å	10.9430(3)
b/Å	12.3084(3)
c/Å	17.5419(4)
α/°	90
β/°	94.232(2)
γ/°	90
Volume/Å^3	2356.29(10)
Z	4
ρ_{calc}g/cm^3	1.424

μ/mm^{-1}	2.283
F(000)	1008.0
Crystal size/mm^3	0.15 × 0.15 × 0.1
Radiation	Mo Kα (λ = 0.71073)
2Θ range for data collection/°	4.046 to 50.054
Index ranges	-12 ≤ h ≤ 13, -14 ≤ k ≤ 9, -20 ≤ l ≤ 8
Reflections collected	7041
Independent reflections	4132 [R_{int} = 0.0236, R_{sigma} = 0.0396]
Data/restraints/parameters	4132/0/275
Goodness-of-fit on F^2	1.059
Final R indexes [I>=2σ (I)]	R_1 = 0.0338, wR_2 = 0.0857
Final R indexes [all data]	R_1 = 0.0404, wR_2 = 0.0894
Largest diff. peak/hole / e $Å^{-3}$	0.62/-0.52

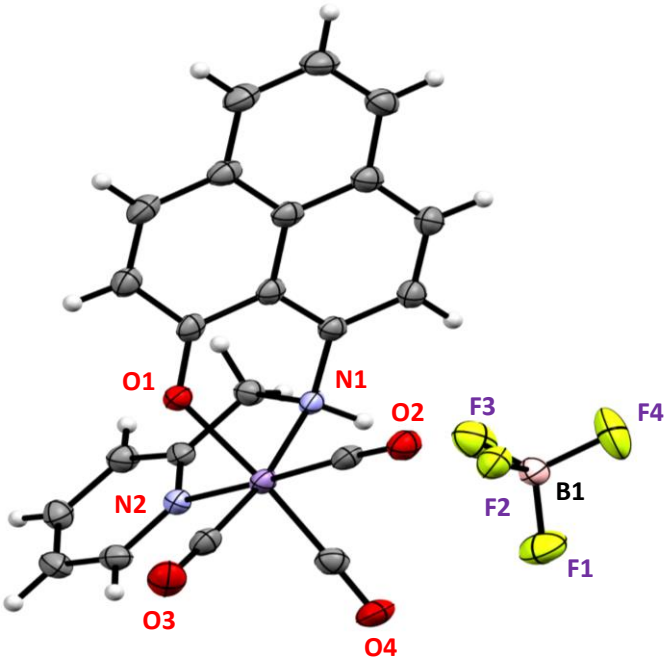

Fig. S16. Molecular structure of **3**. Thermal ellipsoids represent 50% probability. Selected bond distances (Å) and angles (degree) in **3**: Mn-N1 2.083, Mn-N2 2.040, N1-Mn-N2 81.32.

Table S4. Crystal data and structure refinement for 3.

CCDC	2101730
Identification code	SOU_MNAGBF4

Empirical formula	$C_{22}H_{14}BF_4MnN_2O_4$
Formula weight	512.10
Temperature/K	100.00(10)
Crystal system	monoclinic
Space group	$P2_1/c$
a/Å	10.7249(7)
b/Å	14.4773(7)
c/Å	13.6836(6)
α/°	90
β/°	102.311(5)
γ/°	90
Volume/Å^3	2075.8(2)
Z	4
ρ_{calc}g/cm^3	1.639
μ/mm^{-1}	5.816
F(000)	1032.0
Crystal size/mm^3	0.2 × 0.15 × 0.1
Radiation	Cu Kα (λ = 1.54184)
2Θ range for data collection/°	8.438 to 134.56
Index ranges	$-12 \leq h \leq 12$, $-16 \leq k \leq 17$, $-16 \leq l \leq 12$
Reflections collected	16033
Independent reflections	3630 [R_{int} = 0.0404, R_{sigma} = 0.0306]
Data/restraints/parameters	3630/0/307
Goodness-of-fit on F^2	1.069
Final R indexes [I>=2σ (I)]	R_1 = 0.0402, wR_2 = 0.1070
Final R indexes [all data]	R_1 = 0.0469, wR_2 = 0.1124
Largest diff. peak/hole / e Å^{-3}	0.91/-0.39

VII. Computational details.

All theoretical calculations to interpret the experimental observations were performed using Gaussian16 quantum chemistry package[19]. Density Functional Theory (DFT) calculations were performed at B3LYP level of theory[20]. We used LANL2DZ[21] basis set with the relativistic effective core potential for Mn atom and 6-31+g(d) basis for other elements (H, C, N, O, Br). The geometries were optimized without any symmetry constraints. Geometry optimizations were performed starting from crystal structure of complexes.

Optimized structure of 2, 3 and 6.

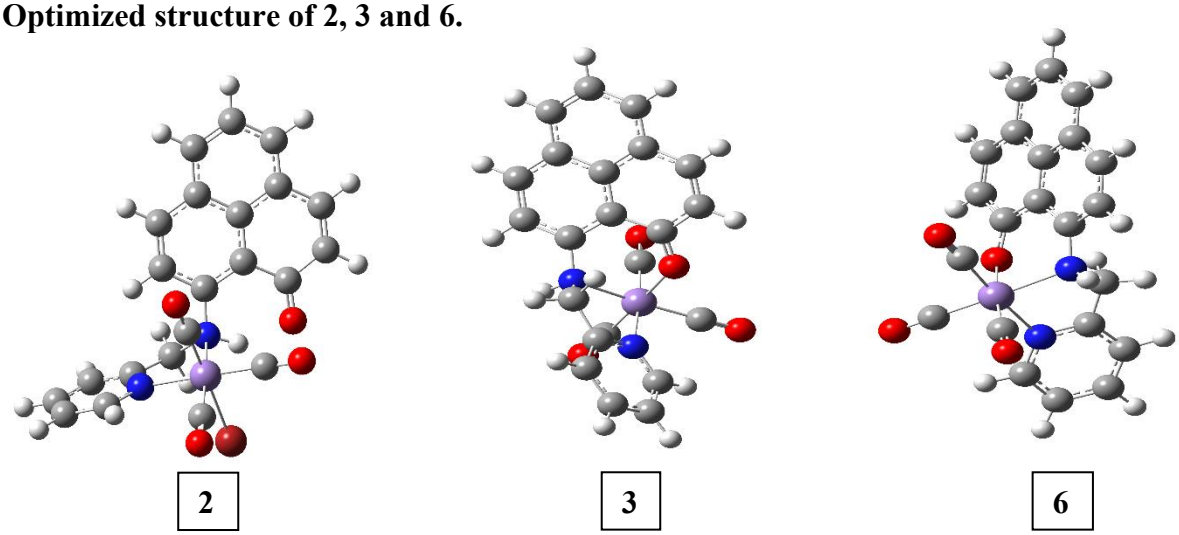

Fig. S17. Optimized structures of compound **2**, **3** and **6** using B3LYP level of theory (with basis set 6-31+g(d) for C, H, N, O, Br and LANL2DZ for Mn).

Molecular Orbitals.

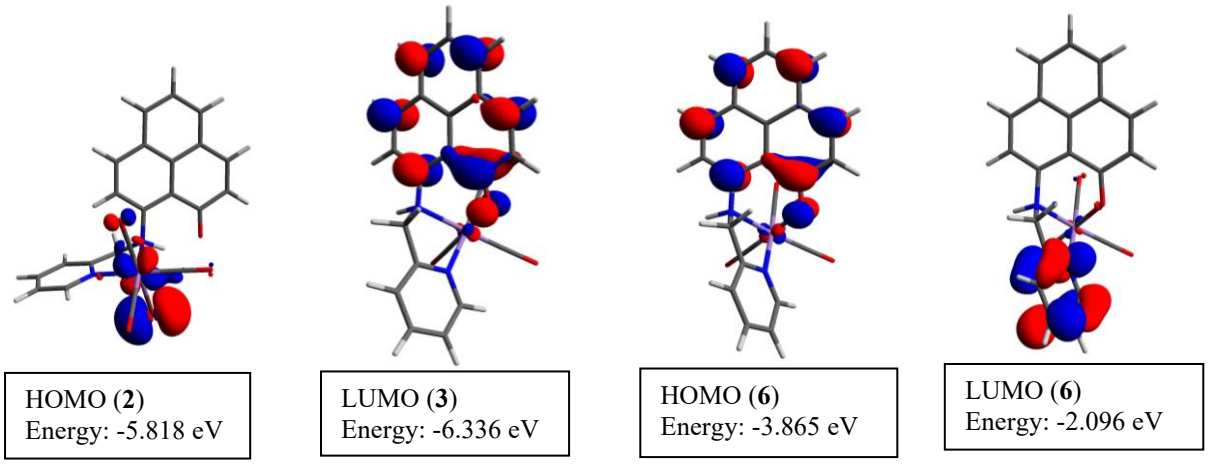

Fig. S18. Calculated MO profiles of **2**, **3** and **6** at the B3LYP/6-31+g(d)/LANL2DZ level of theory (iso value = 0.05).

Table S5. Energies, enthalpies, and free energies (in Hartree) of the optimized structures:

Comp.	ZPE	ΔE	ΔH	ΔG	E	H	G
2	0.315506	0.341498	0.342443	0.257922	-3932.3285	-3932.3275	-3932.4120
3	0.316036	0.339557	0.340501	0.263224	-1360.6832	-1360.6822	-1360.7595
6	0.313250	0.336720	0.337664	0.259984	-1360.8732	-1360.8723	-1360.9499

xyz coordinates.

Compound **2**.

Electronic Energy: -3932.66998 Hartree

No. of imaginary frequency: 0

0 1

Br	-2.82448	-1.80570	-0.96083
Mn	-1.44582	-0.49401	0.75963
O	-3.62466	-1.14307	2.65539
N	-2.36291	1.24342	0.02121
O	-0.09884	-3.05887	1.45851
N	-0.11526	0.00132	-0.95602
H	0.03346	-0.94658	-1.33370
O	1.27450	-2.21993	-1.49359
C	4.70376	-1.83533	-0.54581
H	5.62563	-2.41234	-0.50328
C	3.61248	1.69583	0.22860
C	2.31317	-0.25557	-0.59008
C	-1.96651	1.65295	-1.20138
C	-0.93738	0.80116	-1.89934

H	-0.30287	1.41488	-2.54987
H	-1.47273	0.07619	-2.52134
C	1.15246	0.54442	-0.60414
C	2.30127	-1.66707	-1.05523
C	3.56085	-2.40663	-0.99382
H	3.51964	-3.44064	-1.32200
C	2.42484	2.46948	0.16424
H	2.46030	3.51667	0.45512
C	3.54978	0.32436	-0.15993
C	4.75056	-0.45290	-0.12208
C	-2.52318	2.77552	-1.81998
H	-2.17287	3.07413	-2.80402
C	4.84460	2.25380	0.65848
H	4.87134	3.29990	0.95421
C	5.93988	0.13300	0.30881
H	6.84460	-0.47011	0.33676
C	1.23481	1.91339	-0.24007
H	0.33644	2.52076	-0.25092
C	5.99147	1.48344	0.70311
H	6.93102	1.91465	1.03617
C	-0.60690	-2.06763	1.16729
C	-3.52400	3.49170	-1.16708
H	-3.97346	4.36375	-1.63373
C	-3.93327	3.06511	0.09737
H	-4.70837	3.58570	0.65040
C	-3.32426	1.94439	0.65281
H	-3.61358	1.58470	1.63376
C	-2.76908	-0.89477	1.92050
O	0.00225	0.97944	2.87132
C	-0.53782	0.41373	2.01459

Compound **3**.

Electronic Energy: -1361.022756 Hartree

No. of imaginary frequency: 0

1 1

Mn	-1.45212	-0.97120	-0.06613
O	-0.26421	-0.14161	1.41526
O	-2.80034	-2.66295	1.98423
N	-0.42320	0.50644	-1.21737
H	-0.70843	0.38149	-2.18805
O	0.49287	-3.17192	-0.58100
N	-2.75202	0.65701	0.19504
O	-3.17769	-1.93600	-2.27858
C	1.01898	0.38168	-1.16255
C	-0.88636	1.86653	-0.77721
H	-0.24076	2.18640	0.04452
H	-0.75614	2.59060	-1.58989
C	-2.31271	1.83511	-0.29442
C	1.68454	0.29719	0.07367
C	-2.50913	-1.57890	-1.41014
C	-3.10761	2.98205	-0.29726
H	-2.72189	3.90828	-0.71292
C	-3.99775	0.60009	0.70844
H	-4.32232	-0.36318	1.08496
C	-4.84335	1.70386	0.75808
H	-5.83517	1.60168	1.18571
C	3.11250	0.33646	0.08497
C	3.12647	0.35851	-2.35905
H	3.67180	0.36099	-3.29914
C	3.82689	0.36505	1.32093
C	1.72218	0.27729	2.57514

H	1.16287	0.23212	3.50416
C	0.96707	0.14120	1.35143
C	1.74253	0.39399	-2.36807
H	1.20918	0.44390	-3.31466
C	5.26733	0.37521	-1.10784
H	5.81473	0.37590	-2.04674
C	-4.39255	2.91895	0.24110
H	-5.02933	3.79851	0.25133
C	3.84398	0.35452	-1.14057
C	3.08058	0.36797	2.55487
H	3.63376	0.41809	3.48988
C	5.22222	0.40092	1.30661
H	5.76093	0.43034	2.25052
C	-0.24561	-2.31225	-0.38144
C	-2.28782	-2.02208	1.17986
C	5.94373	0.39864	0.09598
H	7.02879	0.41850	0.11536

Compound **6**.

Electronic Energy: -1361. 209967 Hartree

No. of imaginary frequency: 0

0 2

Mn	-1.43732	-0.94849	-0.19982
O	-0.35522	-0.22212	1.36324
O	-2.73429	-2.89262	1.63336
N	-0.44373	0.67589	-1.14296
H	-0.72796	0.69985	-2.12159
O	0.56541	-3.02581	-0.93227
N	-2.78391	0.60254	0.24839
O	-3.07775	-1.69262	-2.55221
C	1.00804	0.57046	-1.11086

C	-0.90738	1.94201	-0.49723
H	-0.27143	2.10968	0.37529
H	-0.76680	2.79316	-1.17595
C	-2.33486	1.84173	-0.03501
C	1.66539	0.28150	0.11955
C	-2.43908	-1.41099	-1.62541
C	-3.13495	2.97453	0.14080
H	-2.74147	3.95519	-0.11071
C	-4.03437	0.46305	0.72696
H	-4.35708	-0.55073	0.93697
C	-4.88375	1.54294	0.94672
H	-5.88068	1.37296	1.34018
C	3.10064	0.33085	0.13683
C	3.12050	0.79558	-2.27831
H	3.66920	0.97197	-3.19972
C	3.81589	0.12692	1.36050
C	1.69371	-0.21721	2.52732
H	1.13288	-0.44639	3.42946
C	0.94540	-0.05967	1.32801
C	1.73083	0.80802	-2.28127
H	1.19566	1.01398	-3.20811
C	5.25451	0.61501	-1.02403
H	5.80466	0.80122	-1.94350
C	-4.42568	2.82658	0.64386
H	-5.06246	3.69404	0.79294
C	3.83732	0.58262	-1.07010
C	3.06831	-0.12333	2.54841
H	3.60768	-0.26660	3.48253
C	5.22977	0.17757	1.35497
H	5.76387	0.02236	2.28969

C	-0.18542	-2.19965	-0.64479
C	-2.23437	-2.14906	0.90465
C	5.93513	0.41588	0.17533
H	7.02182	0.44585	0.19173

VIII. ^{1}H and ^{13}C NMR spectra of alcohols.

Fig. 19. ^{1}H NMR spectrum of 4-Chlorobenzyl alcohol (**5a**) in $CDCl_3$.

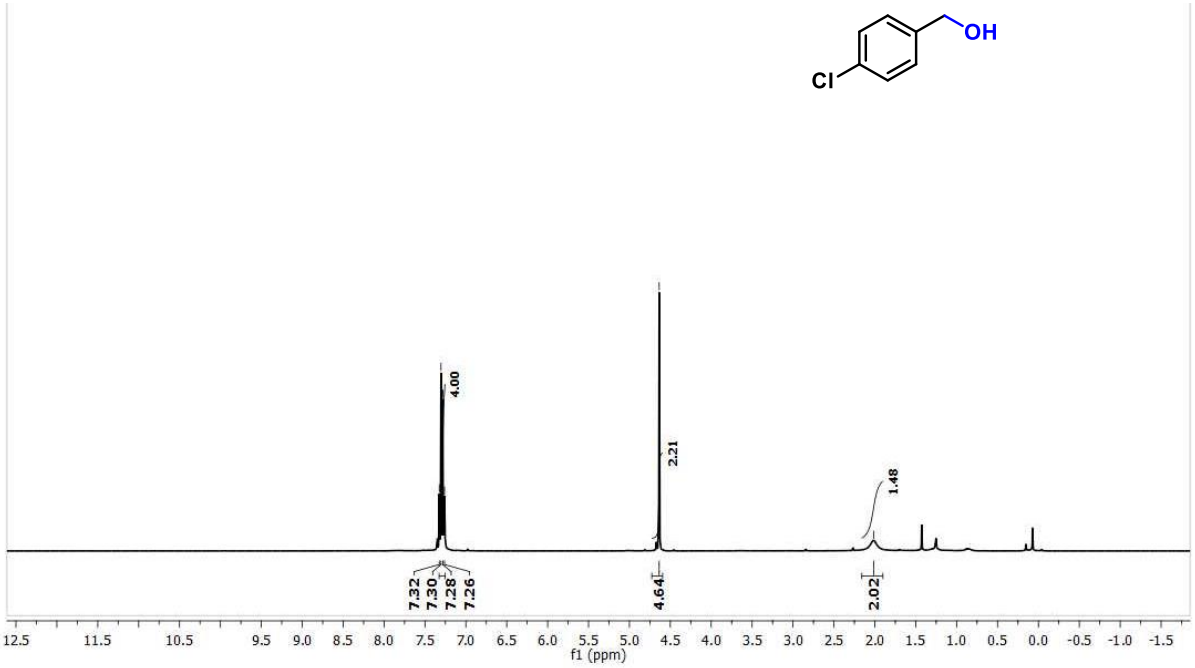

Fig. 20. $^{13}C\{^{1}H\}$ NMR spectrum of 4-Chlorobenzyl alcohol (**5a**) in $CDCl_3$.

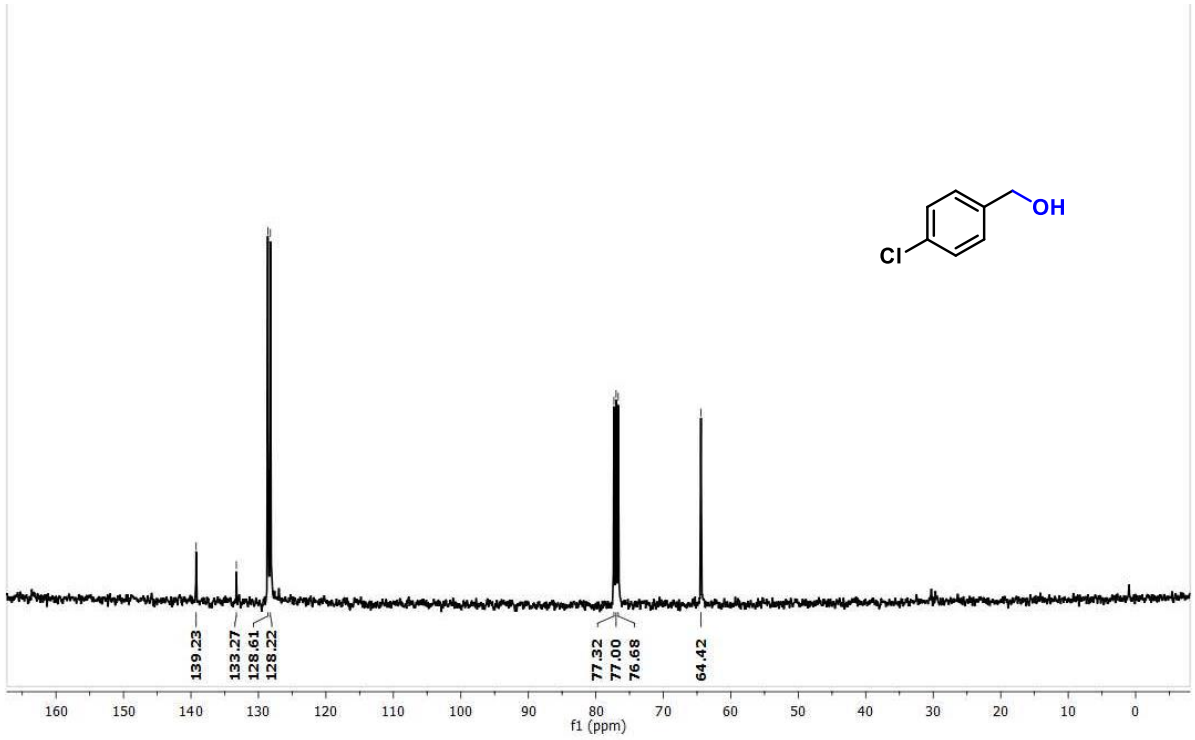

Fig. 21. ^{1}H NMR spectrum of Benzyl alcohol (**5b**) in $CDCl_3$.

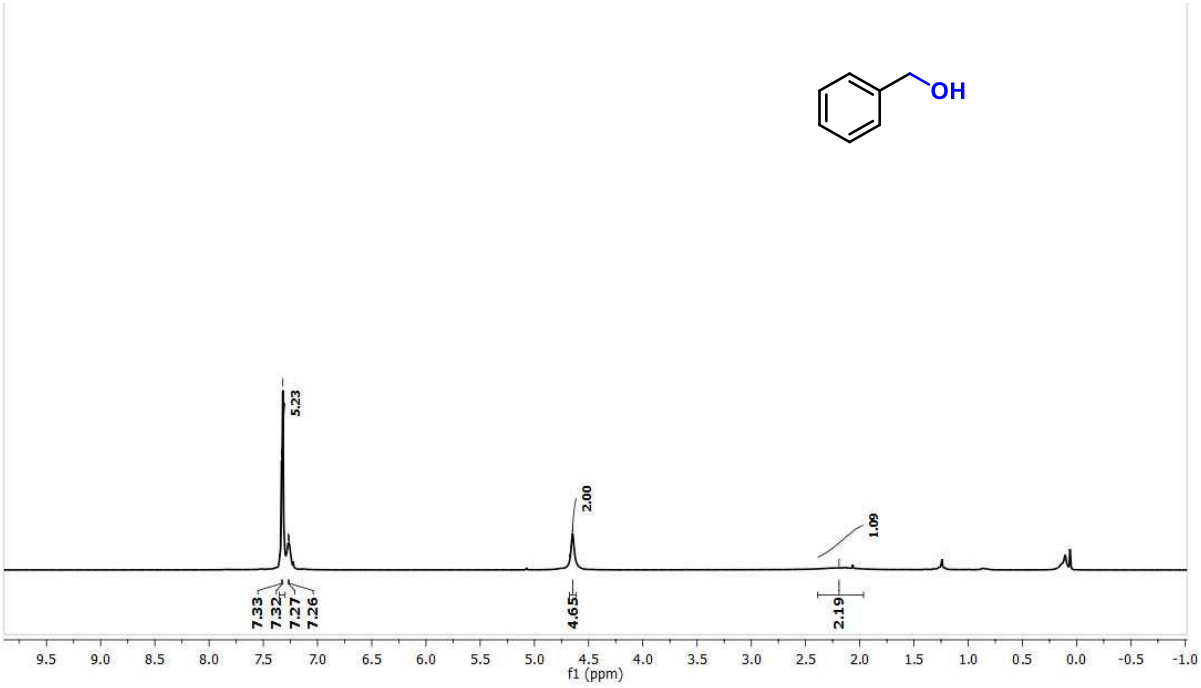

Fig. 22. $^{13}C\{^{1}H\}$ NMR spectrum of Benzyl alcohol (**5b**) in $CDCl_3$.

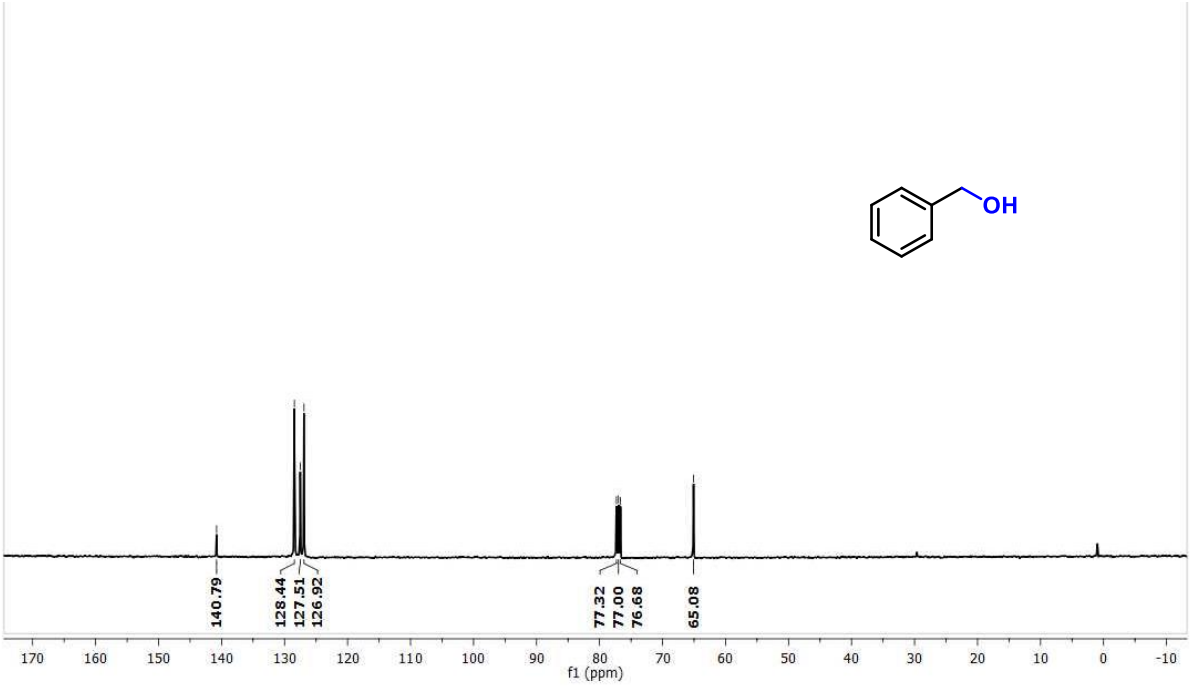

Fig. 23. ^{1}H NMR spectrum of 4-Iodobenzyl alcohol (**5c**) in $CDCl_3$.

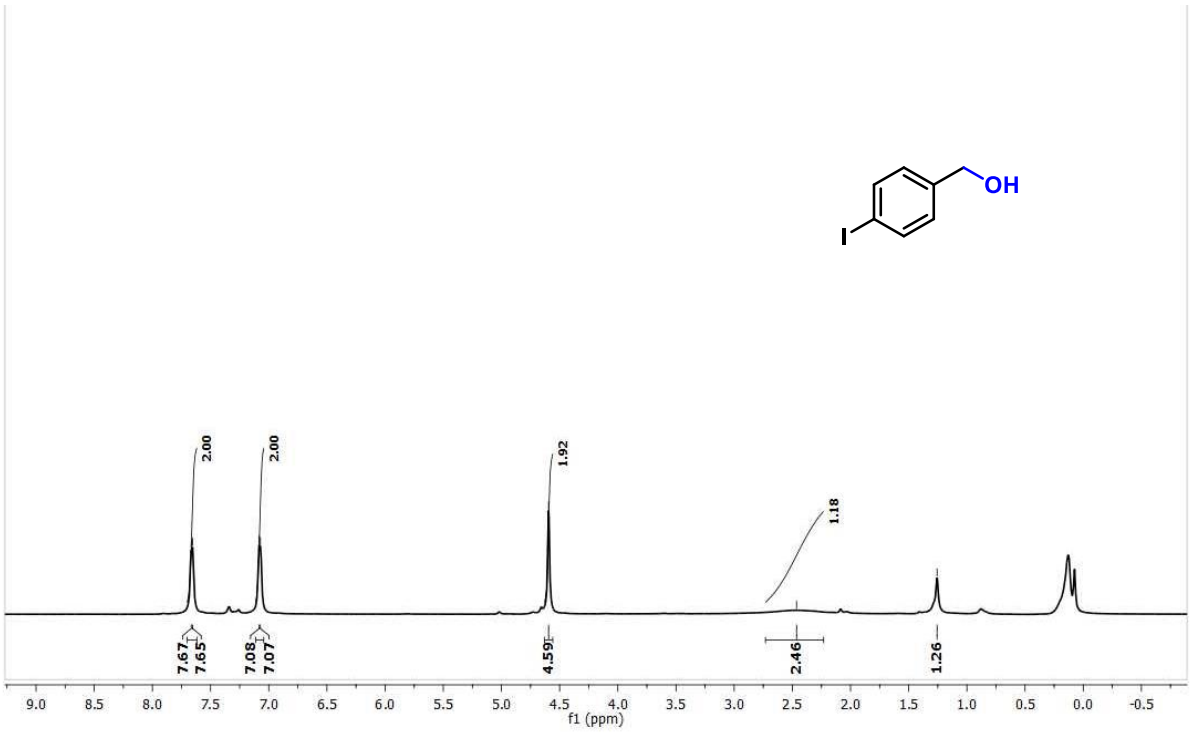

Fig. 24. $^{13}C\{^{1}H\}$ NMR spectrum of 4-Iodobenzyl alcohol (**5c**) in $CDCl_3$.

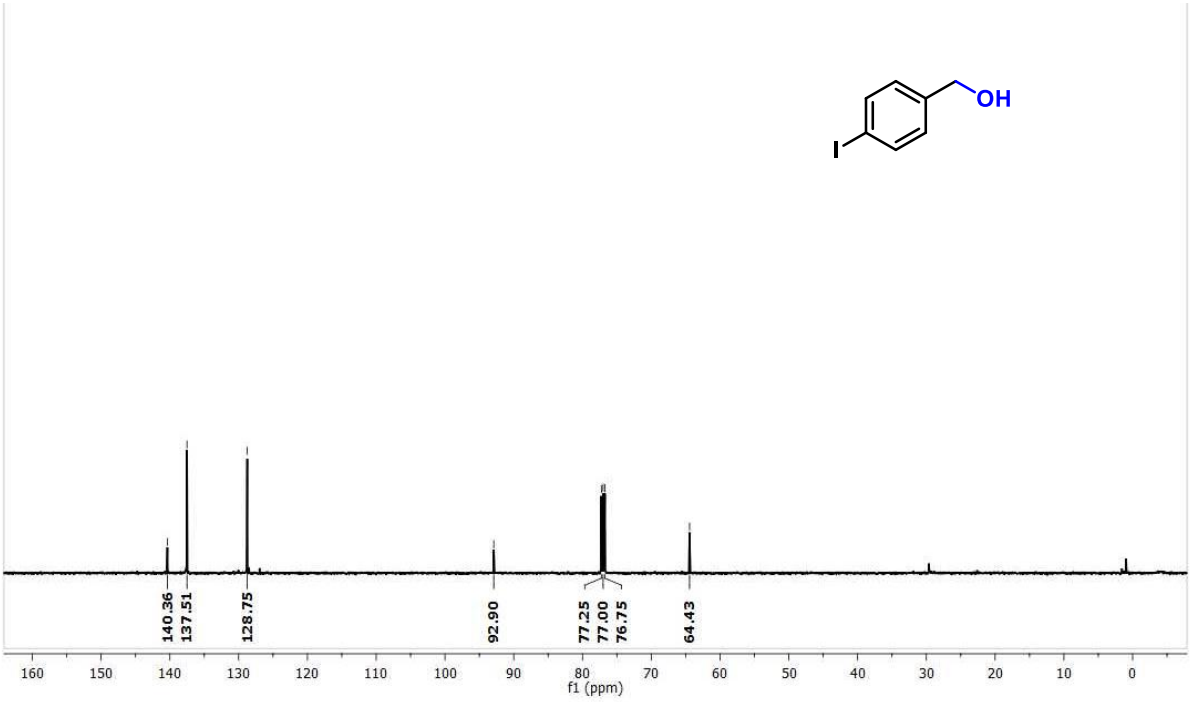

Fig. 25. ^{1}H NMR spectrum of 4-Methoxybenzyl alcohol (**5d**) in $CDCl_3$.

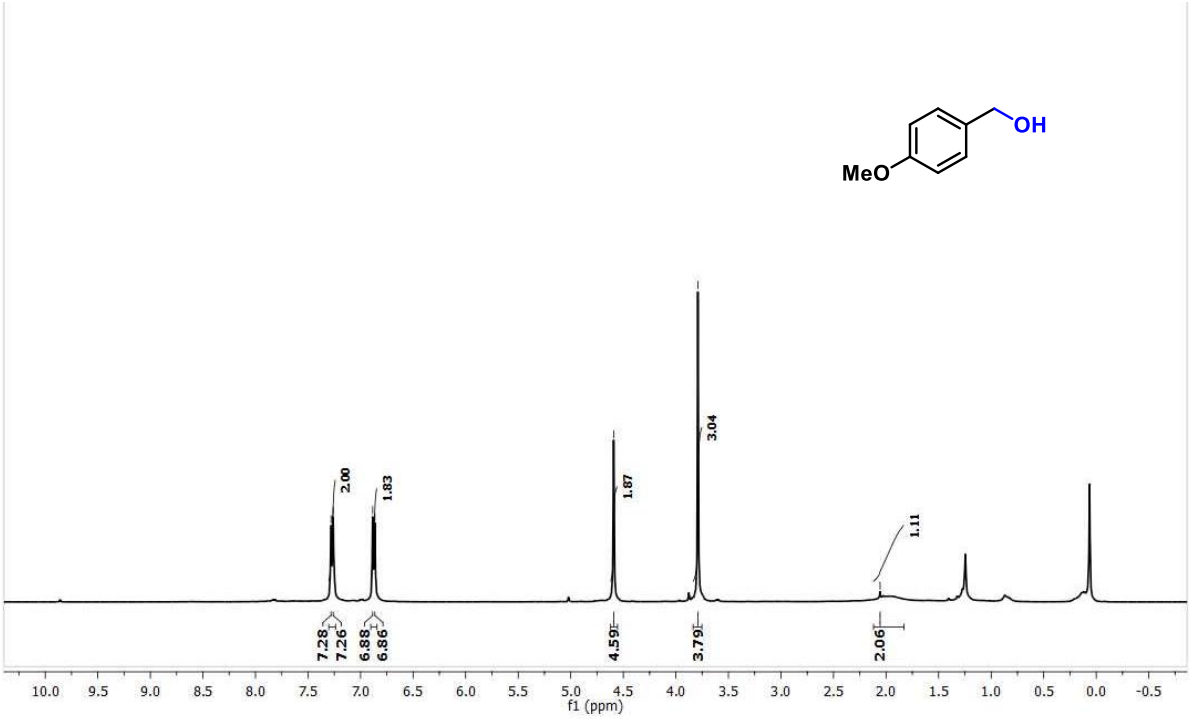

Fig. 26. $^{13}C\{^{1}H\}$ NMR spectrum of 4-Methoxybenzyl alcohol (**5d**) in $CDCl_3$.

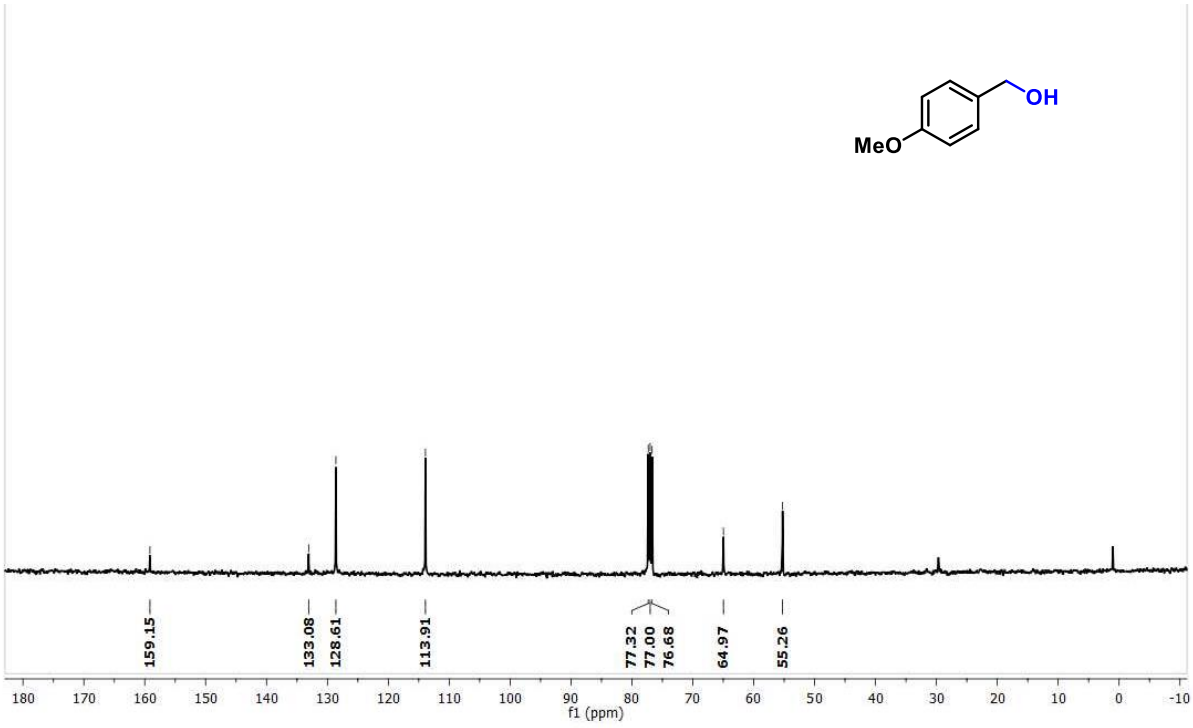

Fig. 27. ^{1}H NMR spectrum of 3-Bromobenzyl alcohol (**5e**) in $CDCl_3$.

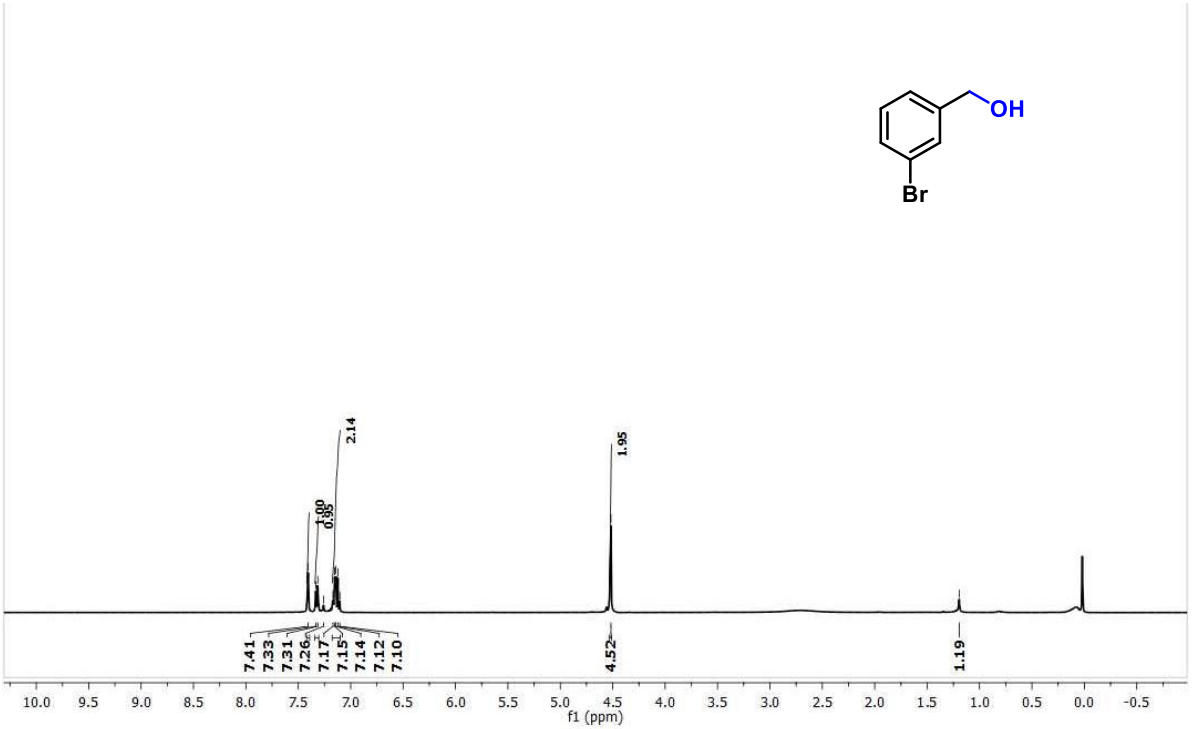

Fig. 28. $^{13}C\{^{1}H\}$ NMR spectrum of 3-Bromobenzyl alcohol (**5e**) in $CDCl_3$.

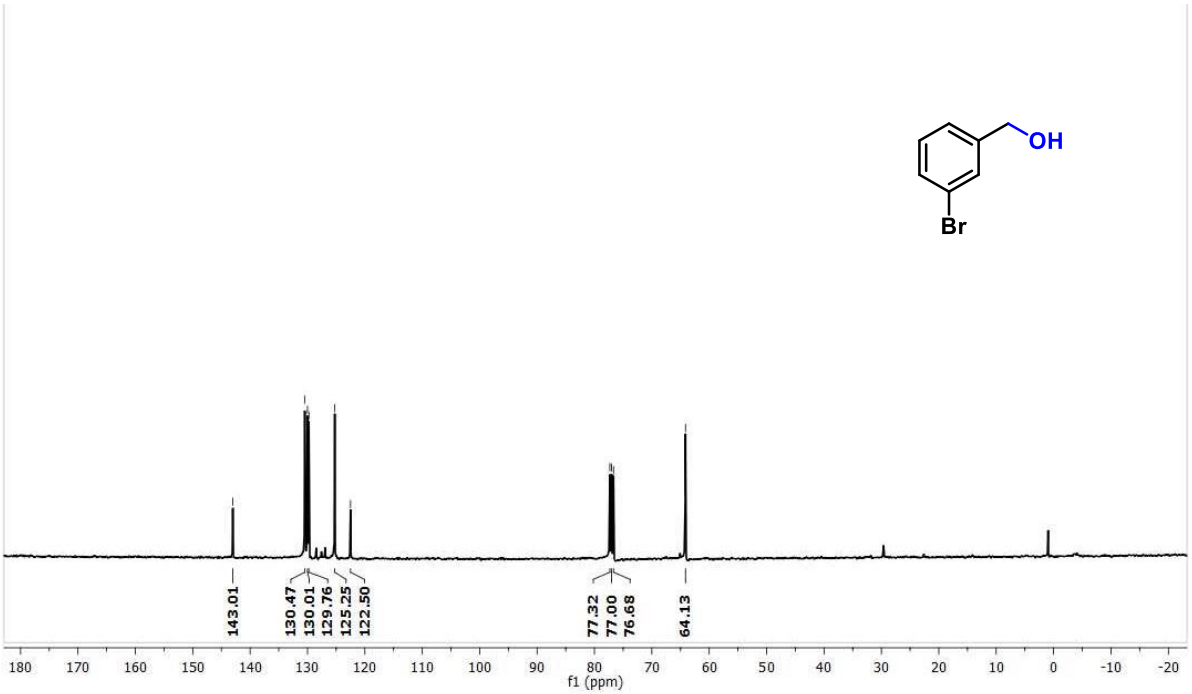

Fig. 29. ^{1}H NMR spectrum of 2-Methoxybenzyl alcohol (**5f**) in $CDCl_3$.

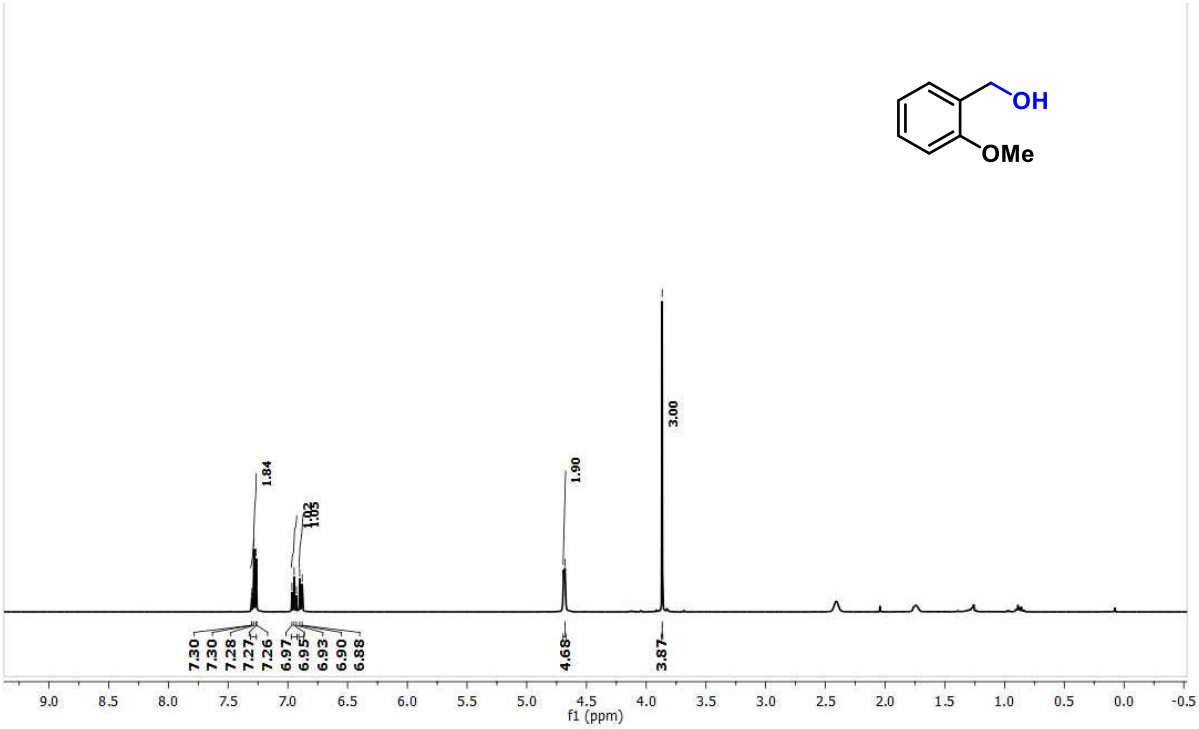

Fig. 30. $^{13}C\{^{1}H\}$ NMR spectrum of 2-Methoxybenzyl alcohol (**5f**) in $CDCl_3$.

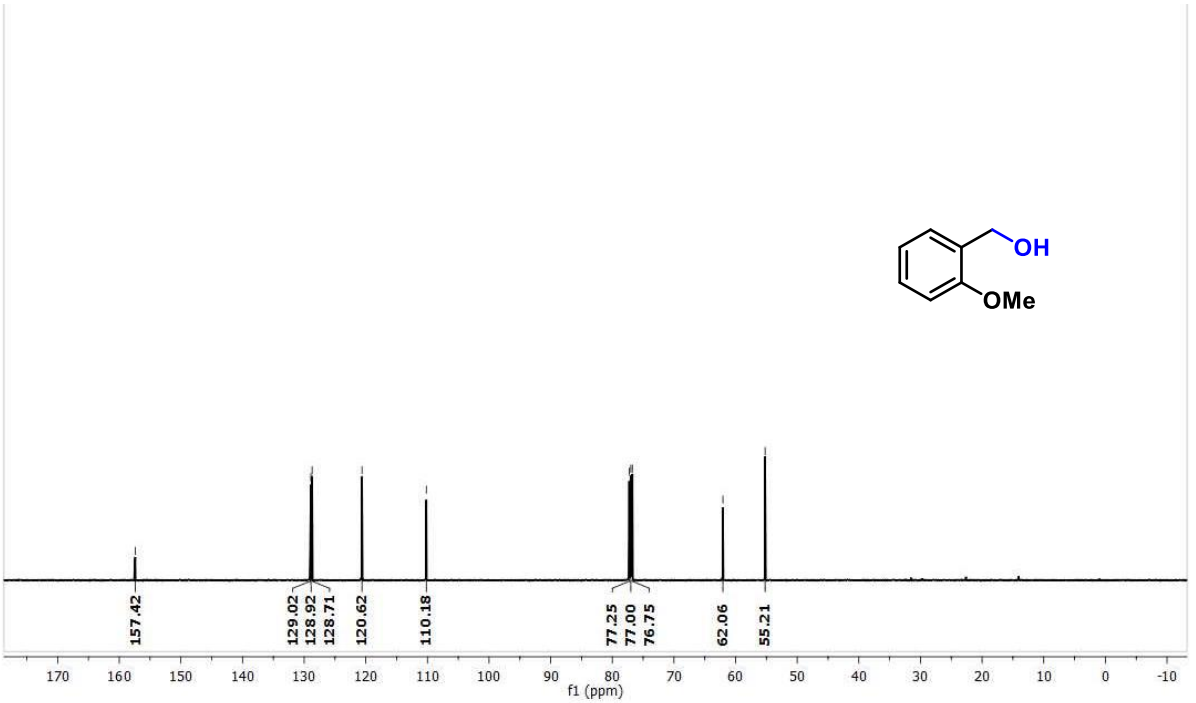

Fig. 31. ^{1}H NMR spectrum of 2-Chlorobenzyl alcohol (**5g**) in $CDCl_3$.

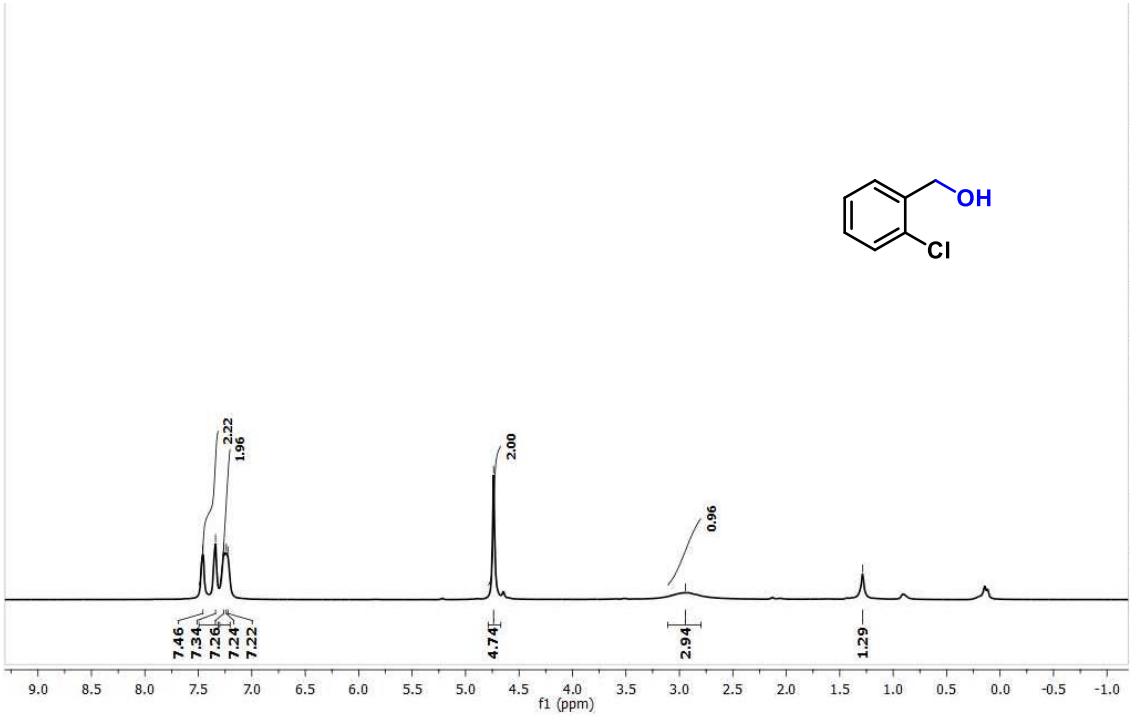

Fig. 32. $^{13}C\{^{1}H\}$ NMR spectrum of 2-Chlorobenzyl alcohol (**5g**) in $CDCl_3$.

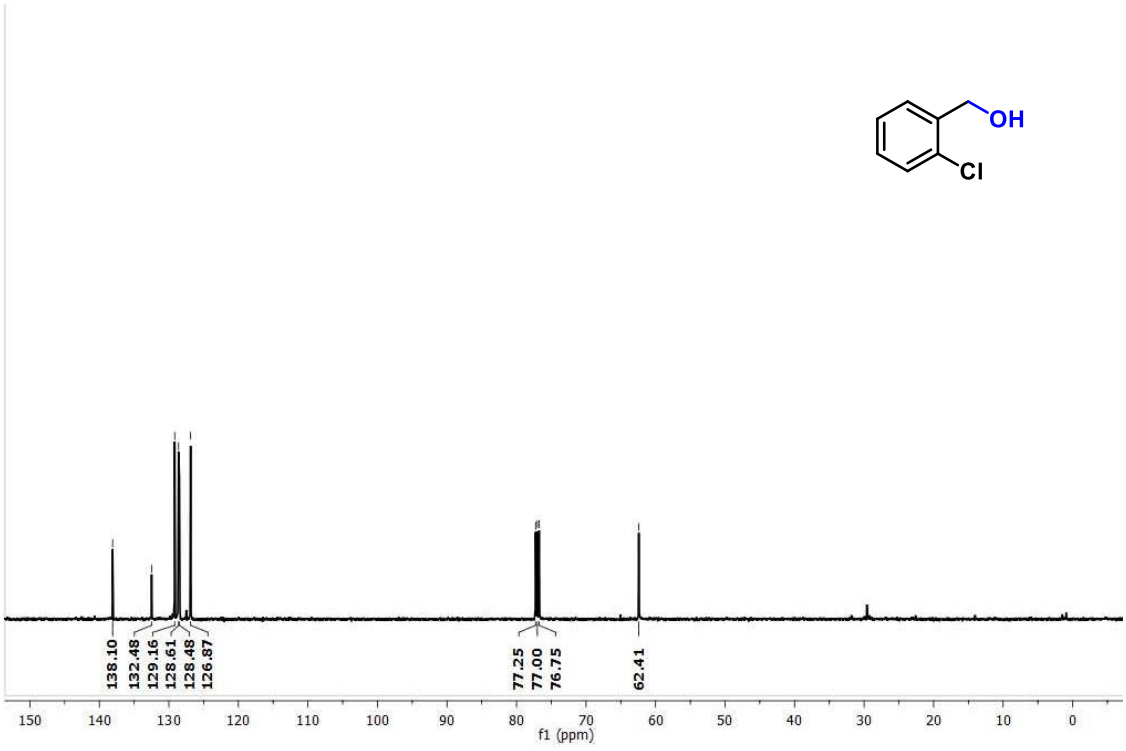

Fig. 33. ^{1}H NMR spectrum of 2-Phenylbenzyl alcohol (**5h**) in $CDCl_3$.

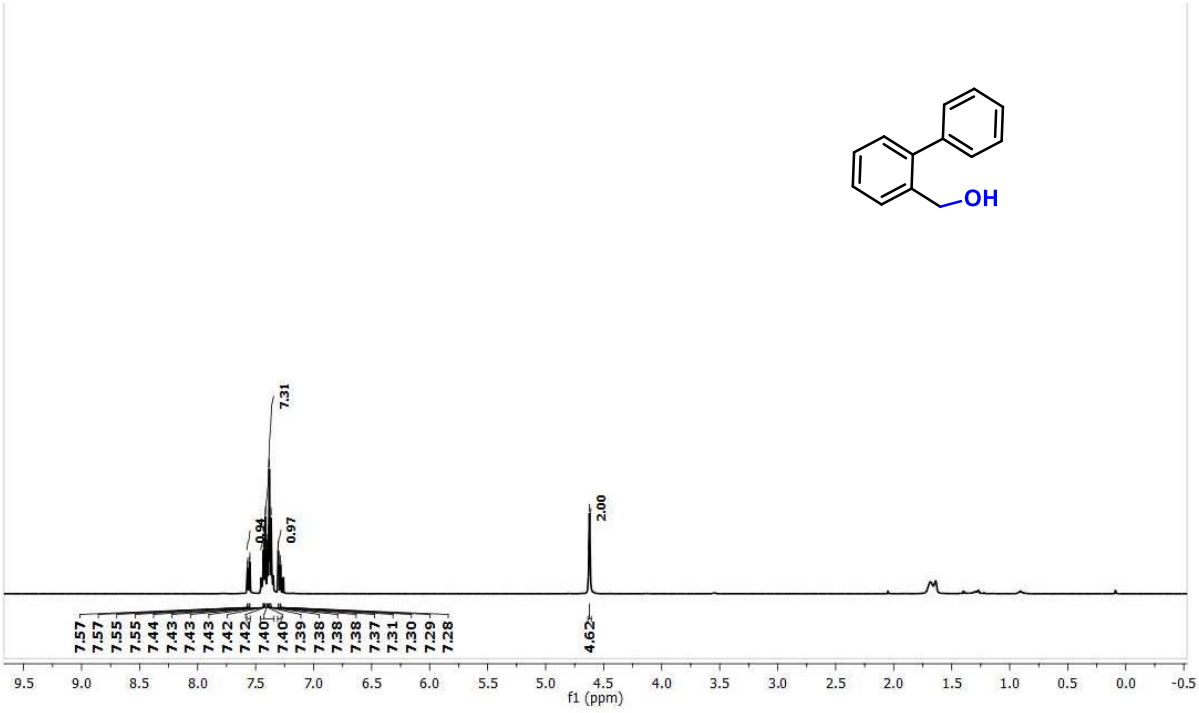

Fig. 34. $^{13}C\{^{1}H\}$ NMR spectrum of 2-Phenylbenzyl alcohol (**5h**) in $CDCl_3$.

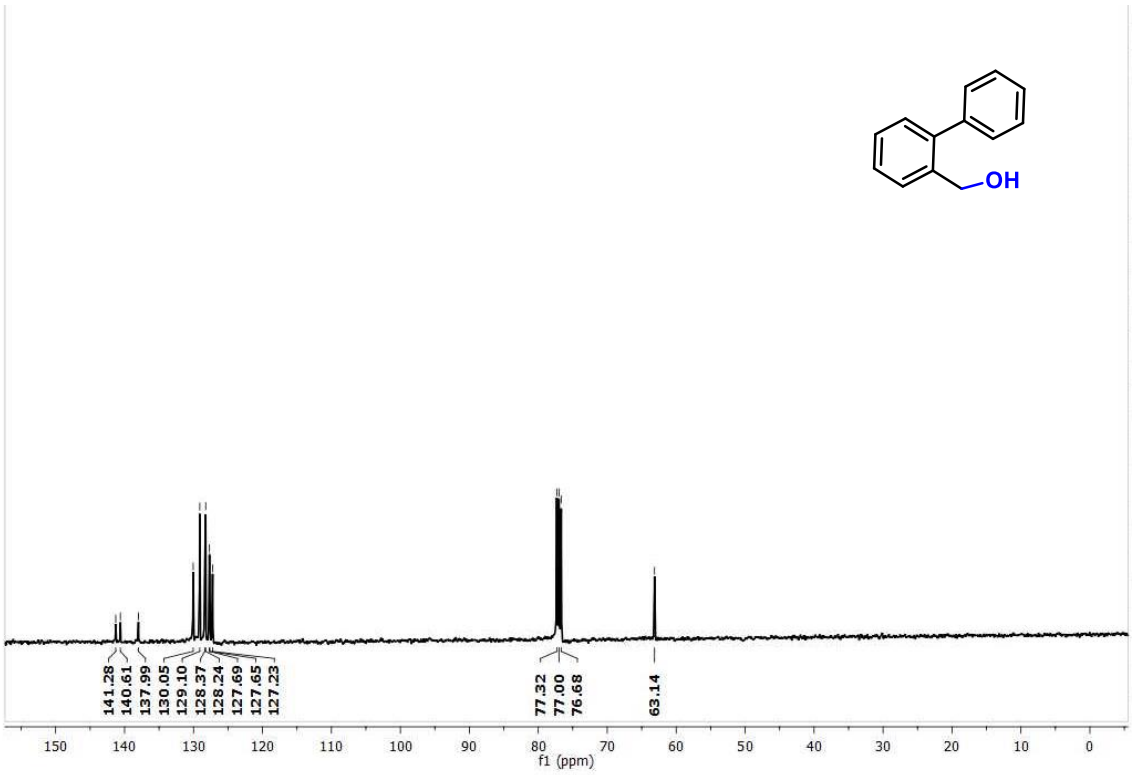

Fig. 35. ^{1}H NMR spectrum of 2-Thiophenemethanol (**5i**) in $CDCl_3$.

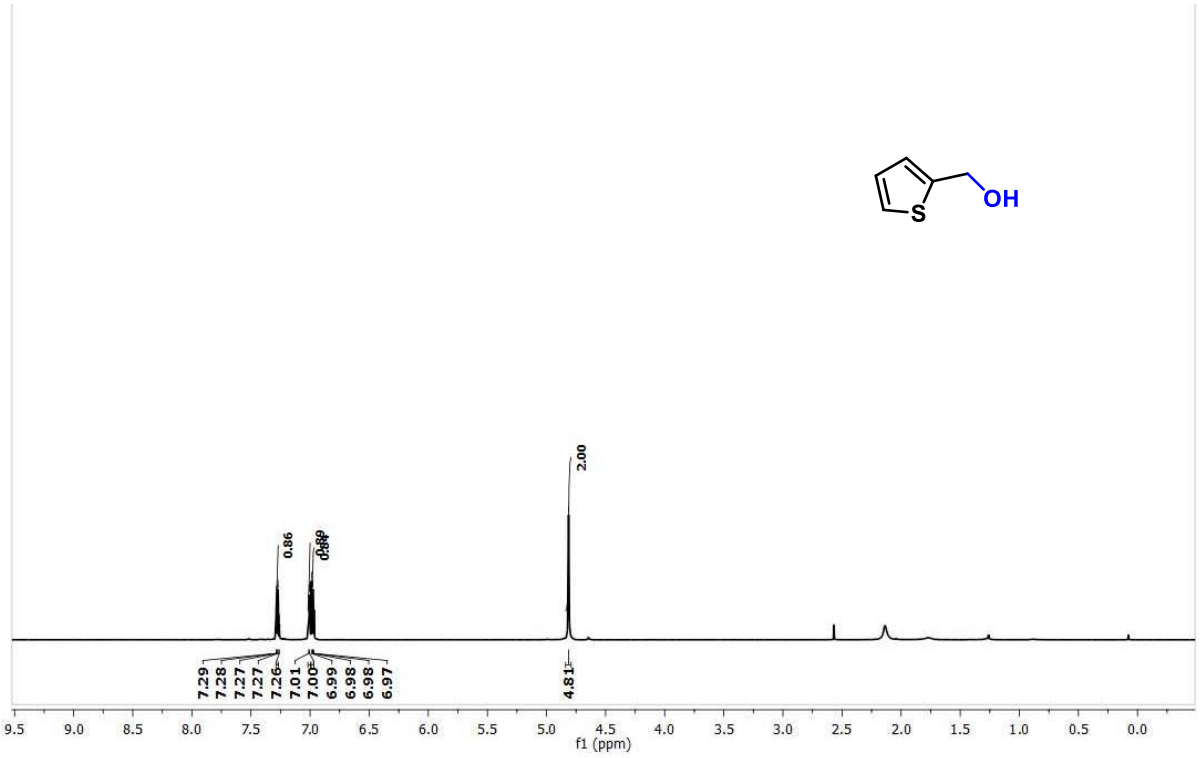

Fig. 36. $^{13}C\{^{1}H\}$ NMR spectrum of 2-Thiophenemethanol (**5i**) in $CDCl_3$.

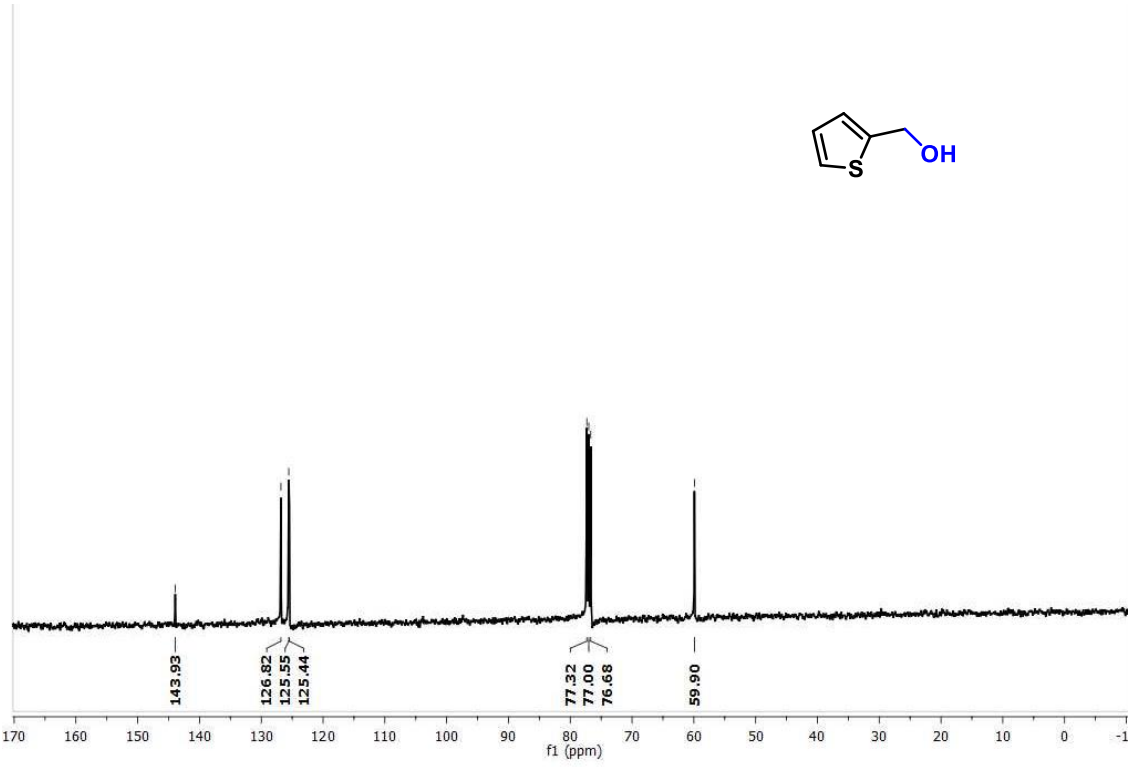

Fig. 37. ^{1}H NMR spectrum of 4-Phenyl-1-butanol (**5j**) in $CDCl_3$.

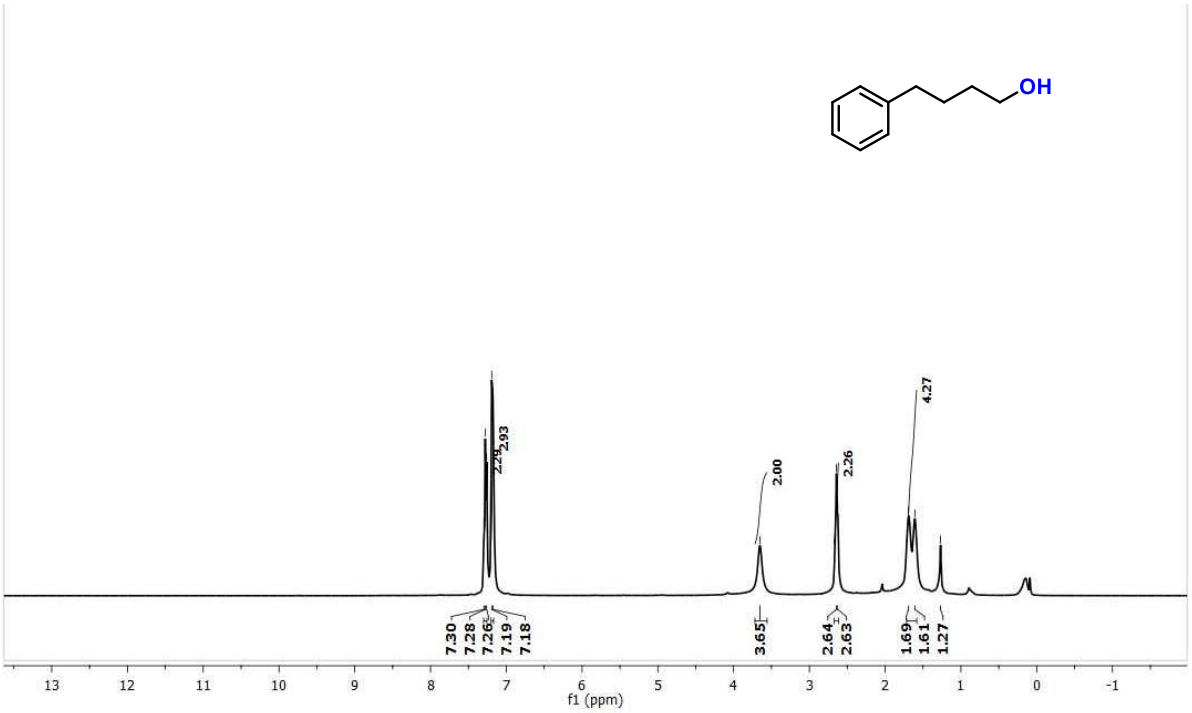

Fig. 38. $^{13}C\{^{1}H\}$ NMR spectrum of 4-Phenyl-1-butanol (**5j**) in $CDCl_3$.

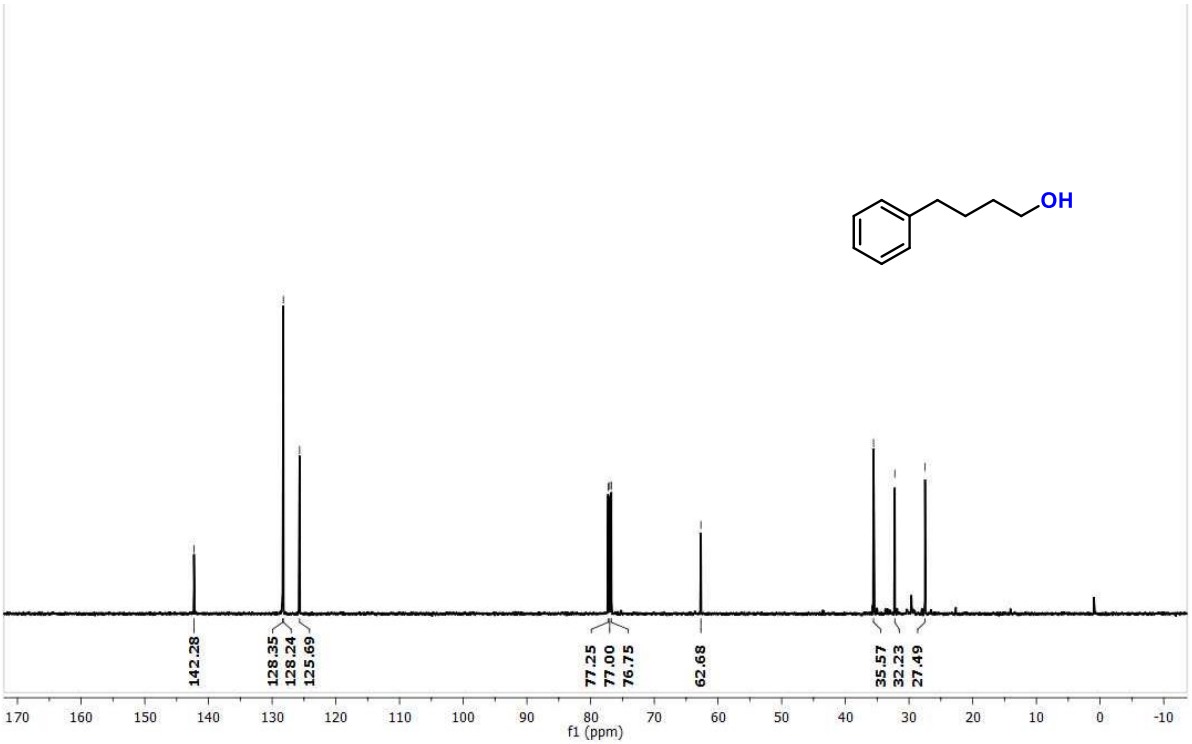

Fig. 39. ^{1}H NMR spectrum of Cyclohexane-1-methanol (**5k**) in $CDCl_3$.

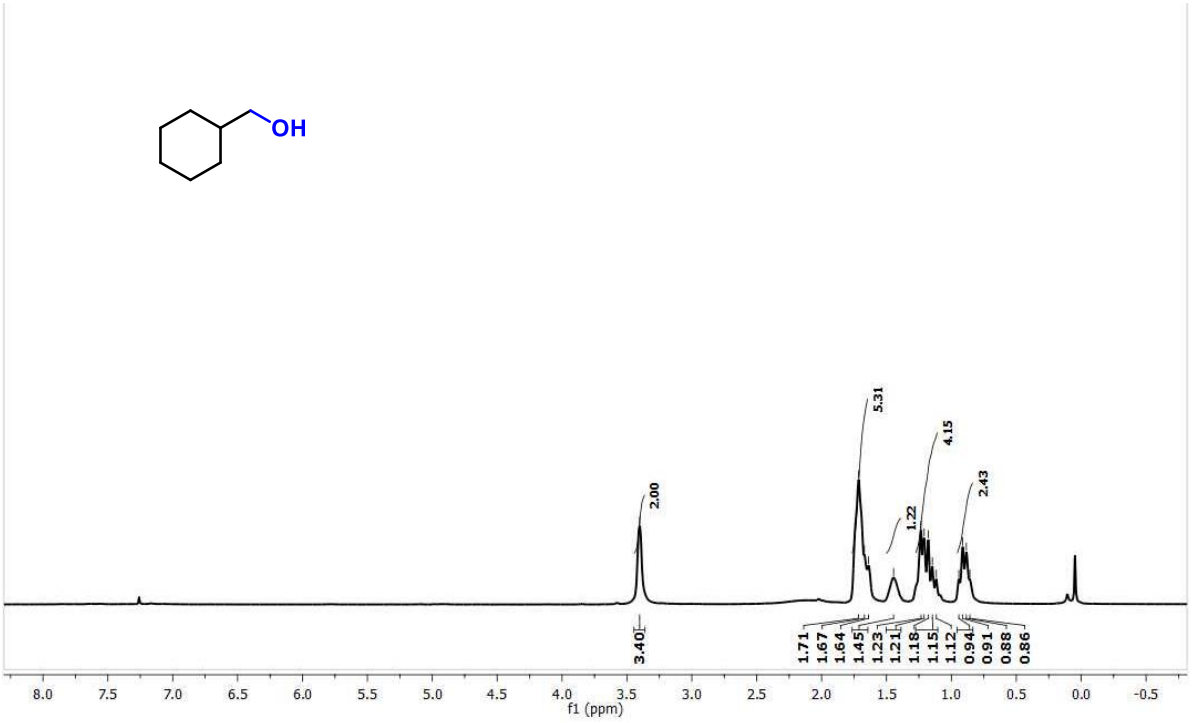

Fig. 40. $^{13}C\{^{1}H\}$ NMR spectrum of Cyclohexane-1-methanol (**5k**) in $CDCl_3$.

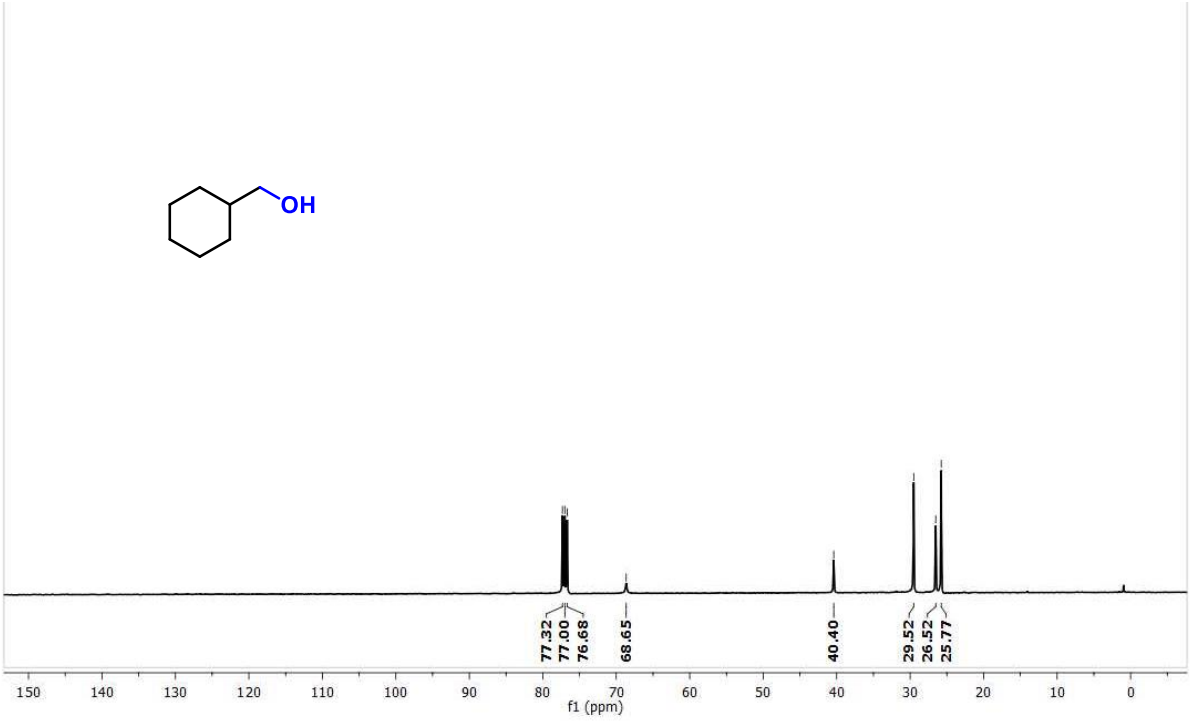

Fig. 41. ^{1}H NMR spectrum of Adamentane-1-methanol (**5l**) in $CDCl_3$.

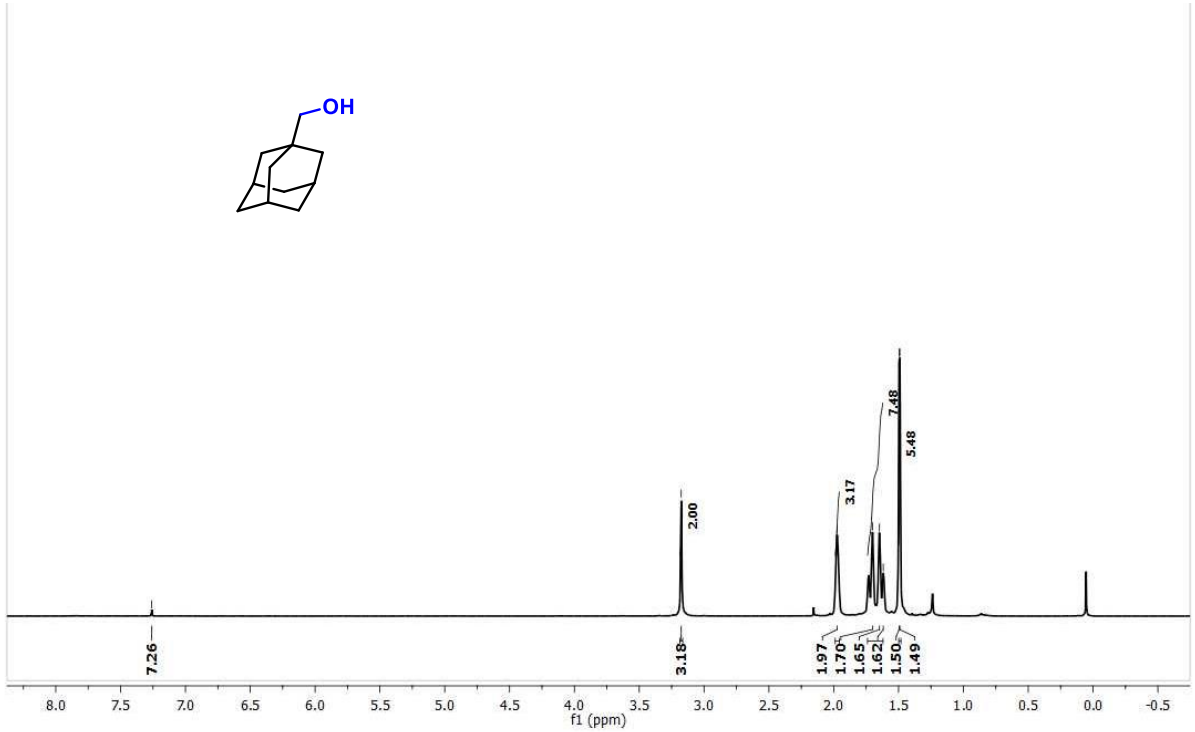

Fig. 42. $^{13}C\{^{1}H\}$ NMR spectrum of Adamentane-1-methanol (**5l**) in $CDCl_3$.

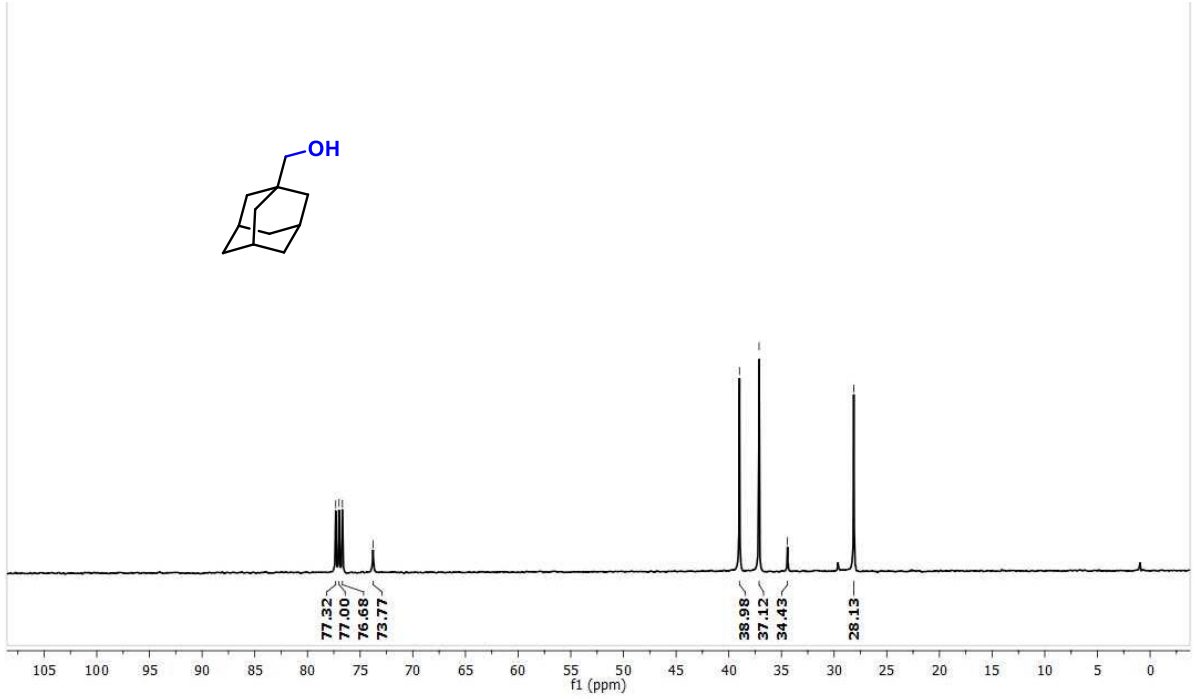

Fig. 43. ^{1}H NMR spectrum of Cinnamyl alcohol (**5m**) in $CDCl_3$.

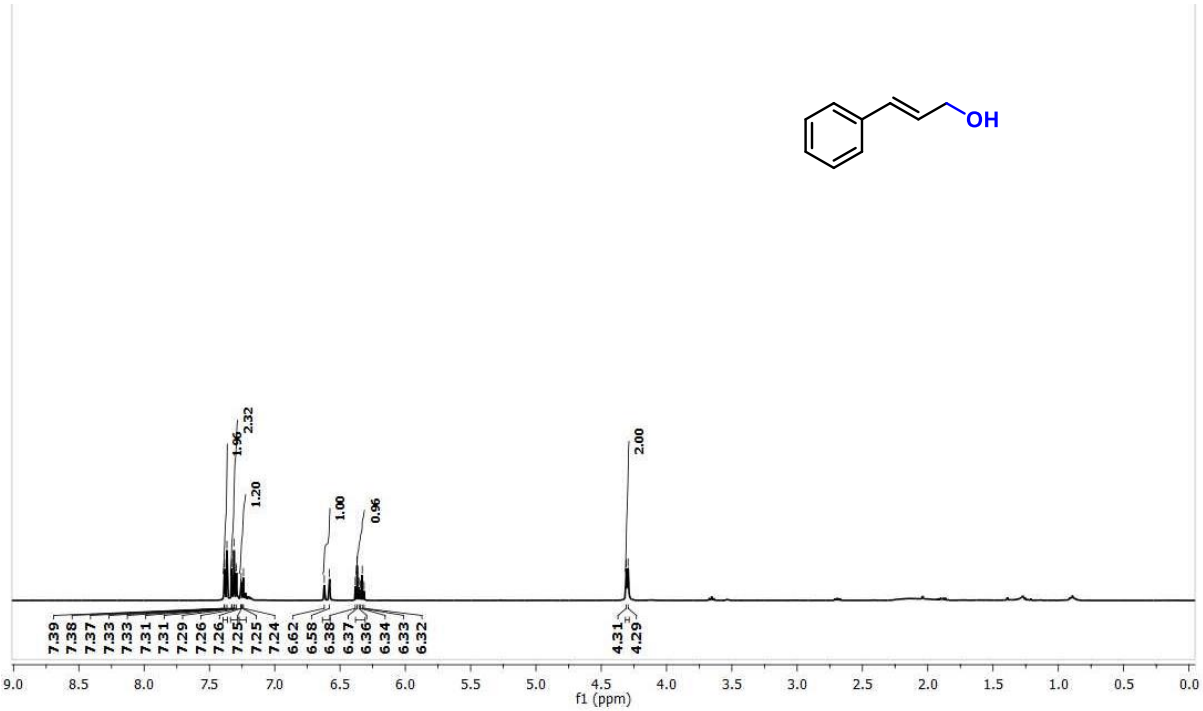

Fig. 44. $^{13}C\{^{1}H\}$ NMR spectrum of Cinnamyl alcohol (**5m**) in $CDCl_3$.

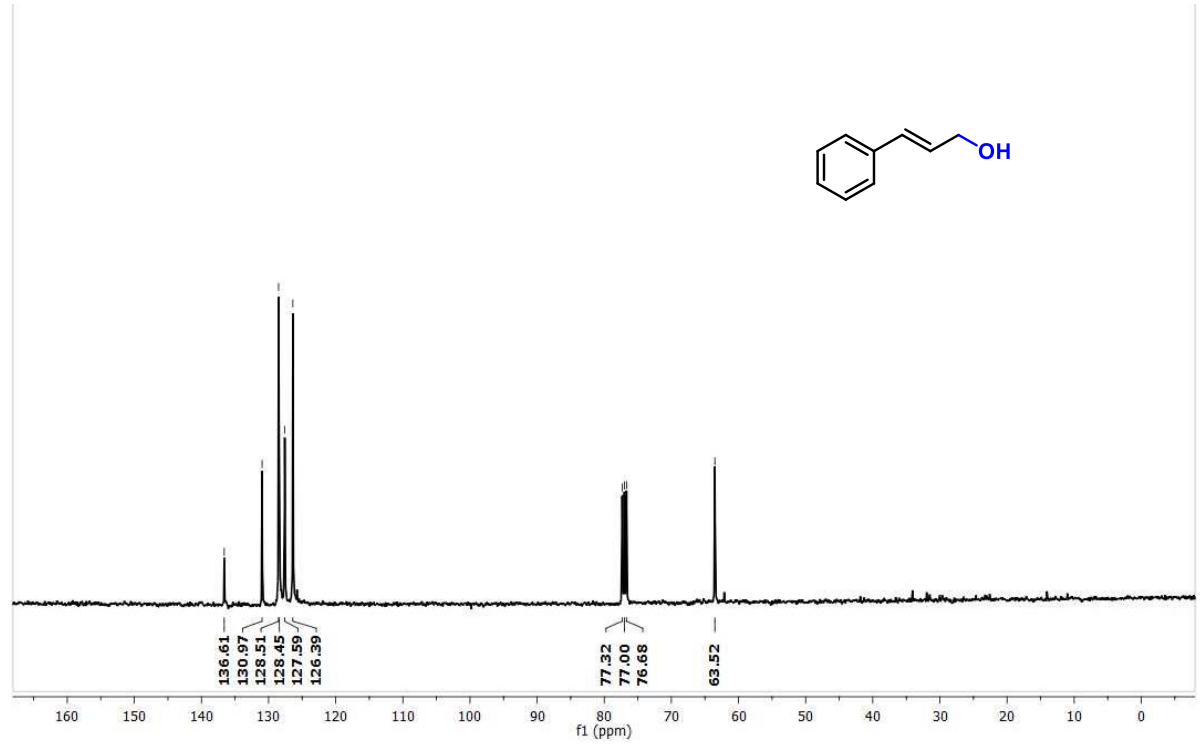

Fig. 45. ^{1}H NMR spectrum of 1-Hexanol (**5n**) in $CDCl_3$.

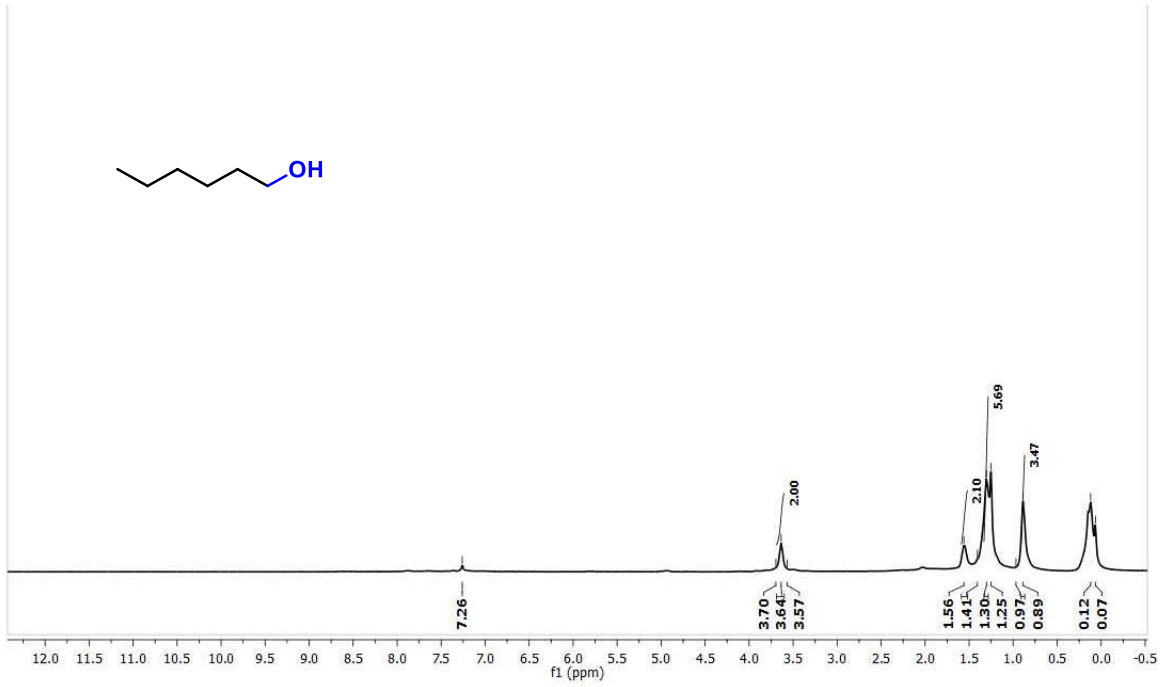

Fig. 46. $^{13}C\{^{1}H\}$ NMR spectrum of 1-Hexanol (**5n**) in $CDCl_3$.

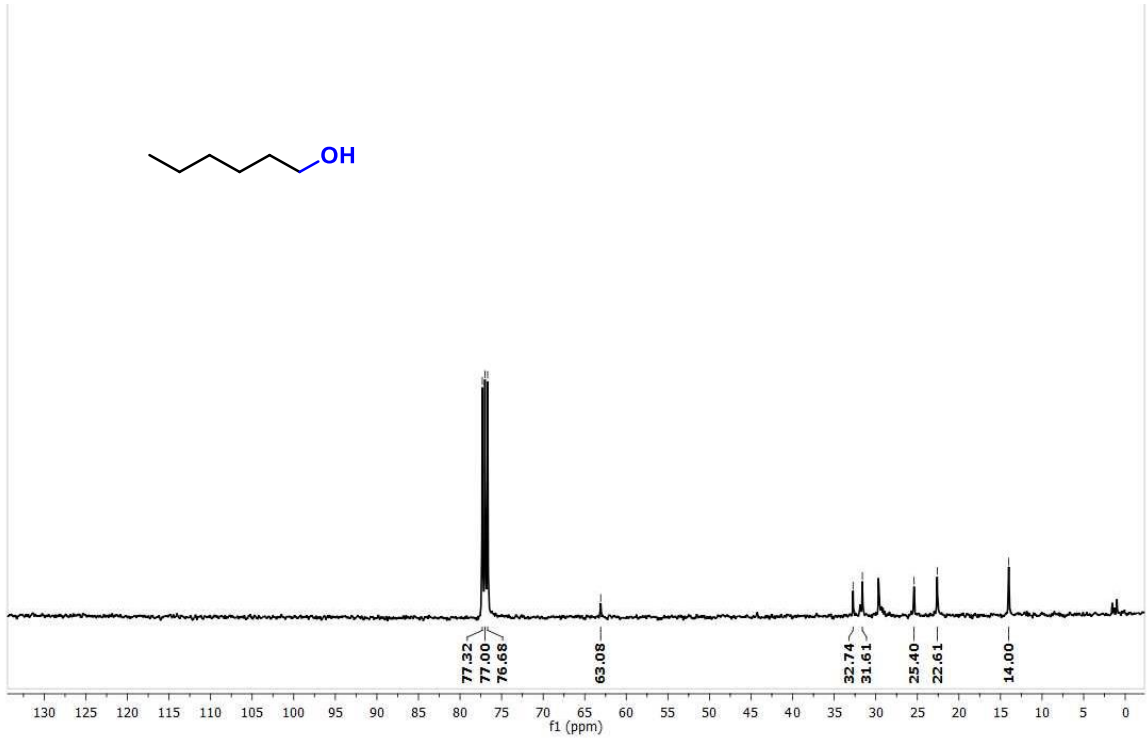

Fig. 47. ^{1}H NMR spectrum of Capric alcohol or 1-Decanol (**5o**) in $CDCl_3$.

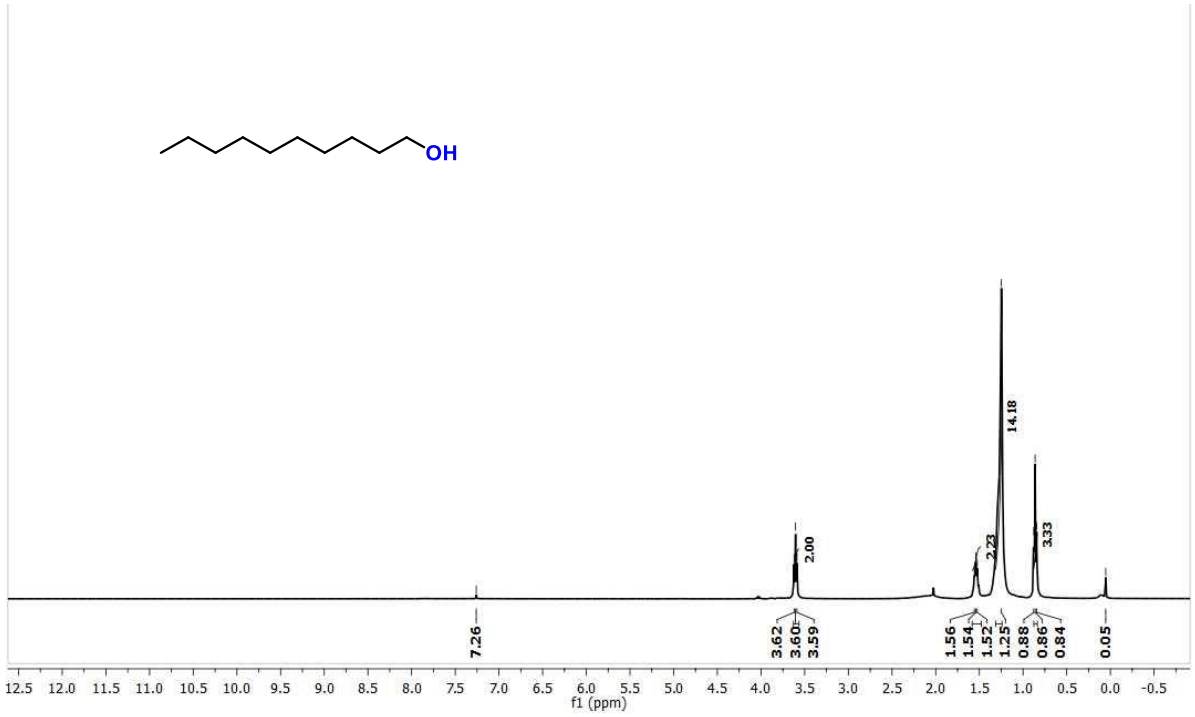

Fig. 48. $^{13}C\{^{1}H\}$ NMR spectrum of Capric alcohol or 1-Decanol (**5o**) in $CDCl_3$.

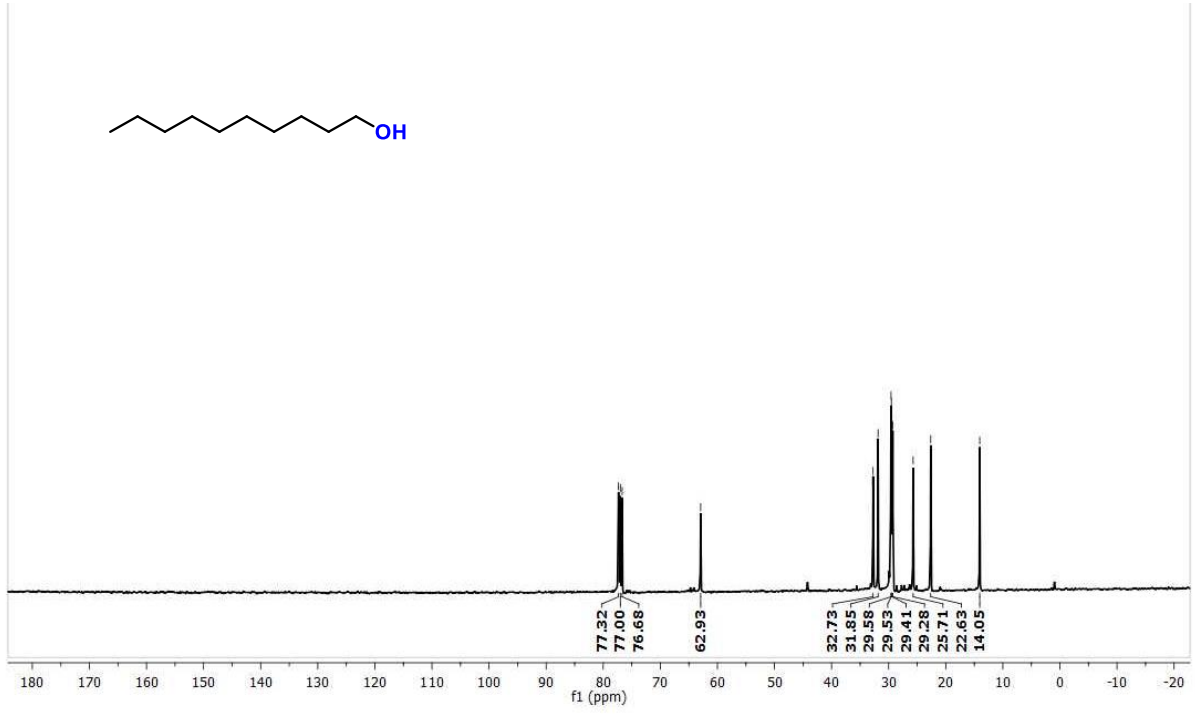

Fig. 49. ^{1}H NMR spectrum of Lauryl alcohol or 1-dodecanol (**5p**) in $CDCl_3$.

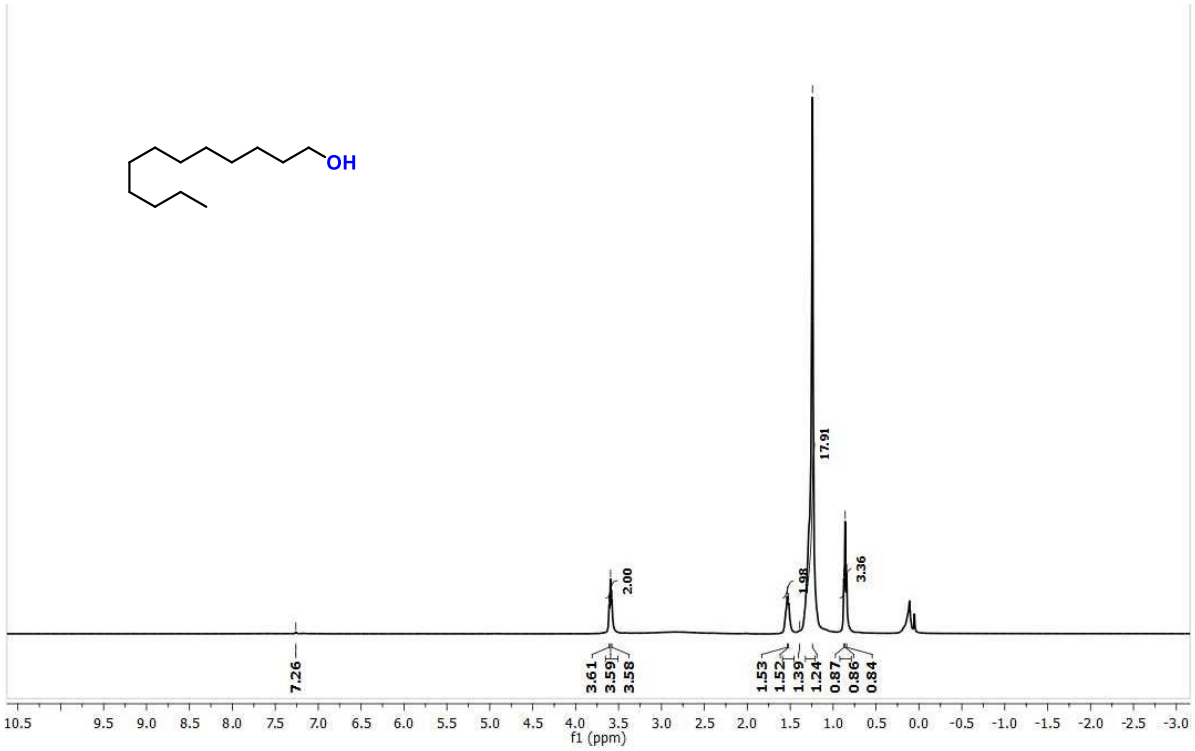

Fig. 50. $^{13}C\{^{1}H\}$ NMR spectrum of Lauryl alcohol or 1-dodecanol (**5p**) in $CDCl_3$.

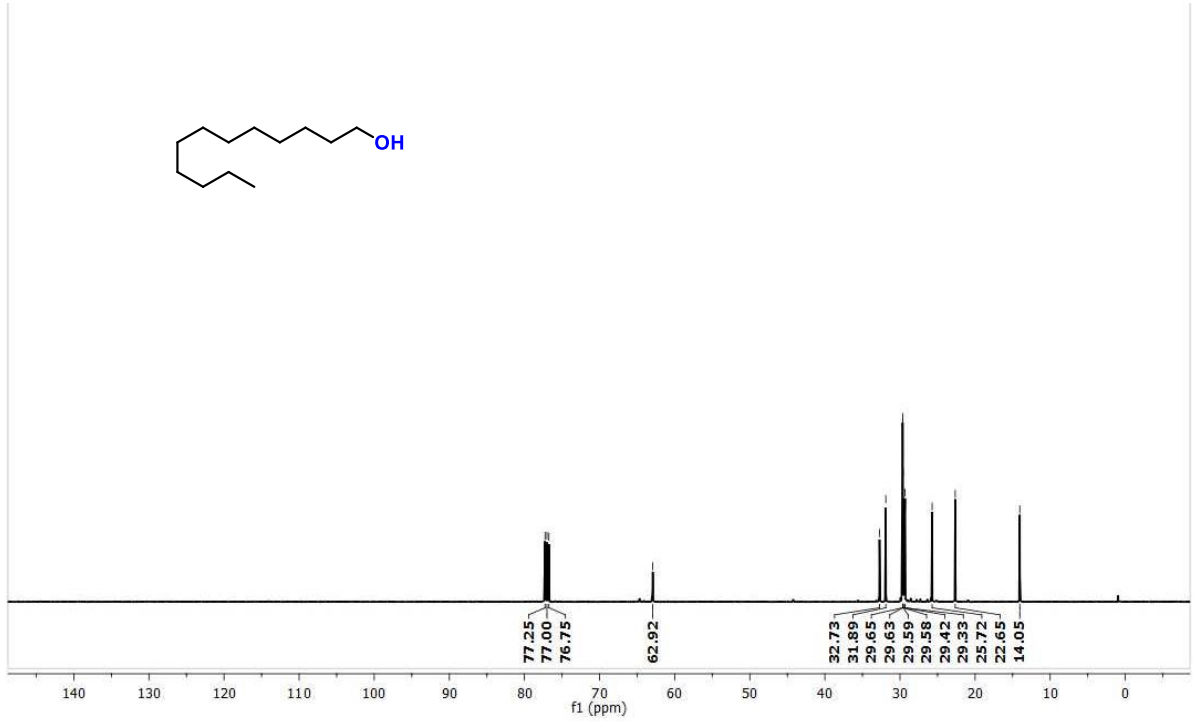

Fig. 51. ^{1}H NMR spectrum of Myristyl alcohol or 1-tetradecanol (**5q**) in $CDCl_3$.

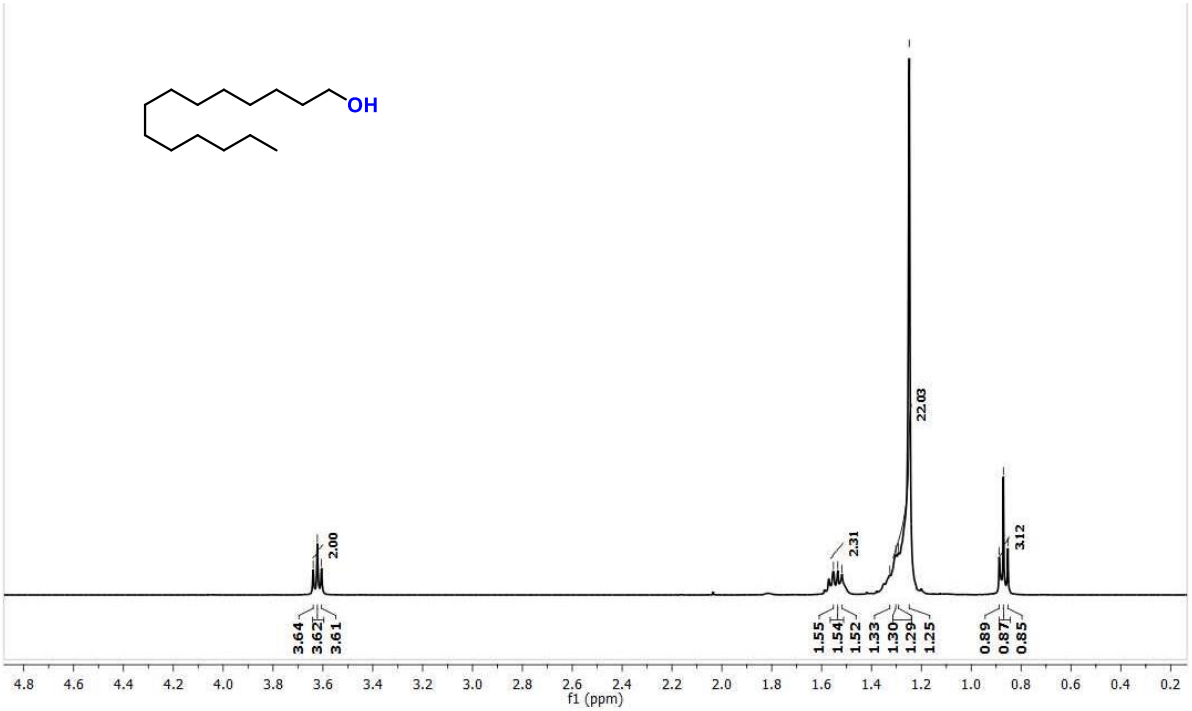

Fig. 52. $^{13}C\{^{1}H\}$ NMR spectrum of Myristyl alcohol or 1-tetradecanol (**5q**) in $CDCl_3$.

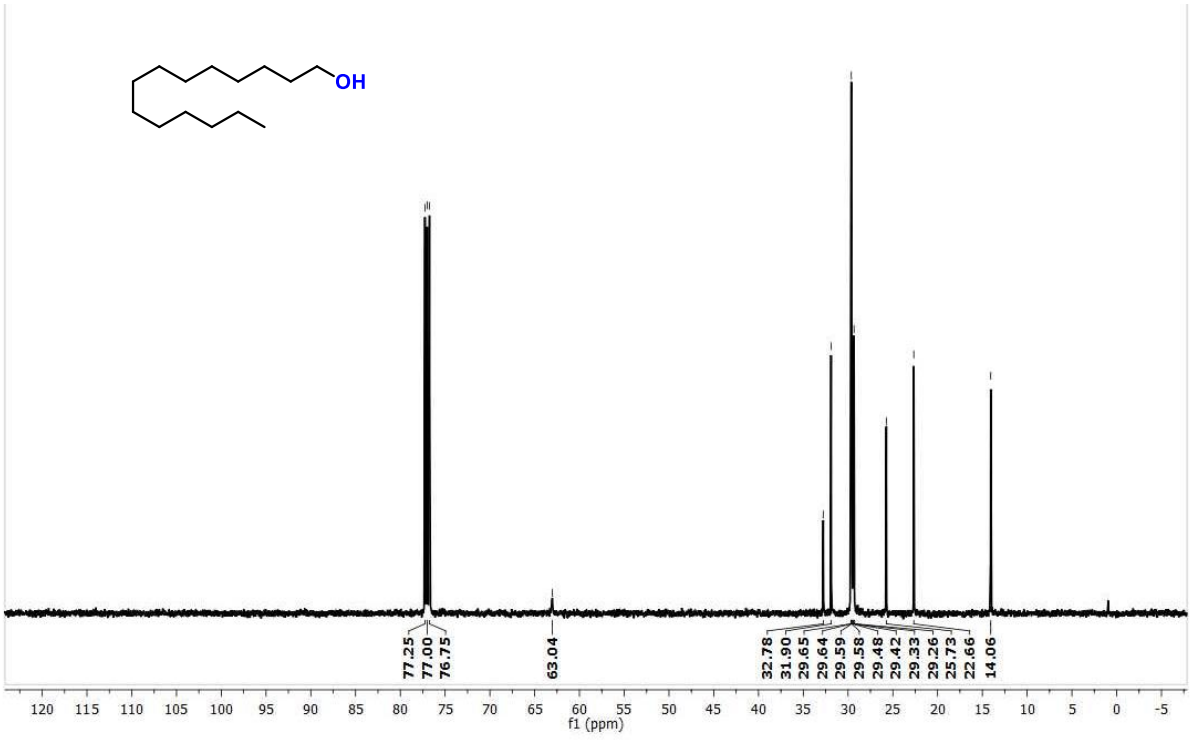

Fig. 53. ^{1}H NMR spectrum of Steryl alcohol or 1-octaecanol (**5r**) in $CDCl_3$.

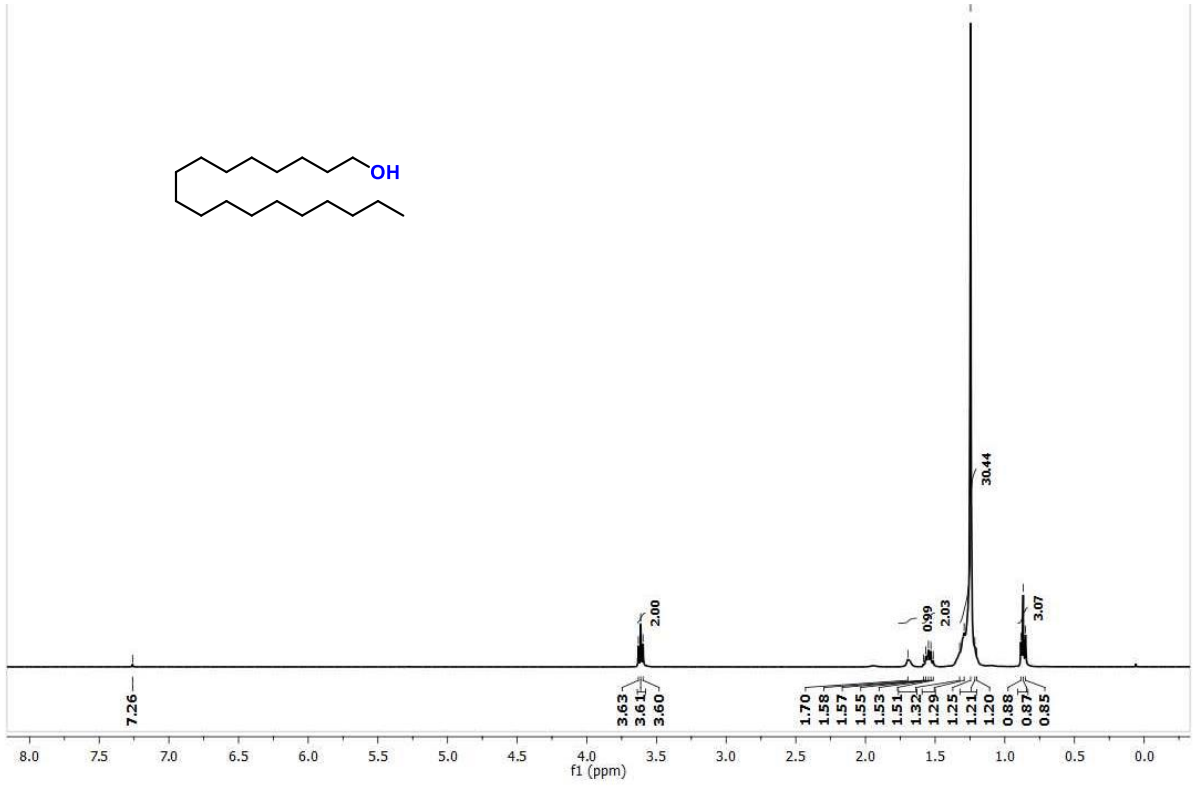

Fig. 54. $^{13}C\{^{1}H\}$ NMR spectrum of Steryl alcohol or 1-octaecanol (**5r**) in $CDCl_3$.

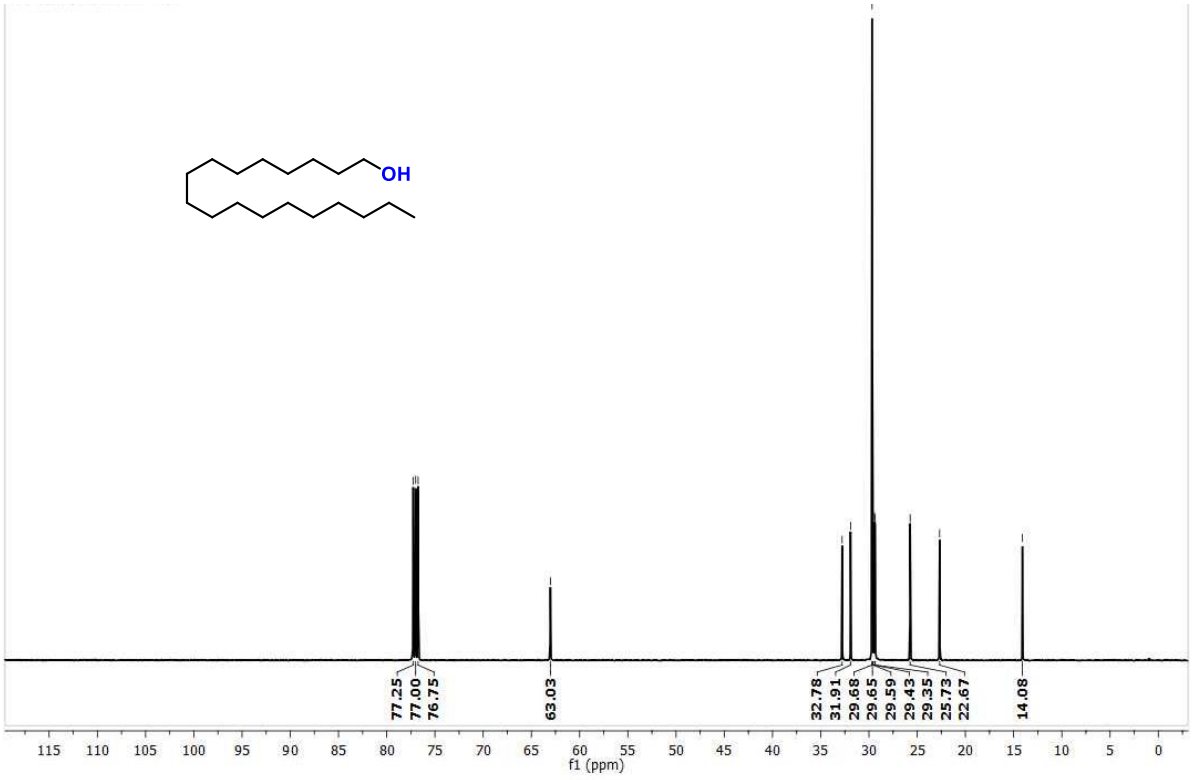

Fig. 55. ^{1}H NMR spectrum of Oleyl alcohol (**5t**) in $CDCl_3$.

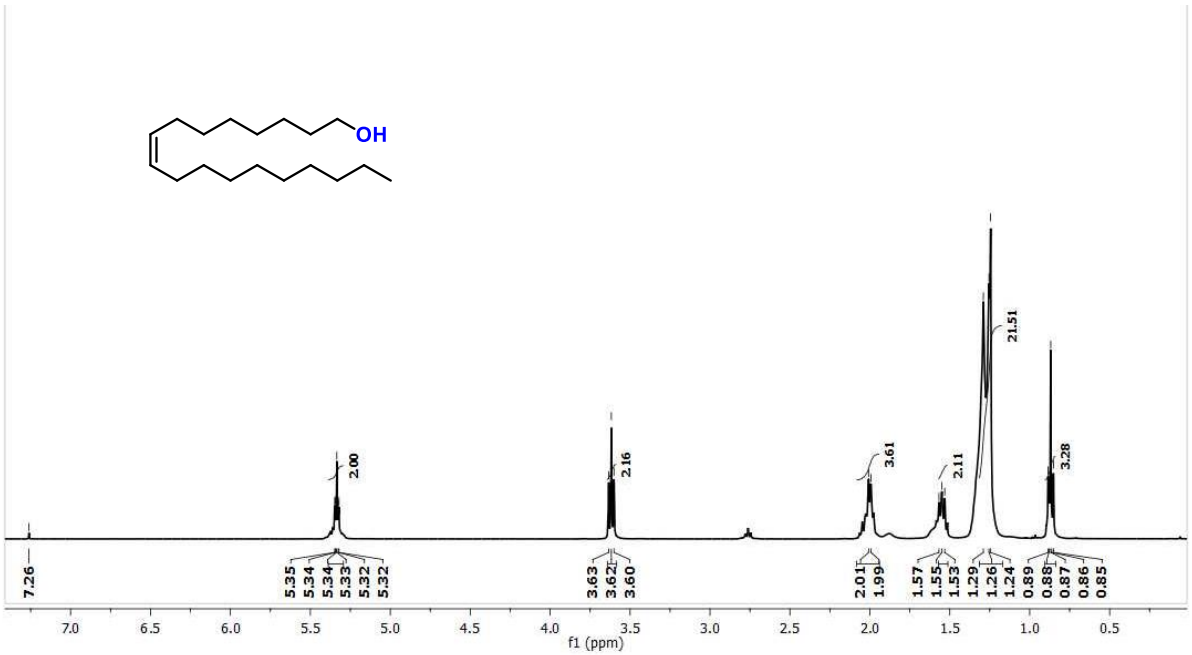

Fig. 56. $^{13}C\{^{1}H\}$ NMR spectrum of Oleyl alcohol (**5t**) in $CDCl_3$.

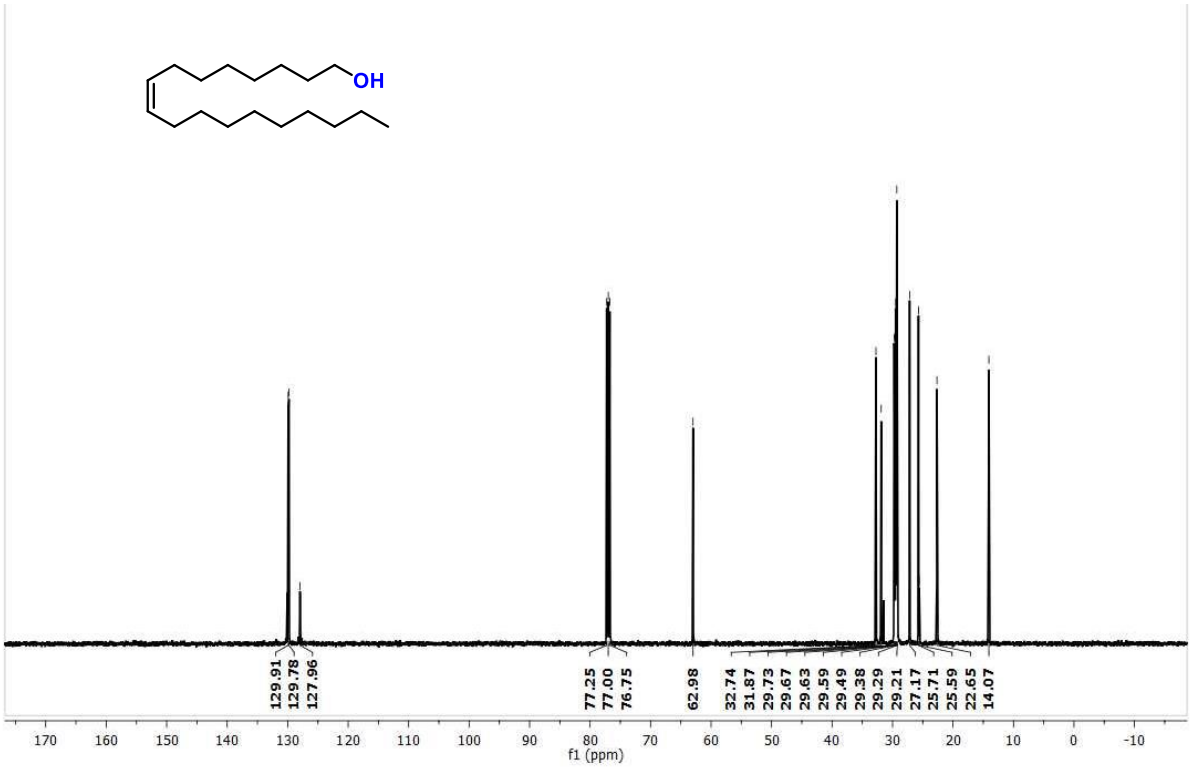

Fig. 57. ^{1}H NMR spectrum of 1-Undecylenic alcohol (**5u**) in $CDCl_3$.

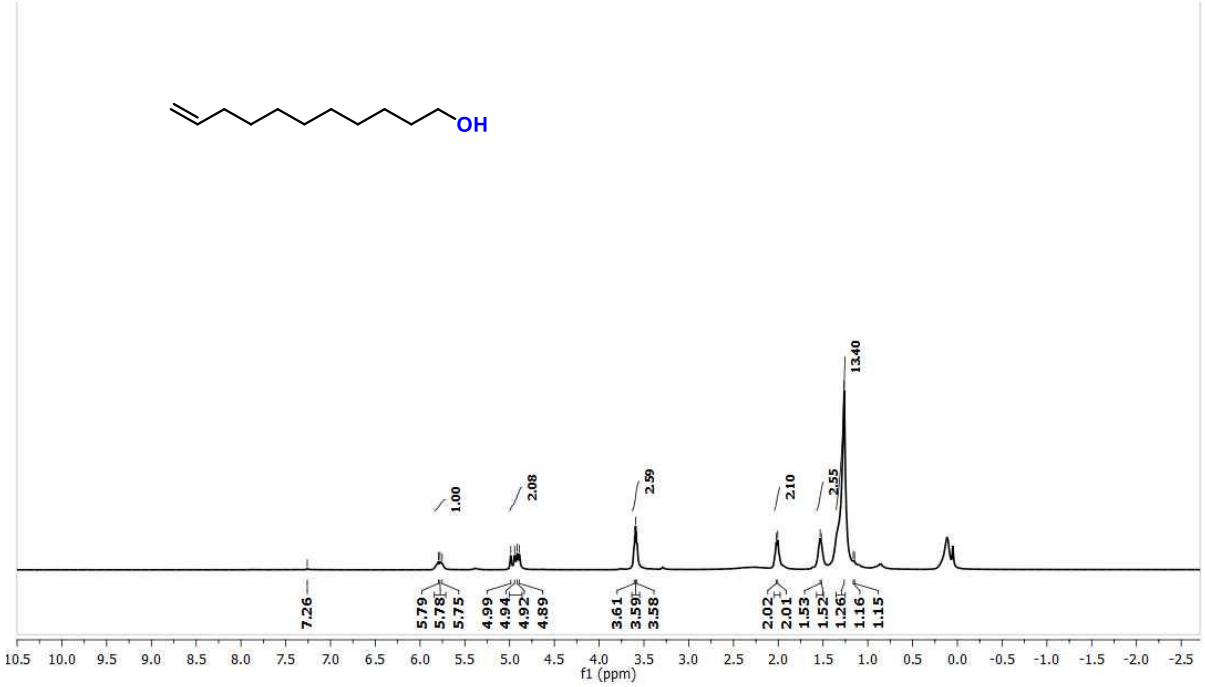

Fig. 58. $^{13}C\{^{1}H\}$ NMR spectrum of 1-Undecylenic alcohol (**5u**) in $CDCl_3$.

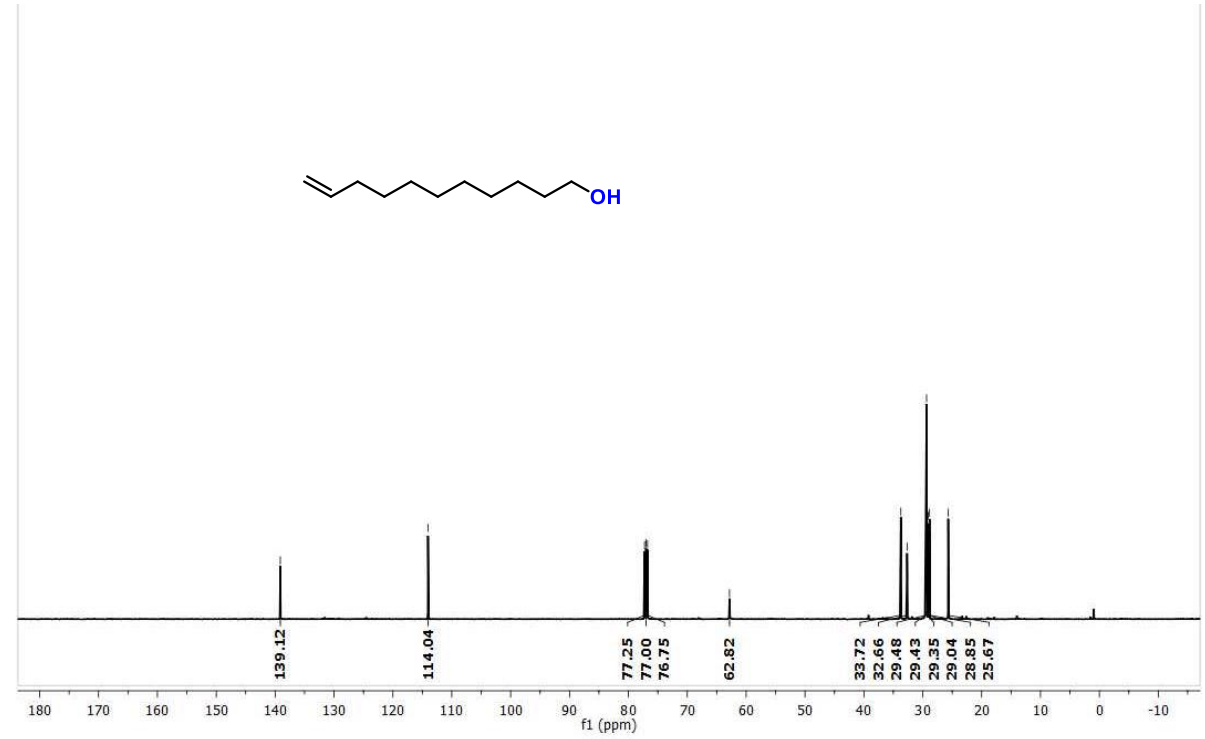

Fig. 59. ^{1}H NMR spectrum of 1,4-Undecandiol (**5v**) in $CDCl_3$.

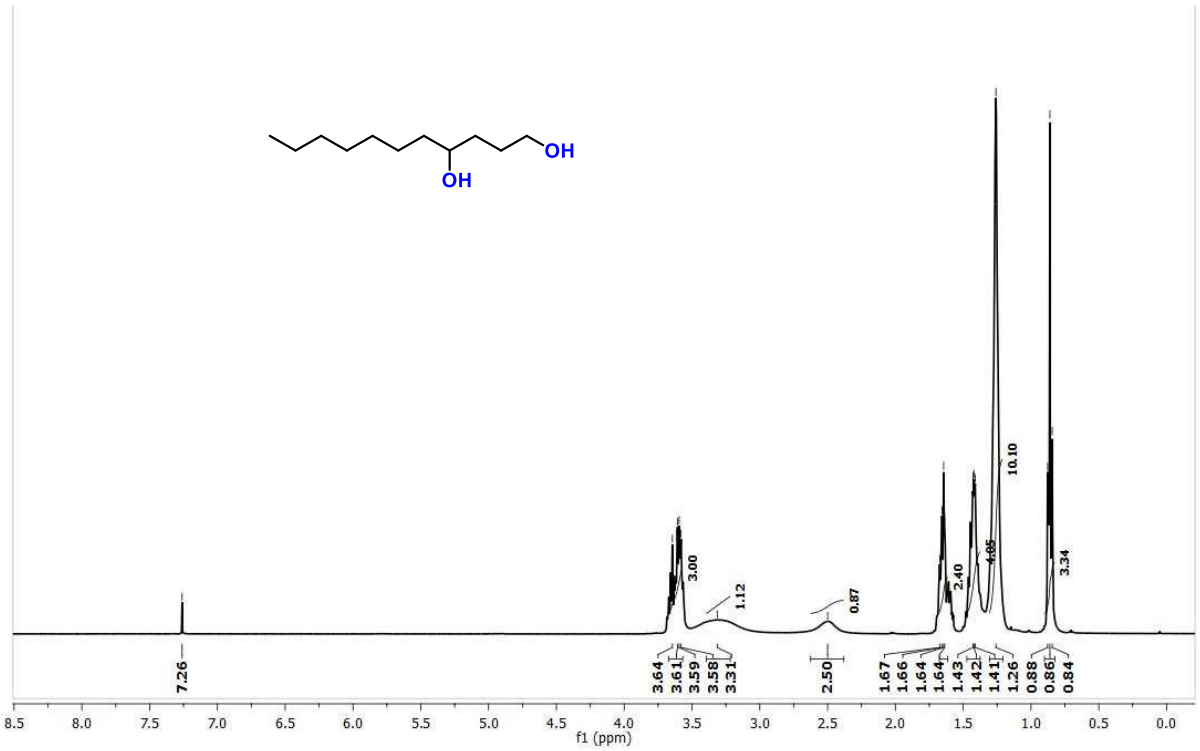

Fig. 60. $^{13}C\{^{1}H\}$ NMR spectrum of 1,4-Undecandiol (**5v**) in $CDCl_3$.

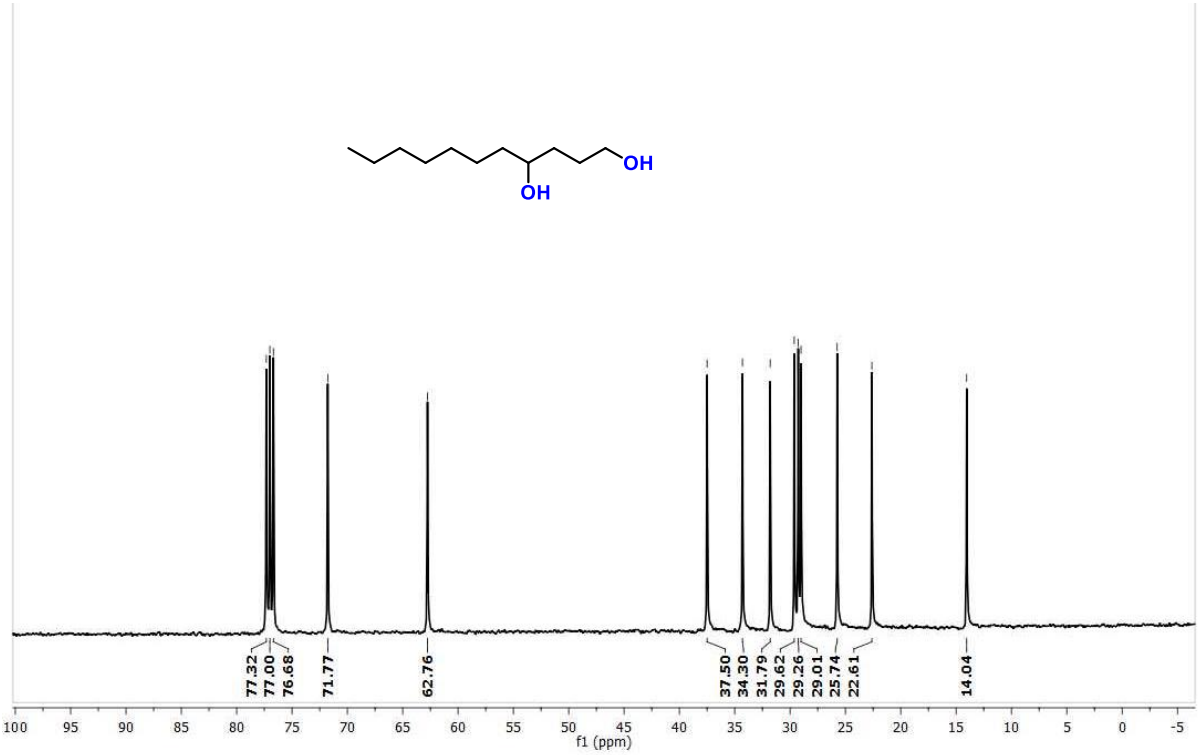

Fig. 61. ^{1}H NMR spectrum of 2-(4-isobutylphenyl)propan-1-ol (**5w**) in $CDCl_3$.

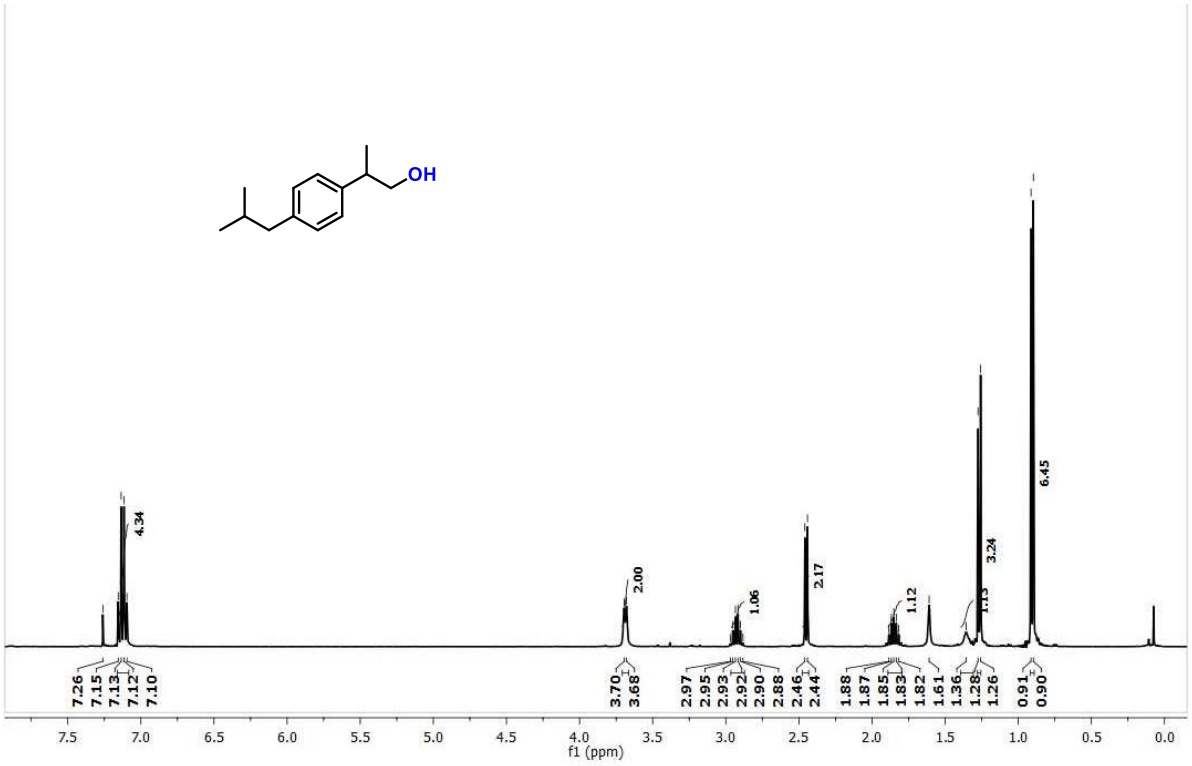

Fig. 62. $^{13}C\{^{1}H\}$ NMR spectrum of 2-(4-isobutylphenyl)propan-1-ol (**5w**) in $CDCl_3$.

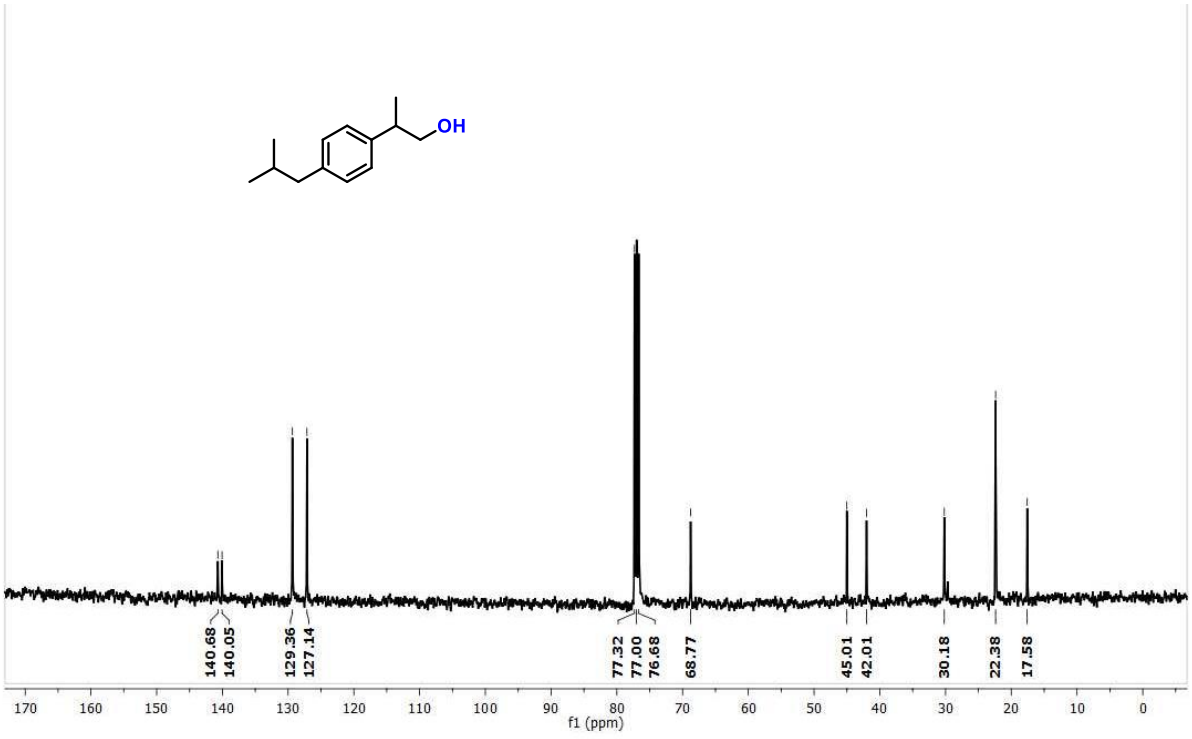

Fig. 63. ^{1}H NMR spectrum of 4-(hydroxymethyl)-N,N-dipropylbenzenesulfonamide (**5x**) in $CDCl_3$.

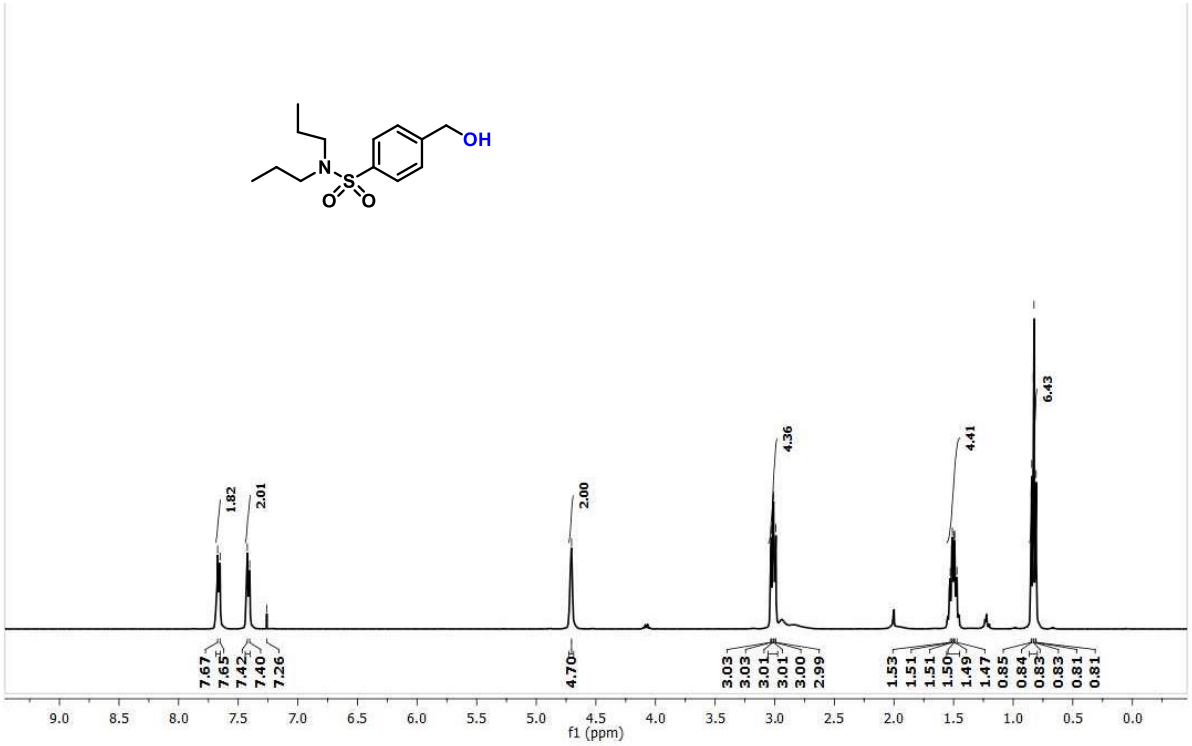

Fig. 64. $^{13}C\{^{1}H\}$ NMR spectrum of 4-(hydroxymethyl)-N,N-dipropylbenzenesulfonamide (**5x**) in $CDCl_3$.

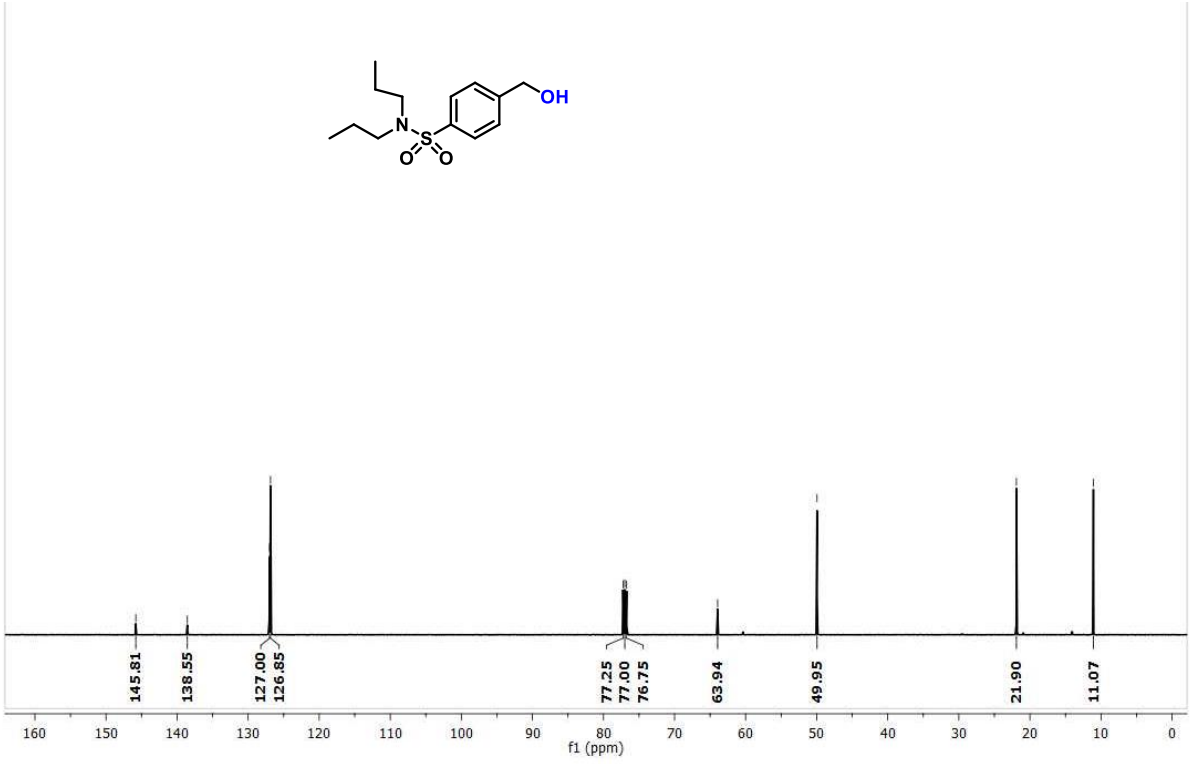

Fig. 65. ^{1}H NMR spectrum of 2-(2-fluoro-[1,1'-biphenyl]-4-yl)propan-1-ol (**5y**) in $CDCl_3$.

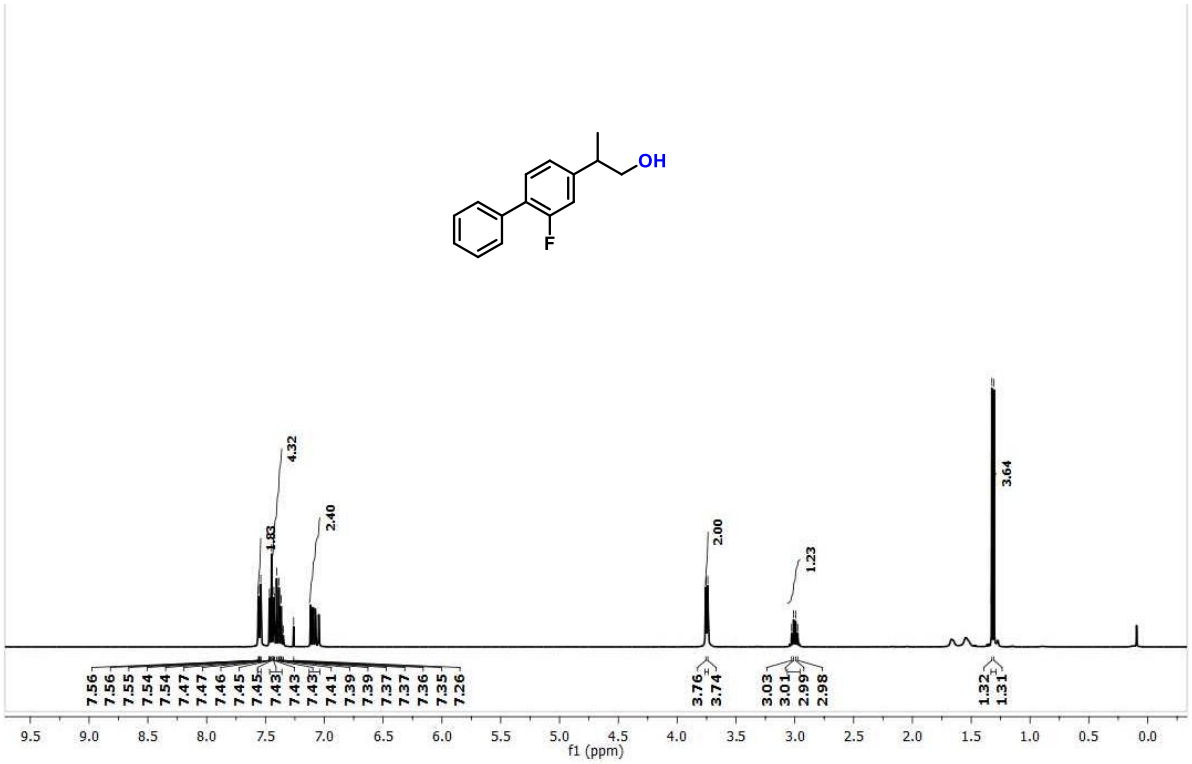

Fig. 66. $^{13}C\{^{1}H\}$ NMR spectrum of 2-(2-fluoro-[1,1'-biphenyl]-4-yl)propan-1-ol (**5y**) in $CDCl_3$.

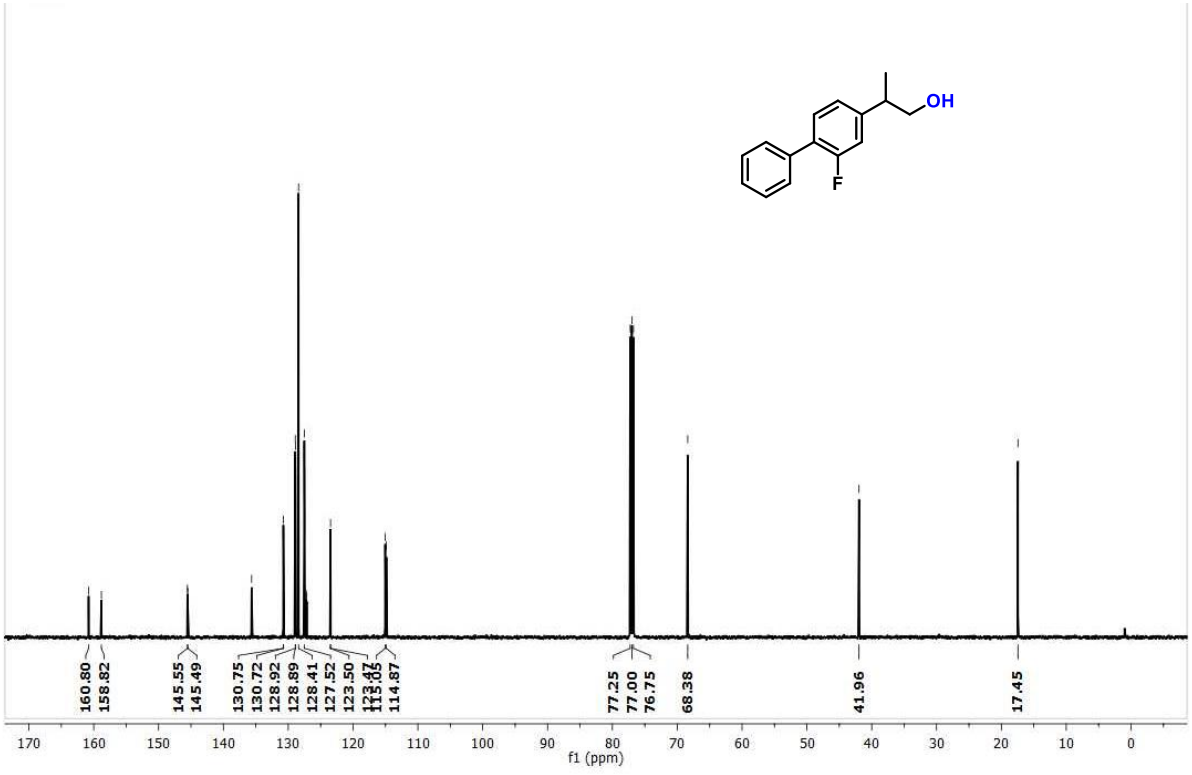

Fig. 67. ^{1}H NMR spectrum of 3-(4,5-diphenyloxazol-2-yl)propan-1-ol (**5z**) in $CDCl_3$.

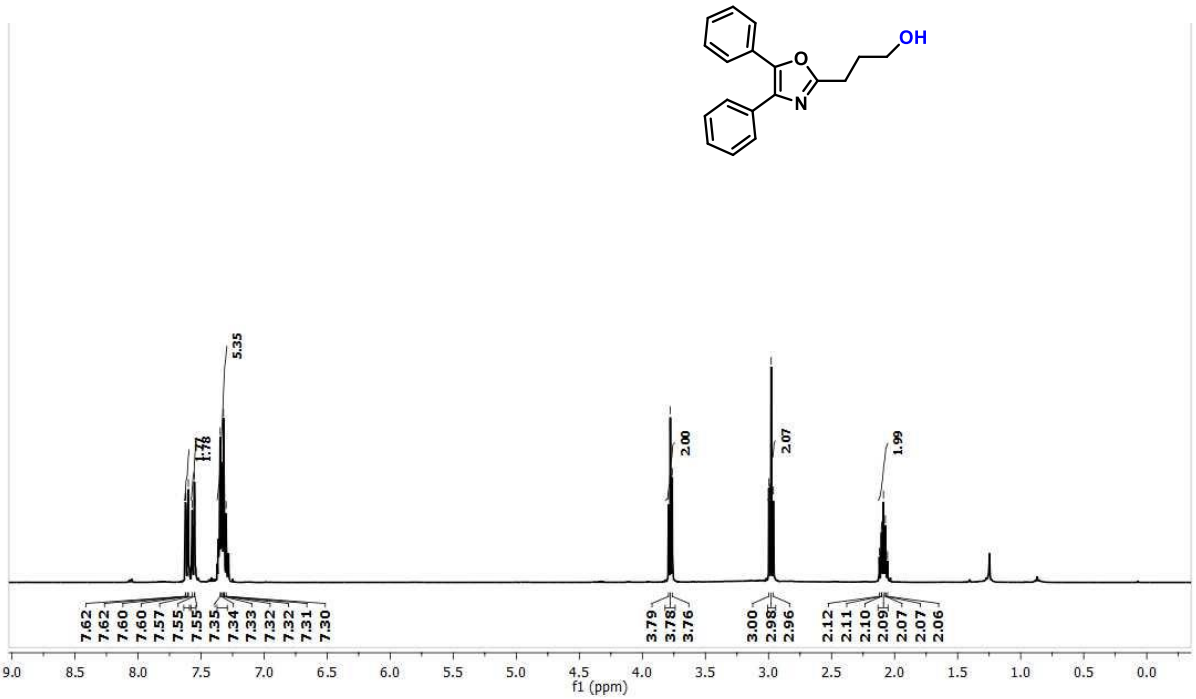

Fig. 68. $^{13}C\{^{1}H\}$ NMR spectrum of 3-(4,5-diphenyloxazol-2-yl)propan-1-ol (**5z**) in $CDCl_3$.

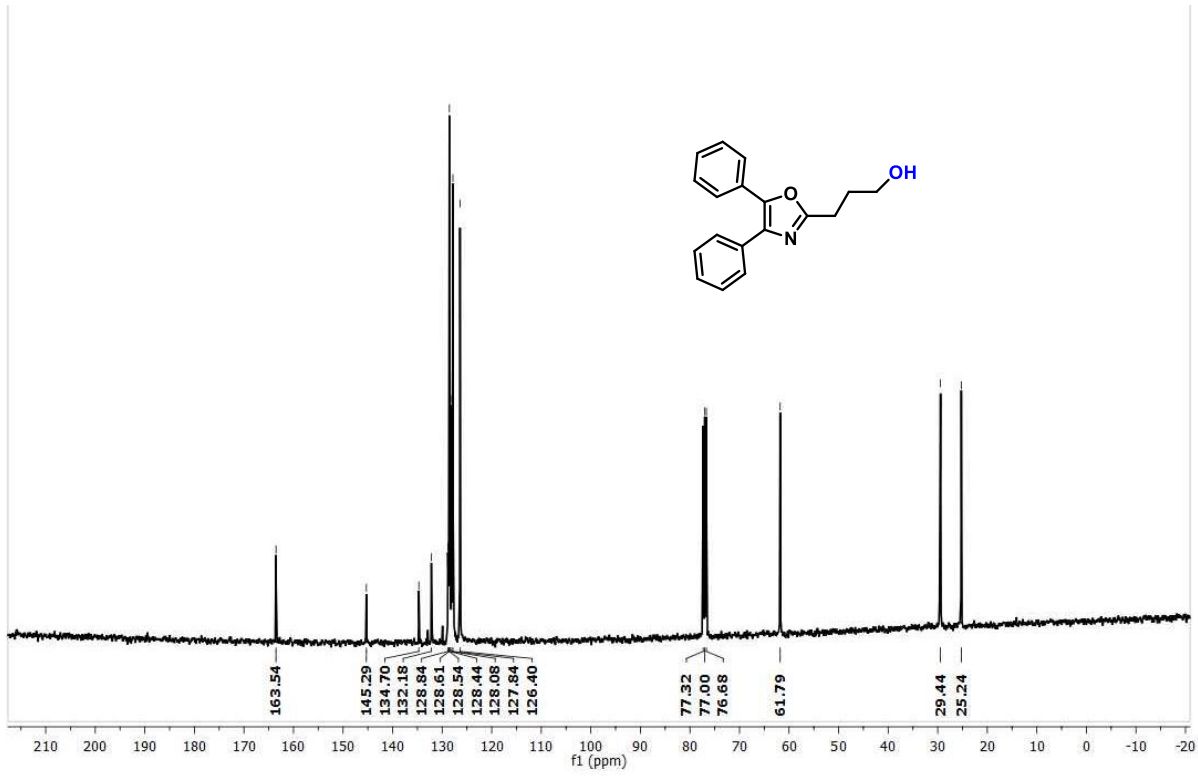

Fig. 69. ^{1}H NMR spectrum of **10'** after flash column of the reaction mixture in $CDCl_3$.

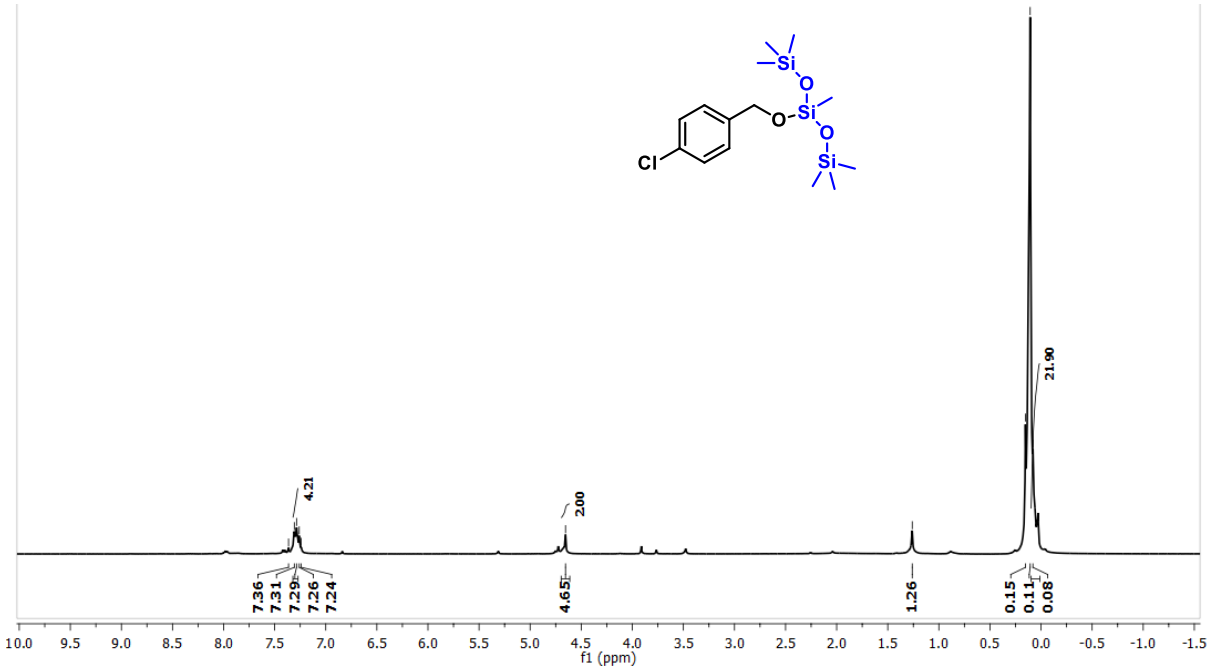

Fig. 70. $^{13}C\{^{1}H\}$ NMR spectrum of **10'** after flash column of the reaction mixture in $CDCl_3$.

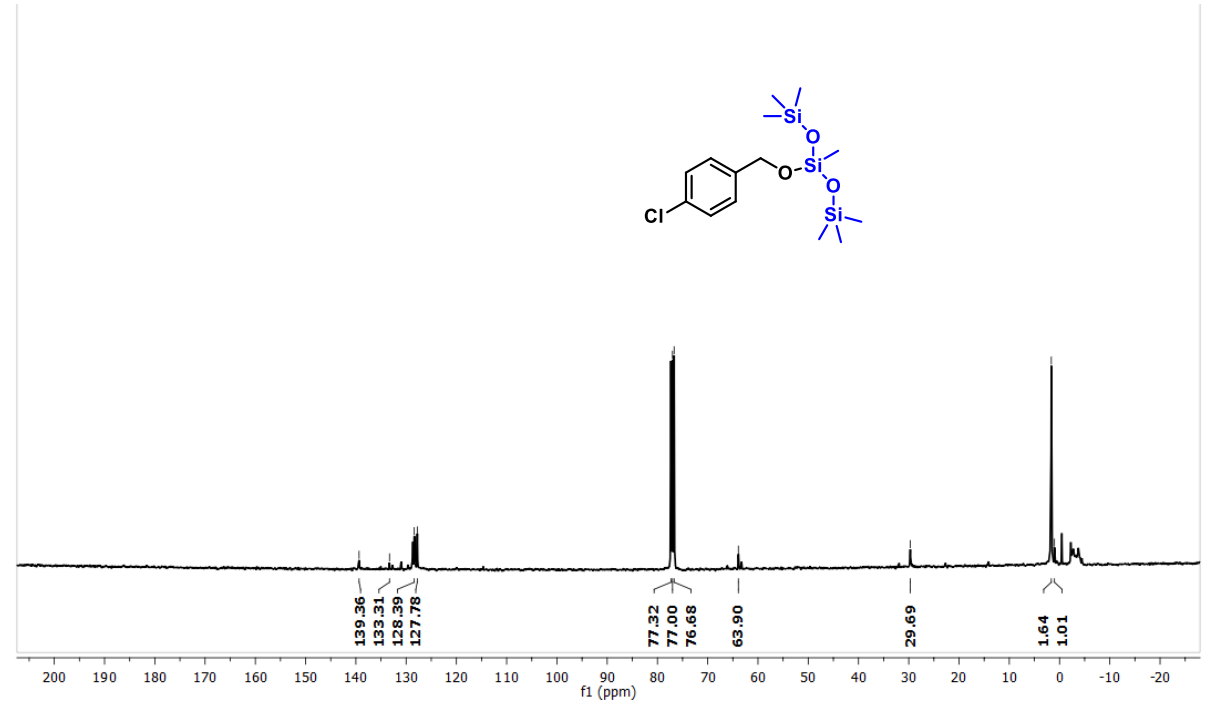

T 71. ^{29}Si NMR spectrum of **10'** after flash column of the reaction mixture in $CDCl_3$.

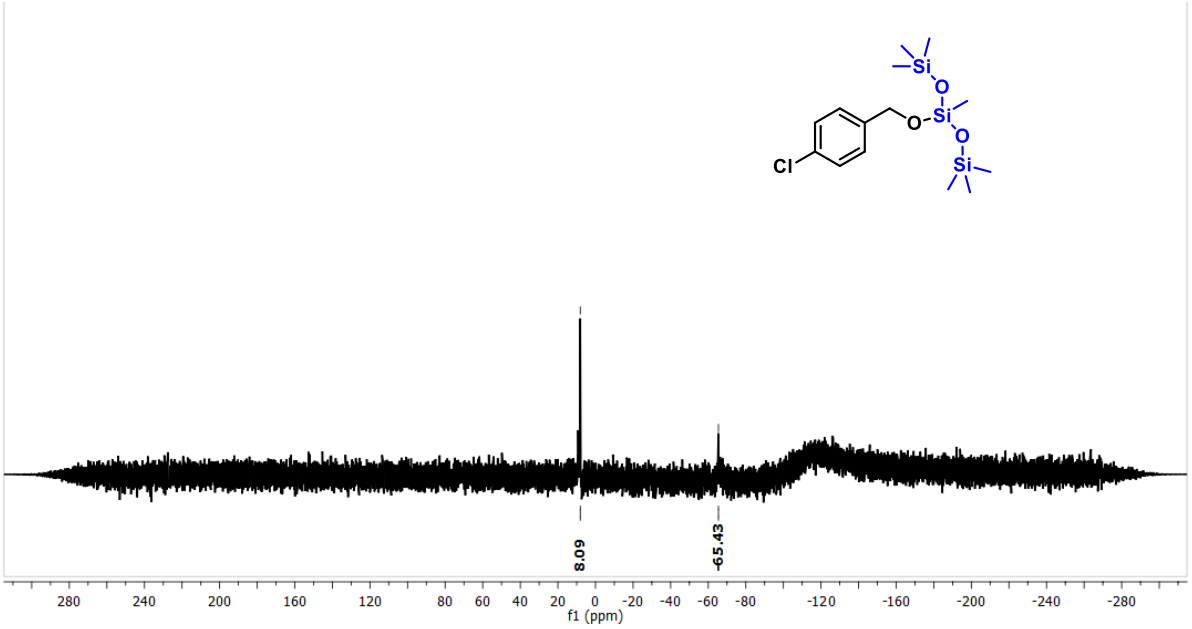

References:

1. Moumne, R.; Lavielle, S.; Karoyan, P. *J. Org. Chem.* **2006**, *71*, 3332-3334.

2. Chakraborty, S.; Das, A.; Ahmed, J.; Barman, S.; Mandal, S. K. *Chem. Commun.* **2020**, *56*, 13788-13791.

3. Martinez-Ferrate, O.; Chatterjee, B.; Werle, C.; Leitner, W. *Catal. Sci. Technol.* **2019**, *9*, 6370-6378.

4. Amberchan, G.; Snelling, R. A.; Moya, E.; Landi, M.; Lutz, K.; Gatihi, R.; Singaram, B. *J. Org. Chem.* **2021**, *86*, 6207-6227.

5. Oates, C. L.; Widegren, M. B.; Clarke, M. L. *Chem. Commun.* **2020**, *56*, 8635-8638.

6. Behera, R. R.; Ghosh, R.; Panda, S.; Khamari, S.; Bagh, B. *Org. Lett.* **2020**, *22*, 3642-3648.

7. Pandey, V. K.; Tiwari, C. S.; Rit, A. *Org. Lett.* **2021**, *23*, 1681-1686.

8. Matsubara, K.; Mitsuyama, T.; Shin, S.; Hori, M.; Ishikawa, R.; Koga, Y. *Organometallics* **2021**, *40*, 1379-1387.
9. Choe, H. R.; Han, S. S.; Kim, Y.; Hong, C.; Cho, E. J.; Nam, K. M. *ACS Appl. Mater. Interfaces* **2021**, *13*, 1714-1722.
10. Choudhary, P.; Bahuguna, A.; Kumar, A.; Dhankhar, S. S.; Nagaraja, C. M.; Krishnan, V. *Green Chem.* **2020**, *22*, 5084-5095.
11. Kuhwald, C.; Kirschning, A. *Org. Lett.* **2021**, *23*, 4300-4304.
12. Mahata, S.; Sahu, A.; Shukla, P.; Rai, A. Singh, M.; Rai, V. K. *New J. Chem.* **2018**, *42*, 19945-19952.
13. Kaithal, A.; Hölscher, M.; Leitner, W. *Chem. Sci.* **2021**, *12*, 976-982.
14. Cao, H. Q.; Liu, H. N.; Liu, Z. Y.; Qiao, B.; Zhang, F. G.; Ma, J. A. *Org. Lett.* **2020**, *22*, 6414-6419.
15. Friest, J. A.; Maezato, Y.; Broussy, S.; Blum, P.; Berkowitz, D. B. *J. Am. Chem. Soc.* **2010**, *132*, 5930-5931.
16. Dolomanov, O. V.; Bourhis, L. J.; Gildea, R. J.; Howard, J. A. K.; Puschmann, H. *J. Appl. Cryst.* **2009**, *42*, 339-341.
17. Sheldrick, G. M. *Acta Cryst.* **2015**, *A71*, 3–8.
18. Sheldrick, G.M. *Acta Cryst.* **2015**, *C71*, 3-8.
19. Frisch, M. J. *et al.* Gaussian 16, Revision B.01, Fox, Gaussian, Inc., Wallingford CT, **2016**.
20. Becke, A. D. *J. Chem. Phys.* **1993**, *98*, 5648-5652.
21. Yang, Y.; Weaver, M. N.; Merz, Jr, K. M. *J. Phys. Chem. A* **2009**, *1123*, 9843-9851.